Physical Oceanography & Tidal Engineering

Sharron Lilly

Stephania Hutchins

First Edition, 2012

Table of Contents

Chapter- 1

Physical Oceanography
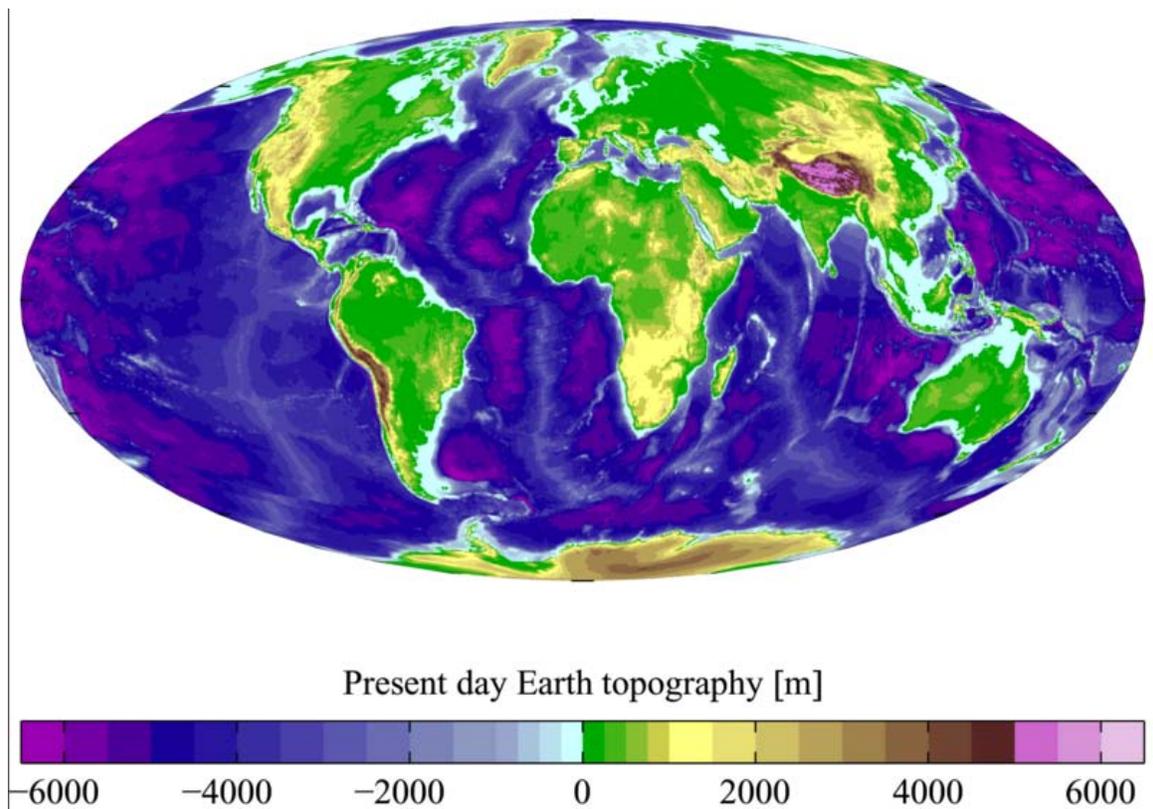
World ocean bathymetry.

Physical oceanography is the study of physical conditions and physical processes within the ocean, especially the motions and physical properties of ocean waters.

Physical oceanography is one of several sub-domains into which oceanography is divided. Others include biological, chemical and geological oceanographies.

The physical setting

Perspective view of the sea floor of the Atlantic Ocean and the Caribbean Sea. The purple sea floor at the center of the view is the Puerto Rico Trench.
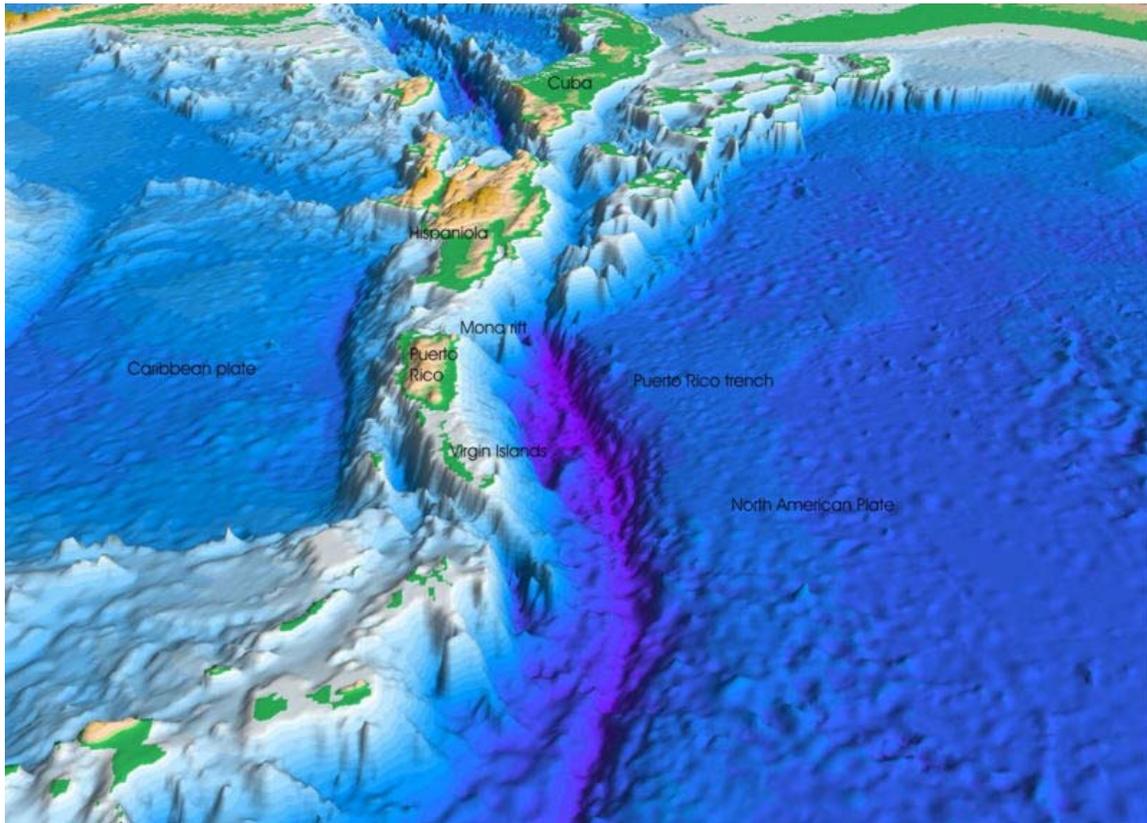
The pioneering oceanographer Matthew Maury said in 1855 *"Our planet is invested with two great oceans; one visible, the other invisible; one underfoot, the other overhead; one entirely envelopes it, the other covers about two thirds of its surface."* The fundamental role of the oceans in shaping Earth is acknowledged by ecologists, geologists, meteorologists, climatologists, geographers and others interested in the physical world. An Earth without oceans would truly be unrecognizable.

Roughly 97% of the planet's water is in its oceans, and the oceans are the source of the vast majority of water vapor that condenses in the atmosphere and falls as rain or snow on the continents. The tremendous heat capacity of the oceans moderates the planet's climate, and its absorption of various gases affects the composition of the atmosphere. The ocean's influence extends even to the composition of volcanic rocks through seafloor metamorphism, as well as to that of volcanic gases and magmas created at subduction zones.

The oceans are far deeper than the continents are tall; examination of the Earth's hypsographic curve shows that the average elevation of Earth's landmasses is only

840 metres (2,760 ft), while the ocean's average depth is 3,800 metres (12,500 ft). Though this apparent discrepancy is great, for both land and sea, the respective extremes such as mountains and trenches are rare.

Area, volume plus mean and maximum depths of oceans (excluding adjacent seas)

Body	Area (10^6km²)	Volume (10^6km³)	Mean depth (m)	Maximum (m)
Pacific Ocean	165.2	707.6	4282	-10911
Atlantic Ocean	82.4	323.6	3926	-8605
Indian Ocean	73.4	291.0	3963	-8047
Southern Ocean	20.3			-7235
Arctic Ocean	14.1		1038	
Caribbean Sea	2.8			-7686

Temperature, salinity and density
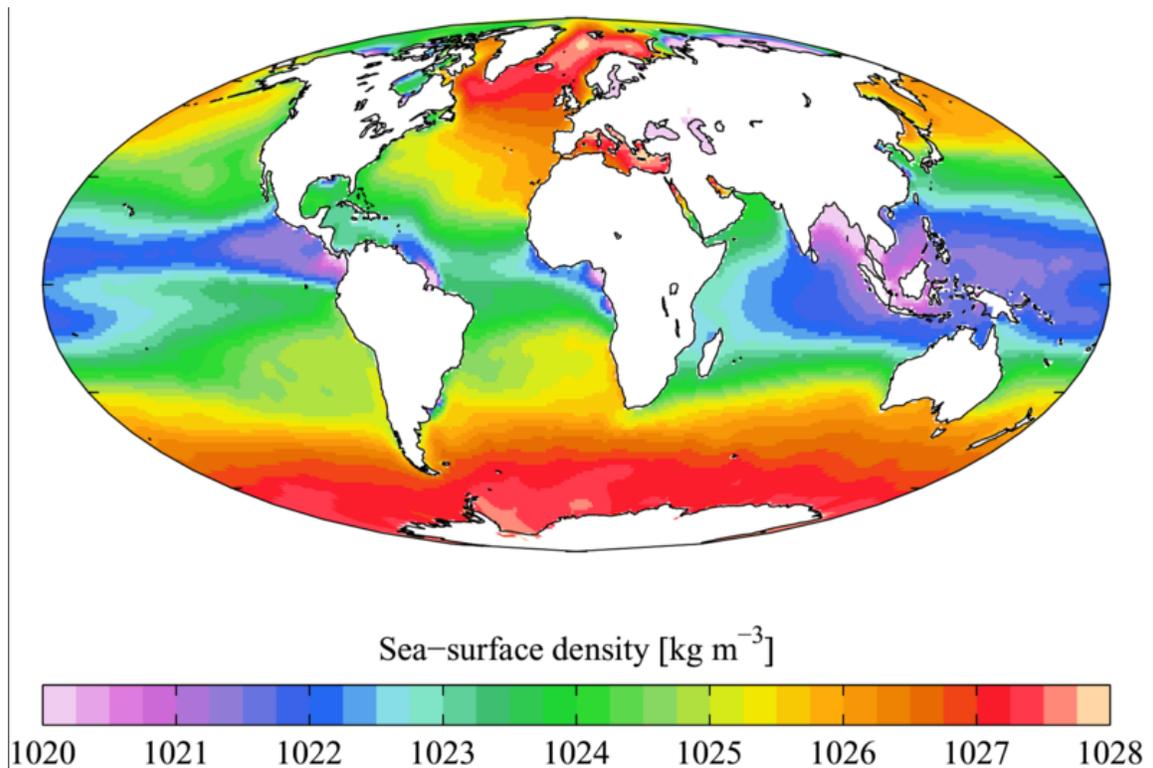

WOA surface density.

Because the vast majority of the world ocean's volume is deep water, the mean temperature of seawater is low; roughly 75% of the ocean's volume has a temperature from 0° – 5°C (Pinet 1996). The same percentage falls in a salinity range between 34–35 ppt (3.4–3.5%) (Pinet 1996). There is still quite a bit of variation, however. Surface

temperatures can range from below freezing near the poles to 35°C in restricted tropical seas, while salinity can vary from 10 to 41 ppt (1.0–4.1%).

The vertical structure of the temperature can be divided into three basic layers, a surface mixed layer, where gradients are low, a thermocline where gradients are high, and a poorly stratified abyss.

In terms of temperature, the ocean's layers are highly latitude-dependent; the thermocline is pronounced in the tropics, but nonexistent in polar waters (Marshak 2001). The halocline usually lies near the surface, where evaporation raises salinity in the tropics, or meltwater dilutes it in polar regions. These variations of salinity and temperature with depth change the density of the seawater, creating the pycnocline.

Circulation
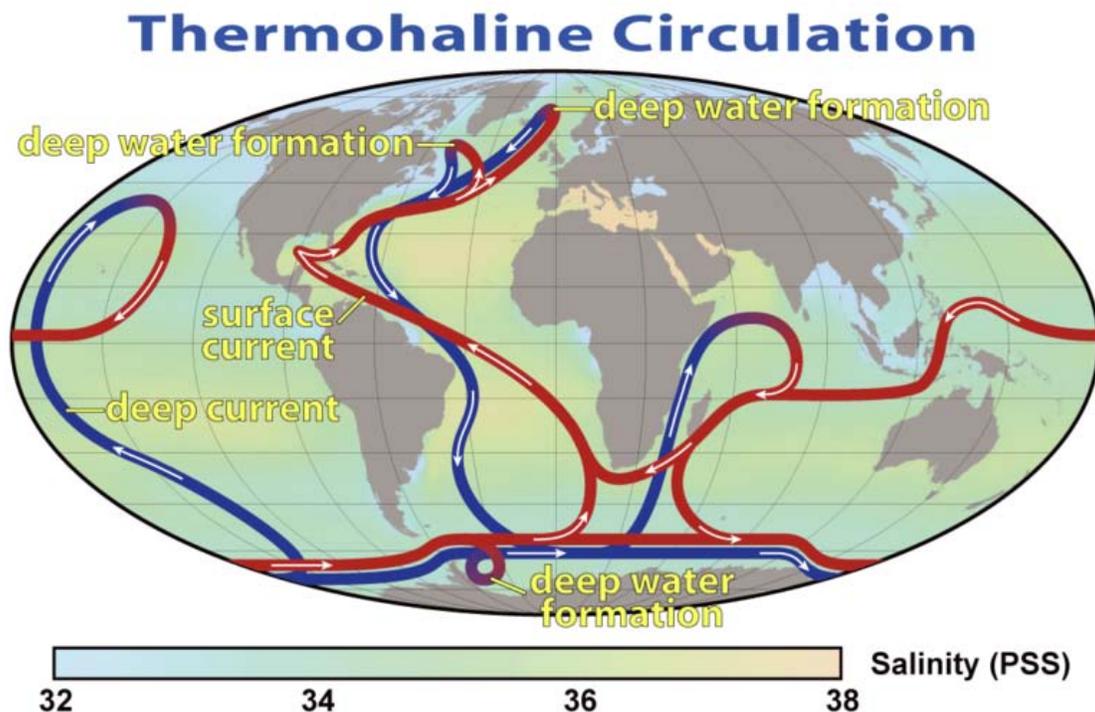
Density-driven thermohaline circulation

The ultimate energy source for the ocean circulation (and for the atmospheric circulation) is the sun. The amount of sunlight absorbed at the surface varies strongly with latitude, being greater at the equator than at the poles, and this engenders fluid motion in both the atmosphere and ocean that acts to redistribute heat from the equator towards the poles, thereby reducing the temperature gradients that would exist in the absence of fluid motion. Perhaps three quarters of this heat is carried in the atmosphere; the rest is carried in the ocean.

The atmosphere is heated from below, which leads to convection, the largest expression of which is the Hadley circulation. By contrast the ocean is heated from above, which tends to suppress convection. Instead ocean deep water is formed in polar regions where cold salty waters sink in fairly restricted areas. This is the beginning of the thermohaline circulation.

Oceanic currents are largely driven by the surface wind stress; hence the large-scale atmospheric circulation is important to understanding the ocean circulation. The Hadley circulation leads to Easterly winds in the tropics and Westerlies in mid-latitudes, which creates an anticyclonic wind stress curl over the subtropical ocean. This leads to slow equatorward flow throughout most of a subtropical ocean basin (the Sverdrup balance). The return flow occurs in an intense, narrow, poleward western boundary current. Like the atmosphere, the ocean is far wider than it is deep, and hence horizontal motion is in general much faster than vertical motion. In the southern hemisphere there is a continuous belt of ocean, and hence the mid-latitude westerlies force the strong Antarctic Circumpolar Current. In the northern hemisphere the land masses prevent this and the ocean circulation is broken into smaller gyres in the Atlantic and Pacific basins.

Coriolis effect

The Coriolis effect results in a deflection of fluid flows (to the right in the Northern Hemisphere and left in the Southern Hemisphere). Because the distance around the Earth decreases as one moves away from the equator, and because the Earth rotates in a counter clockwise direction as seen from the north pole, air and water masses are deflected to the east as they move from the equator to the poles, and to the west as they move from the poles to the equator. This has profound effects on the flow of the oceans. In particular it means the flow goes *around* high and low pressure systems, permitting them to persist for long periods of time. As a result, tiny variations in pressure can produce measurable currents. A slope of one part in one million in sea surface height, for example, will result in a current of 1 cm/s at mid-latitudes. The fact that the Coriolis effect is largest at the poles and weak at the equator results in sharp, relatively steady western boundary currents which are absent on eastern boundaries.

The Coriolis effect is also responsible for coastal upwelling as wind-driven currents tend to forced to the right of the winds in the Northern Hemisphere and to the left of the winds in the Southern Hemisphere. When winds blow either equatorward along an eastern ocean boundary or poleward along a western ocean boundary, water is driven away from the coasts (the so called Ekman transport), and denser water rises from below to replace it.

Ekman transport

Ekman Transport results in the net transport of surface water 90 degrees to the right of the wind in the Northern Hemisphere, and 90 degrees to the left of the wind in the Southern Hemisphere. As the wind blows across the surface of the ocean, it "grabs" onto a thin layer of the surface water. In turn, that thin sheet of water transfers motion energy

to the thin layer of water under it, and so on. However, because of the Coriolis Effect, the direction of travel of the layers of water slowly move farther and farther to the right as they get deeper in the Northern Hemisphere, and to the left in the Southern Hemisphere. In most cases, the very bottom layer of water affected by the wind is at a depth of 100 m – 150 m and is traveling about 180 degrees, completely opposite of the direction that the wind is blowing. Overall, the net transport of water would be 90 degrees from the original direction of the wind.

Langmuir circulation

Langmuir circulation results in the occurrence of thin, visible stripes, called windrows on the surface of the ocean parallel to the direction that the wind is blowing. If the wind is blowing with more than 3 m s^{-1}, it can create parallel windrows alternating upwelling and downwelling about 5–300 m apart. These windrows are created by adjacent ovular water cells (extending to about 6 m (20 ft) deep) alternating rotating clockwise and counterclockwise. In the convergence zones debris, foam and seaweed accumulates, while at the divergencezones plankton are caught and carried to the surface. If there are many plankton in the divergencezone fish are often attracted to feed on them.

Ocean–atmosphere interface

Hurricane Isabel east of the Bahamas on 15 September 2003

At the ocean-atmosphere interface, the ocean and atmosphere exchange fluxes of heat, moisture and momentum.

Heat

The important heat terms at the surface are the sensible heat flux, the latent heat flux, the incoming solar radiation and the balance of long-wave (infrared) radiation. In general, the tropical oceans will tend to show a net gain of heat, and the polar oceans a net loss, the result of a net transfer of energy polewards in the oceans.

The oceans' large heat capacity moderates the climate of areas adjacent to the oceans, leading to a maritime climate at such locations. This can be a result of heat storage in summer and release in winter; or of transport of heat from warmer locations: a particularly notable example of this is Western Europe, which is heated at least in part by the north atlantic drift.

Momentum

Surface winds tend to be of order meters per second; ocean currents of order centimeters per second. Hence from the point of view of the atmosphere, the ocean can be considered effectively stationary; from the point of view of the ocean, the atmosphere imposes a significant wind stress on its surface, and this forces large-scale currents in the ocean.

Through the wind stress, the wind generates ocean surface waves; the longer waves have a phase velocity tending towards the wind speed. Momentum of the surface winds is transferred into the energy flux by the ocean surface waves. The increased roughness of the ocean surface, by the presence of the waves, changes the wind near the surface.

Moisture

The ocean can gain moisture from rainfall, or lose it through evaporation. Evaporative loss leaves the ocean saltier; the Mediterranean and Persian Gulf for example have strong evaporative loss; the resulting plume of dense salty water may be traced through the Straits of Gibraltar into the Atlantic Ocean. At one time, it was believed that evaporation/precipitation was a major driver of ocean currents; it is now known to be only a very minor factor.

Planetary waves

Kelvin Waves

A Kelvin wave is any progressive wave that is channeled between two boundaries or opposing forces (usually between the Coriolis force and a coastline or the equator). There are two types, coastal and equatorial. Kelvin waves are gravity driven and non-dispersive, meaning that the phase speed of the wave at any one frequency will equal the group speed of the wave energy for all frequencies. This means that Kelvin waves can retain their shape and direction over long periods of time. They are usually created by a sudden shift in the wind, such as the change of the trade winds at the beginning of the El Niño-Southern Oscillation.

Coastal Kelvin waves follow shorelines and will always propagate in a counterclockwise direction in the Northern hemisphere (with the shoreline to the right of the direction of travel) and clockwise in the Southern hemisphere.

Equatorial Kelvin waves propagate to the east in the Northern hemisphere and to the west in the Southern hemisphere, using the equator as a guide.

Kelvin waves are known to have very high speeds, typically around 2–3 meters per second. They have wavelengths of thousands of kilometers and amplitudes in the tens of meters.

Rossby Waves

Rossby waves, or planetary waves are huge, slow waves generated in the troposphere by temperature differences between the ocean and the continents. Their major restoring force is the change in Coriolis force with latitude. Their wave amplitudes are usually in the tens of meters and very large wavelengths. They are usually found at low or mid latitudes

There are two types of Rossby waves, barotropic and baroclinic. Barotropic Rossby waves have the highest speeds and do not vary vertically. Baroclinic Rossby waves are much slower.

The special identifying feature of Rossby waves is that the phase velocity of each individual wave always has a westward component, but the group velocity can be in any direction. Usually the shorter Rossby waves have an eastward group velocity and the longer ones have a westward group velocity.

Climate variability
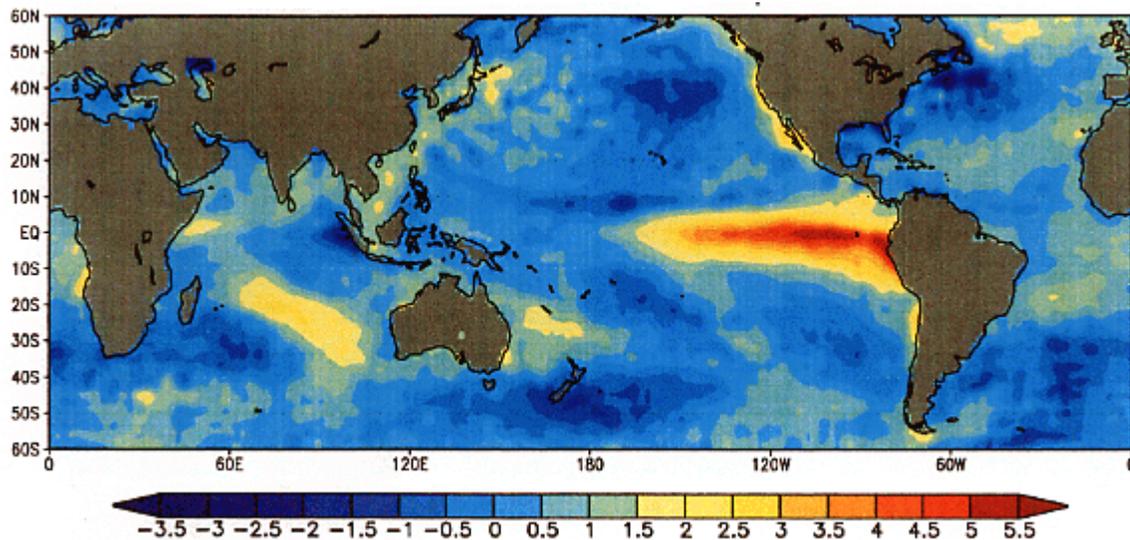
December 1997 chart of ocean surface temperature anomaly [°C] during the last strong El Niño

The interaction of ocean circulation, which serves as a type of heat pump, and biological effects such as the concentration of carbon dioxide can result in global climate changes on a time scale of decades. Known climate oscillations resulting from these interactions, include the Pacific decadal oscillation, North Atlantic oscillation, and Arctic oscillation. The oceanic process of thermohaline circulation is a significant component of heat

redistribution across the globe, and changes in this circulation can have major impacts upon the climate.

La Niña–El Niño

Antarctic circumpolar wave

This is a coupled ocean/atmosphere wave that circles the Southern Ocean about every eight years. Since it is a wave-2 phenomenon (there are two peaks and two troughs in a latitude circle) at each fixed point in space a signal with a period of four years is seen. The wave moves eastward in the direction of the Antarctic Circumpolar Current.

Ocean currents

Among the most important ocean currents are the:

- Antarctic Circumpolar Current
- Deep ocean (density-driven)
- Western boundary currents
    - Gulf Stream
    - Kuroshio Current
    - Labrador Current
    - Oyashio Current
    - Agulhas Current
    - Brazil Current
    - East Australia Current
- Eastern Boundary currents
    - California Current
    - Canary Current
    - Peru Current
    - Benguela Current

Antarctic circumpolar

The ocean body surrounding the Antarctic is currently the only continuous body of water where there is a wide latitude band of open water. It interconnects the Atlantic, Pacific and Indian oceans, and provide an uninterrupted stretch for the prevailing westerly winds to significantly increase wave amplitudes. It is generally accepted that these prevailing winds are primarily responsible for the circumpolar current transport. This current is now thought to vary with time, possibly in an oscillatory manner.

Deep ocean

In the Norwegian Sea evaporative cooling is predominant, and the sinking water mass, the North Atlantic Deep Water (NADW), fills the basin and spills southwards through crevasses in the submarine sills that connect Greenland, Iceland and Britain. It then flows

along the western boundary of the Atlantic with some part of the flow moving eastward along the equator and then poleward into the ocean basins. The NADW is entrained into the Circumpolar Current, and can be traced into the Indian and Pacific basins. Flow from the Arctic Ocean Basin into the Pacific, however, is blocked by the narrow shallows of the Bering Strait.

Western boundary

An idealised subtropical ocean basin forced by winds circling around a high pressure (anticyclonic) systems such as the Azores-Bermuda high develops a gyre circulation with slow steady flows towards the equator in the interior. As discussed by Henry Stommel, these flows are balanced in the region of the western boundary, where a thin fast polewards flow called a western boundary current develops. Flow in the real ocean is more complex, but the Gulf stream, Agulhas and Kuroshio are examples of such currents. They are narrow (approximately 100 km across) and fast (approximately 1.5 m/s).

Equatorwards western boundary currents occur in tropical and polar locations, e.g. the East Greenland and Labrador currents, in the Atlantic and the Oyashio. They are forced by winds circulation around low pressure (cyclonic)

Gulf stream

The Gulf Stream, together with its northern extension, North Atlantic Current, is a powerful, warm, and swift Atlantic ocean current that originates in the Gulf of Mexico, exits through the Strait of Florida, and follows the eastern coastlines of the United States and Newfoundland to the northeast before crossing the Atlantic Ocean.

Kuroshio

The Kuroshio Current is an ocean current found in the western Pacific Ocean off the east coast of Taiwan and flowing northeastward past Japan, where it merges with the easterly drift of the North Pacific Current. It is analogous to the Gulf Stream in the Atlantic Ocean, transporting warm, tropical water northward towards the polar region.

Heat flux

Heat storage

Heat storage and transfer in the ocean is very uneven.

Sea level change

Tide gauges and satellite altimetry suggest an increase in sea level of 1.5–3 mm/yr over the past 100 years.

The IPCC predicts that by 2100, global warming will lead to a sea level rise of 110 to 880 mm.

Rapid variations

Tides

The **Bay of Fundy** is a bay located on the Atlantic coast of North America, on the northeast end of the Gulf of Maine between the provinces of New Brunswick and Nova Scotia.

The rise and fall of the oceans due to tidal effects is a key influence upon the coastal areas. Ocean tides on the planet Earth are created by the gravitational effects of the Sun and Moon. The tides produced by these two bodies are roughly comparable in magnitude, but the orbital motion of the Moon results in tidal patterns that vary over the course of a month.

The ebb and flow of the tides produce a cyclical current along the coast, and the strength of this current can be quite dramatic along narrow estuaries. Incoming tides can also produce a tidal bore along a river or narrow bay as the water flow against the current results in a wave on the surface.

Tide and Current (Wyban 1992) clearly illustrates the impact of these natural cycles on the lifestyle and livelihood of Native Hawaiians tending coastal fishponds. *Aia ke ola ka hana* meaning . . . *Life is in labor*.

Tidal resonance occurs in the Bay of Fundy since the time it takes for a large wave to travel from the mouth of the bay to the opposite end, then reflect and travel back to the mouth of the bay coincides with the timing between this repeating wave that is also reinforced by the tidal rhythm producing the world's highest tides.

As the surface tide oscillates over topography, such as submerged seamounts or ridges, it generates internal waves at the tidal frequency, which are known as internal tides.

Tsunamis

A series of surface waves can be generated due to large-scale displacement of the ocean water. These can be caused by sub-marine landslides, seafloor deformations due to earthquakes, or the impact of a large meteorite.

The waves can travel with a velocity of up to several hundred km/hour across the ocean surface, but in mid-ocean they are barely detectable with wavelengths spanning hundreds of kilometers.

Tsunamis, originally called tidal waves, were renamed because they are not related to the tides. They are regarded as shallow-water waves, or waves in water with a depth less than 1/20 their wavelength. Tsunamis have very large periods, high speeds, and great wave heights.

The primary impact of these waves is along the coastal shoreline, as large amounts of ocean water are cyclically propelled inland and then drawn out to sea. This can result in significant modifications to the coastline regions where the waves strike with sufficient energy.

The tsunami that occurred in Lituya Bay, Alaska on July 9, 1958 was 520 m (1,710 ft) high and is the biggest tsunami ever measured, almost 90 m (300 ft) taller than the Sears Tower in Chicago and about 110 m (360 ft) taller than the World Trade Center in New York.

Surface waves

The wind generates ocean surface waves, which have a large impact on offshore structures, ships, coastal erosion and sedimentation, as well as harbours. After their generation by the wind, ocean surface waves can travel (as swell) over long distances.

Chapter- 2

Ocean Current
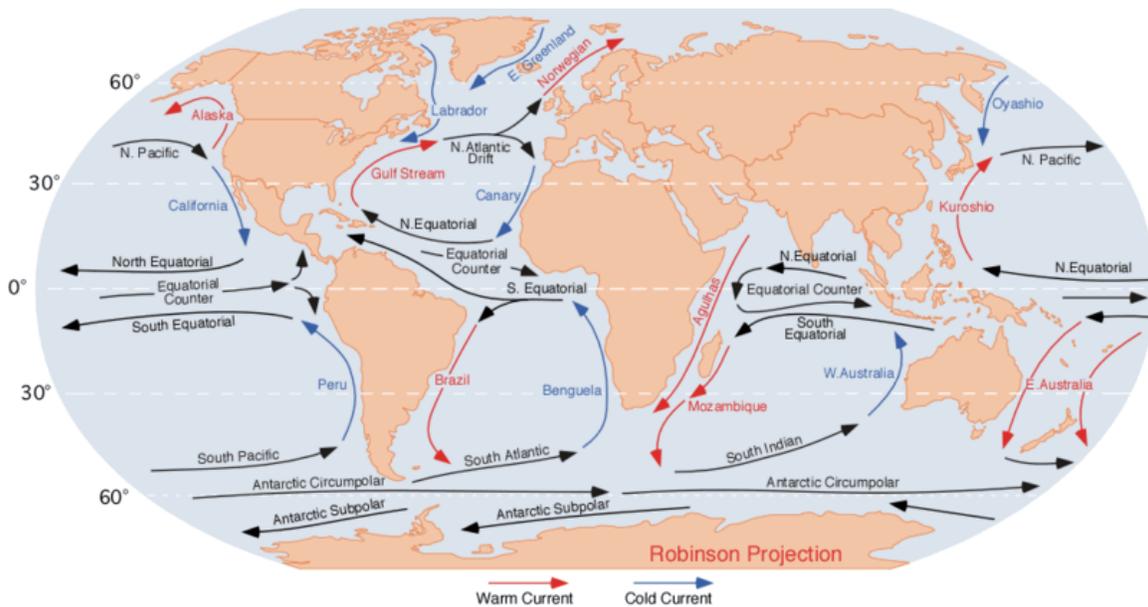
The ocean currents.

An **ocean current** is a continuous, directed movement of ocean water generated by the forces acting upon this mean flow, such as breaking waves, wind, Coriolis force, temperature and salinity differences and tides caused by the gravitational pull of the Moon and the Sun. Depth contours, shoreline configurations and interaction with other currents influence a current's direction and strength.

Ocean currents can flow for great distances, and together they create the great flow of the global conveyor belt which plays a dominant part in determining the climate of many of the Earth's regions. Perhaps the most striking example is the Gulf Stream, which makes northwest Europe much more temperate than any other region at the same latitude. Another example is the Hawaiian Islands, where the climate is cooler (sub-tropical) than the tropical latitudes in which they are located, due to the effect of the California Current.

Function
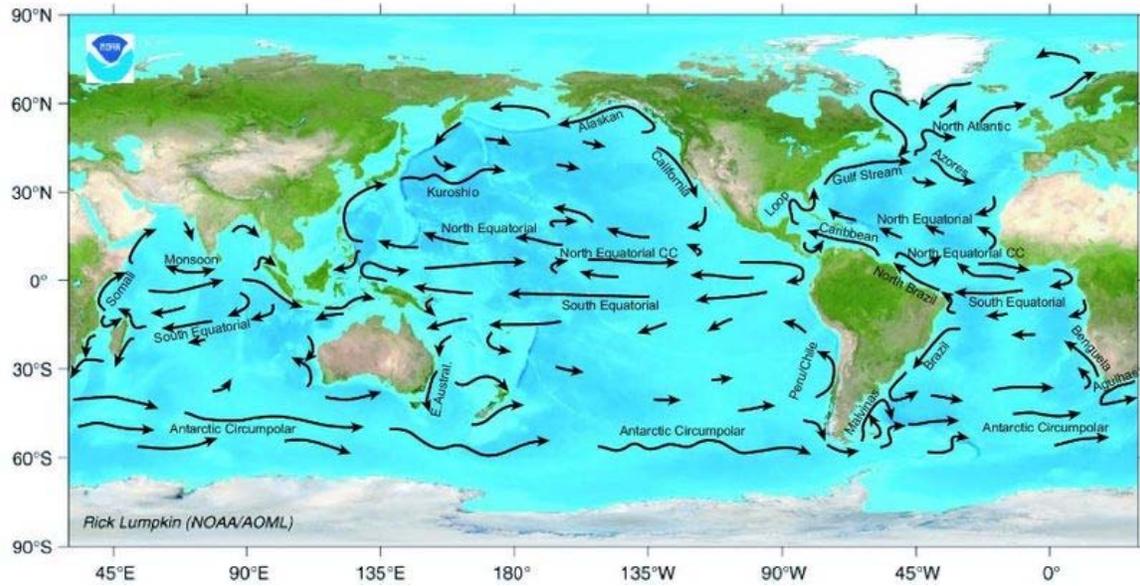
Major ocean surface currents, (Source: NOAA).

Device to record ocean currents.

Surface ocean currents are generally wind driven and develop their typical clockwise spirals in the northern hemisphere and counter-clockwise rotation in the southern hemisphere because of the imposed wind stresses. In wind driven currents, the Ekman spiral effect results in the currents flowing at an angle to the driving winds. The areas of surface ocean currents move somewhat with the seasons; this is most notable in equatorial currents.

Ocean basins generally have a non-symmetric surface current, in that the eastern equatorward-flowing branch is broad and diffuse whereas the western poleward-flowing branch is very narrow. These western boundary currents (of which the gulf stream is an example) are a consequence of basic fluid dynamics.

Deep ocean currents are driven by density and temperature gradients. Thermohaline circulation, also known as the ocean's conveyor belt, refers to the deep ocean density-driven ocean basin currents. These currents, which flow under the surface of the ocean and are thus hidden from immediate detection, are called submarine rivers. These are currently being researched using a fleet of underwater robots called Argo. Upwelling and downwelling areas in the oceans are areas where significant vertical movement of ocean water is observed.

Surface currents make up about 10% of all the water in the ocean. Surface currents are generally restricted to the upper 400 m (1,300 ft) of the ocean. The movement of deep water in the ocean basins is by density driven forces and gravity. The density difference is a function of different temperatures and salinity. Deep waters sink into the deep ocean basins at high latitudes where the temperatures are cold enough to cause the density to increase.

Ocean currents are measured in Sverdrup (Sv), where 1Sv is equivalent to a volume flow rate of 1,000,000 m^3 (35,000,000 cu ft) per second.

Importance
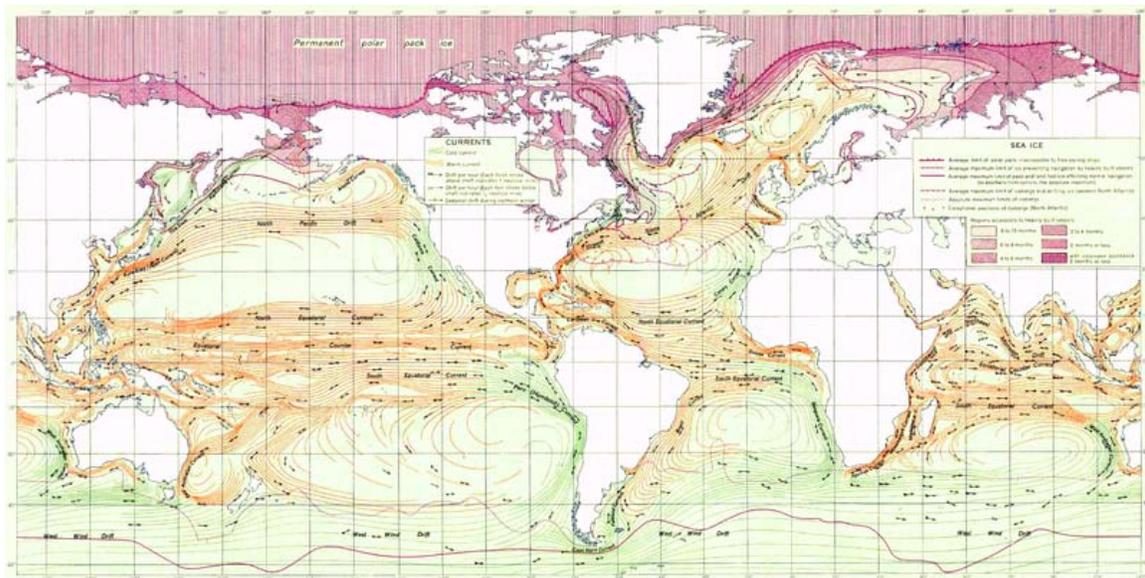
A 1943 map of the world's ocean currents.

Knowledge of surface ocean currents is essential in reducing costs of shipping, since they reduce fuel costs. In the sail-ship era knowledge was even more essential. A good example of this is the Agulhas current, which long prevented Portuguese sailors from reaching India. Even today, the round-the-world sailing competitors employ surface currents to their benefit. Ocean currents are also very important in the dispersal of many life forms. An example is the life-cycle of the eel.

Ocean currents are important in the study of marine debris, and vice versa. These currents also affect temperatures throughout the world. For example, the current that brings warm water up the north Atlantic to northwest Europe stops ice from forming by the shores, which would block ships from entering and exiting ports.

Ocean gyre
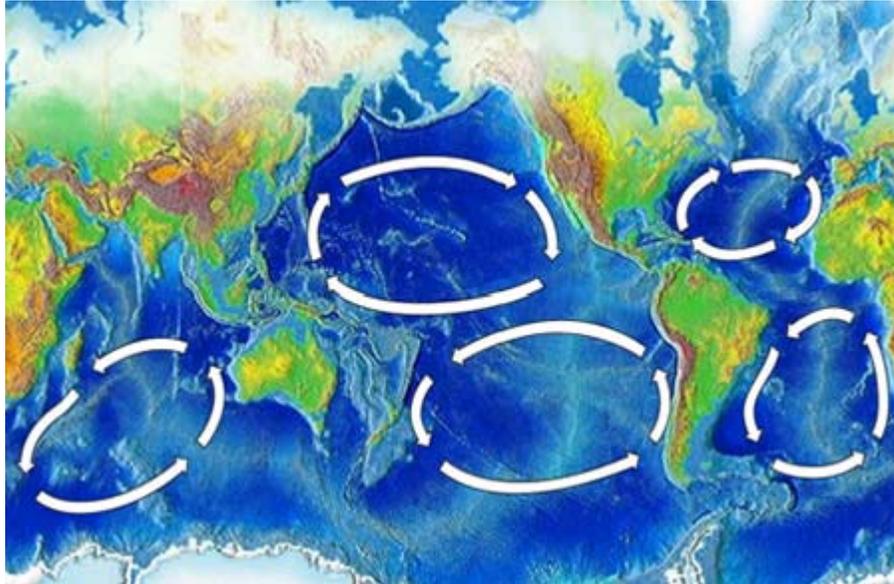
The five major ocean gyres

A **gyre** in oceanography is any large system of rotating ocean currents, particularly those involved with large wind movements. Gyres are caused by the Coriolis Effect; planetary vorticity along with horizontal and vertical friction, which determine the circulation patterns from the wind curl (torque). The term *gyre* can be used to refer to any type of vortex in the air or the sea, even one that is man-made, but it is most commonly used in oceanography, to refer to the major ocean systems.

Major gyres

The following are the five most notable gyres:

- North Atlantic Gyre
- South Atlantic Gyre
- Indian Ocean Gyre
- North Pacific Gyre
- South Pacific Gyre

Description of above five most notable gyres: -
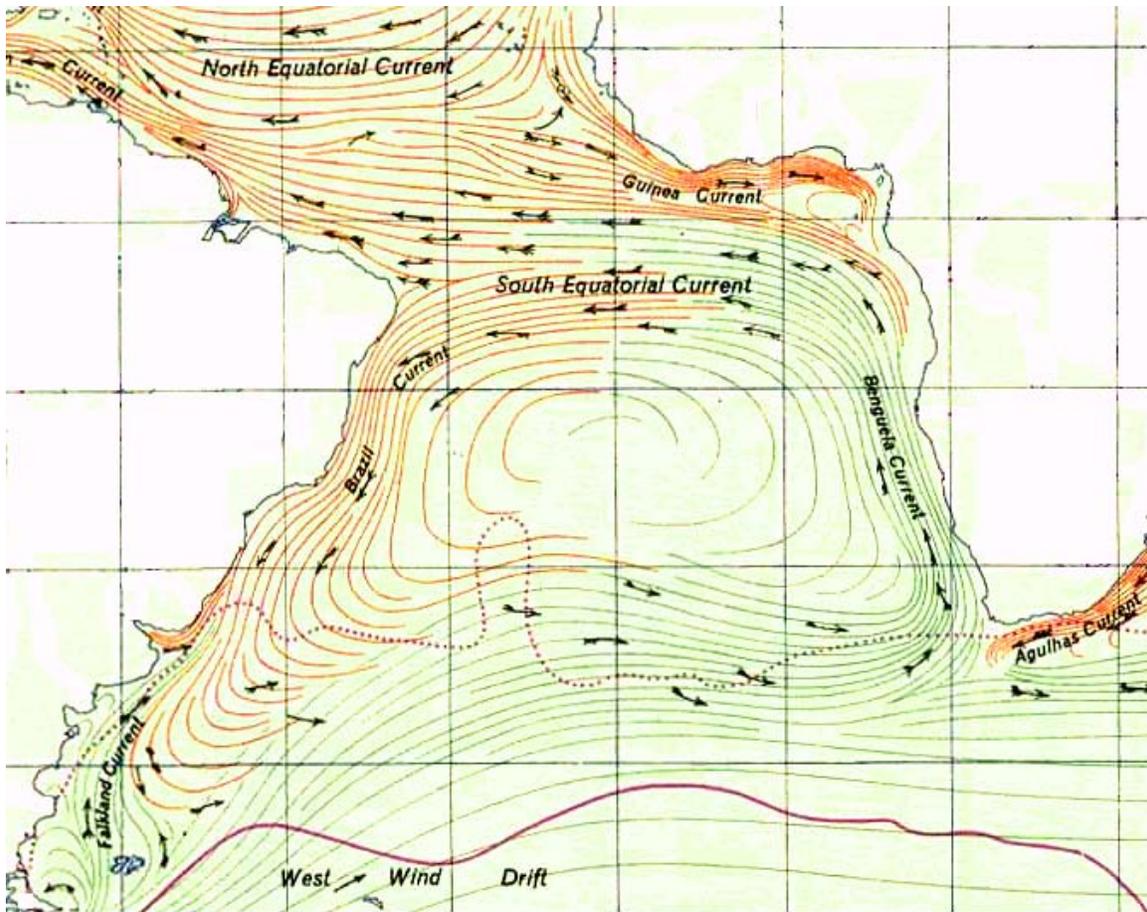
North Atlantic Gyre

The five major oceanic gyres.

The **North Atlantic Gyre**, located in the Atlantic Ocean, is one of the five major oceanic gyres, and contains the Sargasso Sea. This gyre is similar to the North Pacific Gyre by way that this gyre traps man-made ocean debris in the North Atlantic Garbage Patch, similar to the Great Pacific Garbage Patch in the North Pacific.

South Atlantic Gyre

The South Atlantic Gyre.

The **South Atlantic Gyre** is the southern branch of the subtropical gyre in the south Atlantic. This gyre is heavily influenced by northwesterly winds that drive a broad eastward drift, which makes it difficult to distinguish between the northern boundary of the subtropical gyre and the southern boundary of the Antarctic Circumpolar Current.

Southern boundary

South of this gyre is the Antarctic Circumpolar Current. This current flows from West to East around Antarctica. Another name for this current is the West Wind Drift. This current allows Antarctica to maintain its huge ice sheet by keeping warm ocean waters away. At approximately 125Sv, this current is the largest ocean current.

Northern boundary

North of this gyre is the Brazil Current. This current flows south along the south Brazilian coast to the mouth of Rio de la plata. Its a western boundary current, as is the Gulf Stream, but it is considerably weaker.
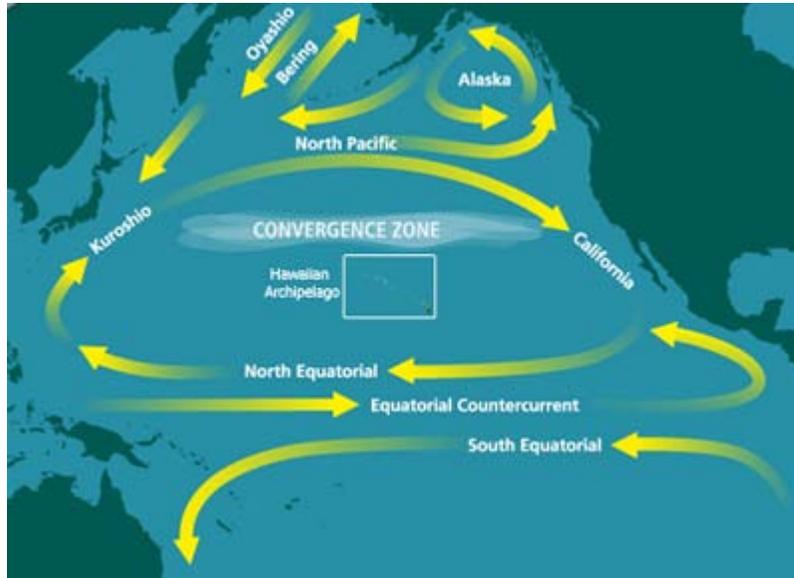
Indian Ocean Gyre
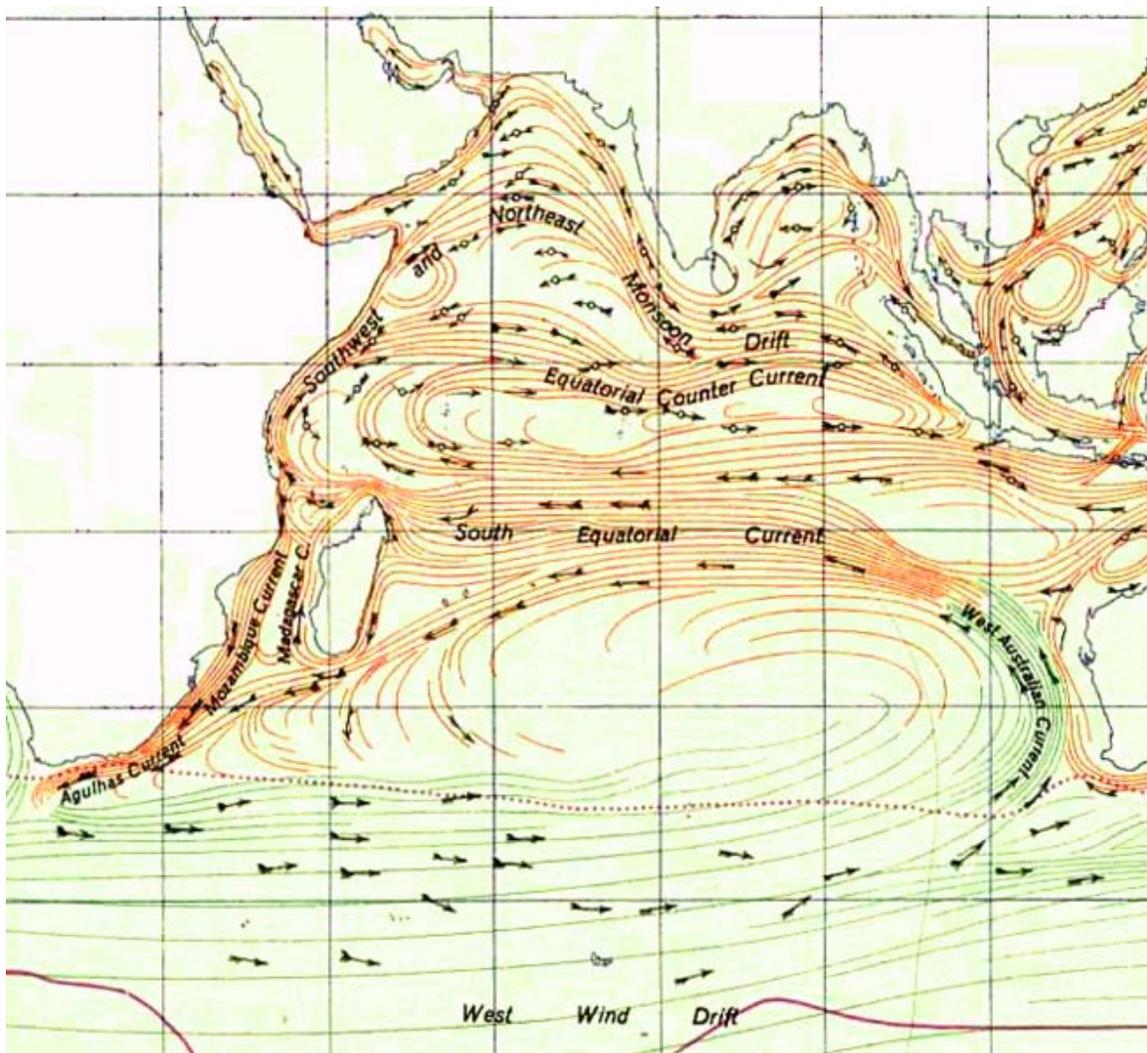
The Indian Ocean Gyre.

The **Indian Ocean Gyre**, located in the Indian Ocean, is one of the five major oceanic gyres.

North Pacific Gyre

The main ocean currents involved with the North Pacific Gyre

The **North Pacific Gyre**, located in the northern Pacific Ocean, is one of the five major oceanic gyres. This gyre comprises most of the northern Pacific Ocean. It is the largest ecosystem on our planet. It is located between the equator and 50° N latitude and occupies an area of approximately 20 million square kilometers. The gyre has a clockwise circular pattern and comprises four prevailing ocean currents: the North Pacific Current to the north, the California Current to the east, the North Equatorial Current to the south, and the Kuroshio Current to the west. It is the site of an unusually intense collection of man-made marine debris, known as the Great Pacific Garbage Patch.

South Pacific Gyre

The **South Pacific Gyre** is the Earth's biggest system of ocean currents, located south of the equator between South America and Australia. It is mostly inactive and contains little marine life.

Sediment
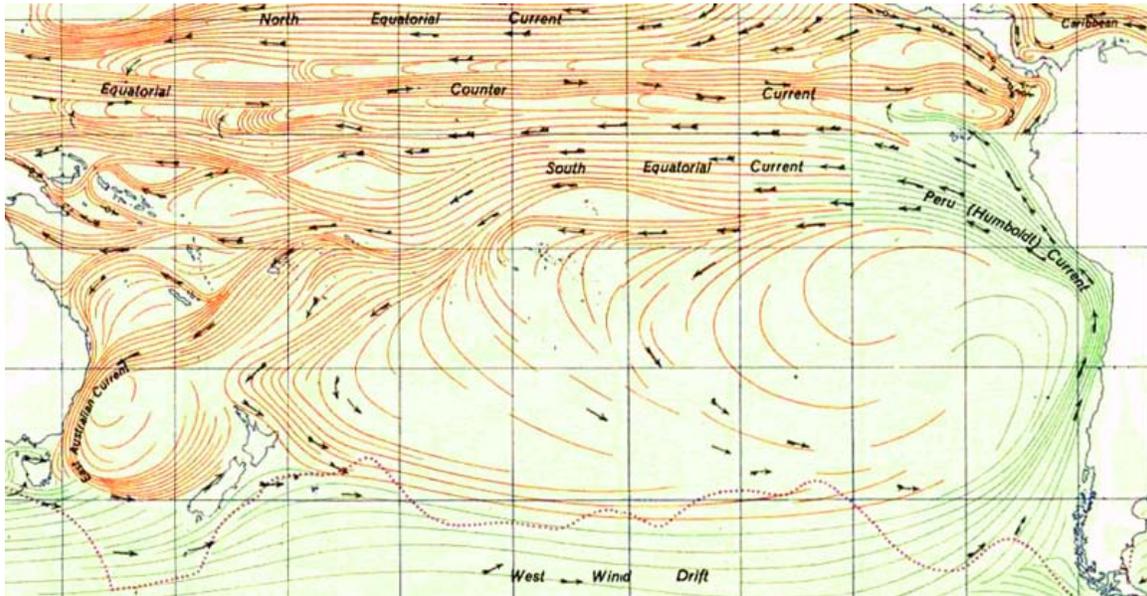
The South Pacific Gyre.

The gyre's sediment accumulates very slowly, approximately 0.1 to 1 m (0.3 to 3.3 ft) every million years. Its ecosystem has very little living matter and contains low amounts of life and has low growth and reproduction rates. At all depths in the gyre's sediment, mean cell abundances and net rates of respiration are several orders of magnitude lower than those of other subseafloor communities at the same depths. Because of the low respiration rates and thin consistency of the sediment in the area, most of the spaces between the sediment columns contain oxygen. This results in the sedimentary community of the SPG generally requiring oxygen to function, unlike previously explored subseafloor communities. Though per-cell, the respiration rates of this community are a couple orders of magnitude higher than in most subseafloor ecosystems living without oxygen, they may soon be decreasing to the approximate rates of the South Pacific Gyre. Sediment from the South Pacific Gyre contains far fewer living cells than other areas. Sediment cores from this area contained a minimum of 1,000 living cells per cubic centimeter, while sediments from closer to the shore can have 1 billion living cells per cubic centimeter, and even areas as far out as the SPG can have 1 million. Little organic matter settles in the sediment of the South Pacific Gyre because the currents around it move so slowly, so the water is very clear.

Water Color

Satellite observations by researchers have shown that some areas in the gyre are greener than the surrounding clear blue water. Their theory is that these green patches are a result of the accumulated waste of marine life. From satellite images, this disintegrated material often looks like living phytoplankton, but the assumed theory that the greener the ocean

water, the more phytoplankton it contains, is not always true. The South Pacific Gyre is an example of this, because it contains these patches of green water, but has very little organism growth.

Other gyres

Tropical gyres
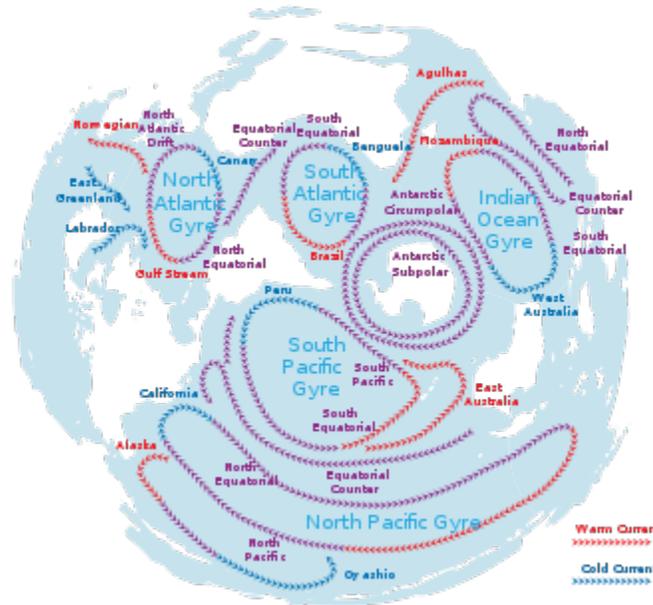
All of the world's larger gyres

Tropical gyres are less unified and tend to be mostly east-west with minor north-south extent.

- Atlantic Equatorial Current System (two counter-rotating circulations)
- Pacific Equatorial Current System
- Indian Monsoon Gyres (two counter-rotating circulations in northern Indian Ocean)

Subtropical gyres

The center of a subtropical gyre is a high pressure zone. Circulation around the high pressure is clockwise in the northern hemisphere and anticlockwise in the southern hemisphere, due to the Coriolis effect. The high pressure in the center is due to the westerly winds on the northern side of the gyre and easterly trade winds on the southern side of the gyre. These cause frictional surface currents towards the latitude at the center of the gyre. The build-up of water in the center of the gyre creates equatorward flow in the upper 1,000 to 2,000 m (3,300 to 6,600 ft) of the ocean, through rather complex

dynamics. This equatorward flow is returned poleward in an intensified western boundary current.

The intensified western boundary current of the North Atlantic Gyre is the Gulf Stream, in the North Pacific it's the Kuroshio Current, in the South Atlantic it's the Brazil Current, in the South Pacific it's the East Australian Current, and in the Indian Ocean it's the Agulhas Current.

Subpolar gyres

Subpolar gyres form at high latitudes (around 60°). Circulation of surface wind and ocean water is anticlockwise in the Northern Hemisphere, around a low-pressure area, such as the persistent Aleutian Low and the Icelandic Low. Surface currents generally move outward from the center of the system. This drives the Ekman transport, which creates an upwelling of nutrient-rich water from the lower depths.

Subpolar circulation in the southern hemisphere is dominated by the Antarctic Circumpolar Current, due to the lack of large landmasses breaking up the Southern Ocean. There are minor gyres in the Weddell Sea and the Ross Sea, the Weddell Gyre and Ross Gyre, which circulate in a clockwise direction.

Chapter- 3

Antarctic Circumpolar Current
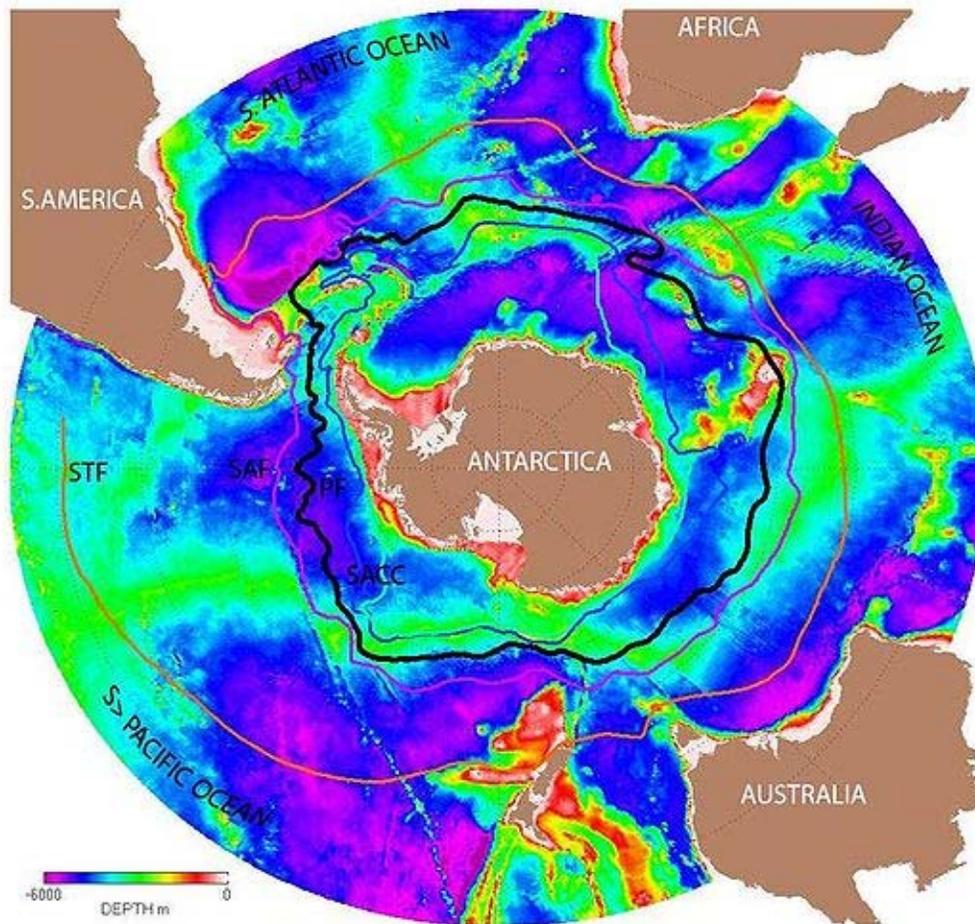
ANTARCTIC CIRCUMPOLAR CURRENT
SEAWATER DENSITY FRONTS (FROM ORSI et al, 1995),
AND BATHYMETRY OF THE SOUTHERN OCEAN (UP TO LATITUDE 25 S)

The Antarctic Circumpolar Current (ACC) is the strongest current system in the world oceans, the one that links the Atlantic, Indian and Pacific basins.

The **Antarctic Circumpolar Current (ACC)** is an ocean current that flows from west to east around Antarctica. An alternative name for the ACC is the **West Wind Drift**. The ACC is the dominant circulation feature of the Southern Ocean and, at approximately 125 Sverdrups, the largest ocean current. It keeps warm ocean waters away from Antarctica, enabling that continent to maintain its huge ice sheet.

The ACC has been known to sailors for centuries; it greatly speeds up any voyages from west to east, but makes sailing extremely difficult from east to west; though this is mostly due to the prevailing westerly winds. The circumstances preceding the Mutiny on the Bounty and Jack London's story "Make Westing" poignantly illustrated the difficulty it caused for mariners seeking to round Cape Horn on the clipper ship route between New York and California. The clipper route, which is the fastest sailing route around the world, follows the ACC around three continental capes - Cape of Good Hope (Africa), Southeast Cape (Australia) and Cape Horn (South America).

The current creates two Antarctic gyres.

Structure

The ACC connects the Atlantic, Pacific and Indian Ocean basins, and as such serves as a principal pathway of exchange between these basins. The current is strongly constrained by landform and bathymetric features. Starting at South America, it flows through the Drake Passage between South America and the Antarctic Peninsula and then is split by the Scotia Arc to the east, with a shallow warm branch flowing to the north in the Falkland Current and a deeper branch passing through the Arc more to the east before also turning to the north. Passing through the Indian Ocean, the current is split by the Kerguelen Plateau in the Indian Ocean, and then moving northward again. Deflection is also seen as it passes over the mid-ocean ridge in the Southeast Pacific.

The current consists of a number of fronts. The northern boundary of the ACC is defined by the Subtropical Front. This marks the boundary between warm, salty subtropical waters (generally with a salinity of greater than 34.9 parts per thousand) and fresher, cooler subpolar waters. Moving southward we find the Subantarctic Front, along which much of the ACC transport is carried, which is defined as the latitude at which a subsurface salinity minimum or a thick layer of unstratified Subantarctic Mode Water first appears. Still further south lies the Polar Front, which is marked by a transition to very cold, relatively fresh, Antarctic Surface Water at the surface. Further south still is the Southern Boundary front, which is determined as the point where very dense abyssal waters upwell to within a few hundred meters of the surface. The bulk of the transport is carried in the middle two fronts. The total transport of the ACC at Drake Passage is estimated to be around 135 Sverdrups (135,000,000 m³/s), or about 135 times the transport of all the world's rivers combined. There is a relatively small addition of flow in the Indian Ocean, with the transport south of Tasmania reaching around 147 Sv, at which point the current is probably the largest on the planet.

Dynamics

The Circumpolar Current is driven by the strong westerly winds which are found in the latitudes of the Southern Ocean.

In latitudes where there are continents, winds blowing on light surface water can simply pile up light water against these continents. But in the Southern Ocean, the momentum imparted to the surface waters cannot be balanced in this way. Different theories of the Circumpolar Current balance the momentum imparted by the winds in different ways. The increasing eastward momentum imparted by the winds causes water parcels to drift outwards from the axis of the Earth's rotation (in other words, northward) as a result of the Coriolis force. This northward transport is balanced by a southward, pressure-driven flow below the depths of the major ridge systems. Some theories connect these flows directly, implying that there is significant upwelling of dense deep waters within the Southern Ocean, transformation of these waters into light surface waters, and a transformation of waters in the opposite direction to the north. Such theories link the magnitude of the Circumpolar Current with the global thermohaline circulation, particularly the properties of the North Atlantic.

Alternatively, ocean eddies, the oceanic equivalent of atmospheric storms, or the large scale meanders of the Circumpolar Current may directly transport momentum downwards in the water column. This is because such flows can produce a net southward flow in the troughs and a net northward flow over the ridges without requiring any transformation of density. In practice both the thermohaline and the eddy/meander mechanisms are likely to be important.

The current flows at a rate of about four km per hour. Recent studies have indicated that the Antarctic Circumpolar Current varies with time. Evidence of this is the Antarctic Circumpolar Wave, a periodic oscillation that affects the climate of much of the southern hemisphere. There is also the Antarctic oscillation, which involves changes in the location and strength of Antarctic winds. Trends in the Antarctic Oscillation have been hypothesized to account for an increase in the transport of the Circumpolar Current over the past two decades.

Formation

Published estimates of the onset of the Antarctic Circumpolar Current vary, but it is commonly considered to have started at the Eocene/Oligocene boundary. The isolation of Antarctica and formation of the ACC occurred with the openings of the Tasmanian Seaway and the Drake Passage. The Tasmanian Seaway separates East Antarctica and Australia, and is reported to have opened to water circulation 33.5 Ma. The timing of the opening of the Drake Passage, between South America and the Antarctic Peninsula, is more disputed. Tectonic and sediment evidence show that it could have been open as early as pre 34 Ma, estimates of the opening of the Drake passage are between 20 and 40 Ma. The isolation of Antarctica by the current is credited by many researchers with

causing the glaciation of Antarctica and global cooling in the Miocene Period. Oceanic models have shown that the opening of these two passages limited polar heat convergence and caused a cooling of sea surface temperatures by several degrees, other models have shown that CO_2 levels also played a significant role in the glaciation of Antarctica.

Phytoplankton

Antarctic sea ice cycles seasonally, in February-March the amount of sea ice is lowest, and in August-September the sea ice is at its greatest extent. Ice levels have been monitored by satellite since 1973. Upwelling of deep water under the sea ice brings substantial amounts of nutrients. As the ice melts, the melt water provides stability and the critical depth is well below the mixing depth, which allows for a positive net primary production. As the sea ice recedes epontic algae dominate the first phase of the bloom, and a strong bloom dominate by diatoms follows the ice melt south .

Another phytoplankton bloom occurs more to the north near the antarctic convergence, here nutrients are present from thermohaline circulation. Phytoplankton blooms are dominated by diatoms and grazed by copepods in the open ocean, and by krill closer to the continent. Diatom production continues through the summer, and populations of krill are sustained, bringing large stocks of whales, seals, and fish to the area .

Phytoplankton blooms are believed to be limited by irradiance in the austral (southern hemisphere) spring, and by biologically available iron in the summer. Much of the biology in the area occurs along the major fronts of the current, the Subtropical, SubAntarctic, and the Antarctic Polar fronts, these are areas associated with well defined temperature changes. Size and distribution of phytoplankton are also related to fronts. Microphytoplankton ($>20\mu m$) are found at fronts and at sea ice boundaries, while nanophytoplankton ($<20\mu m$) are found between fronts.

Studies of phytoplankton stocks in the southern sea have shown that the Antarctic Circumpolar Current is dominated by diatoms, while the Weddell Sea has abundant coccolithophorids and silicoflagellates. Surveys of the SW Indian Ocean have shown phytoplankton group variation based on their location relative to the Polar Front, with diatoms dominating South of the front, and dinoflagellates and flagellates in higher populations North of the front

Some research has been done on Antarctic phytoplankton as a carbon sink. Areas of open water left from ice melt are good areas for phytoplankton blooms. The phytoplankton takes carbon from the atmosphere during photosynthesis. As the blooms die and sink, the carbon can be stored in sediments for thousands of years. This natural carbon sink is estimated to remove 3.5 million tonnes from the ocean each year. 3.5 million tonnes of carbon taken from the ocean and atmosphere is equivalent to 12.8 million tonnes of carbon dioxide.

Studies

An expedition in May 2008 by 19 scientists studied the geology and biology of eight Macquarie Ridge sea mounts, as well as the Antarctic Circumpolar Current to investigate the effects of climate change of the southern Ocean. The circumpolar current merges the waters of the Atlantic, Indian, and Pacific Oceans and carries up to 150 times the volume of water flowing in all of the world's rivers. After studying the circumpolar current it is clear that it strongly influences regional and global climate as well as underwater biodiversity.

Western Boundary Currents

Kuroshio Current
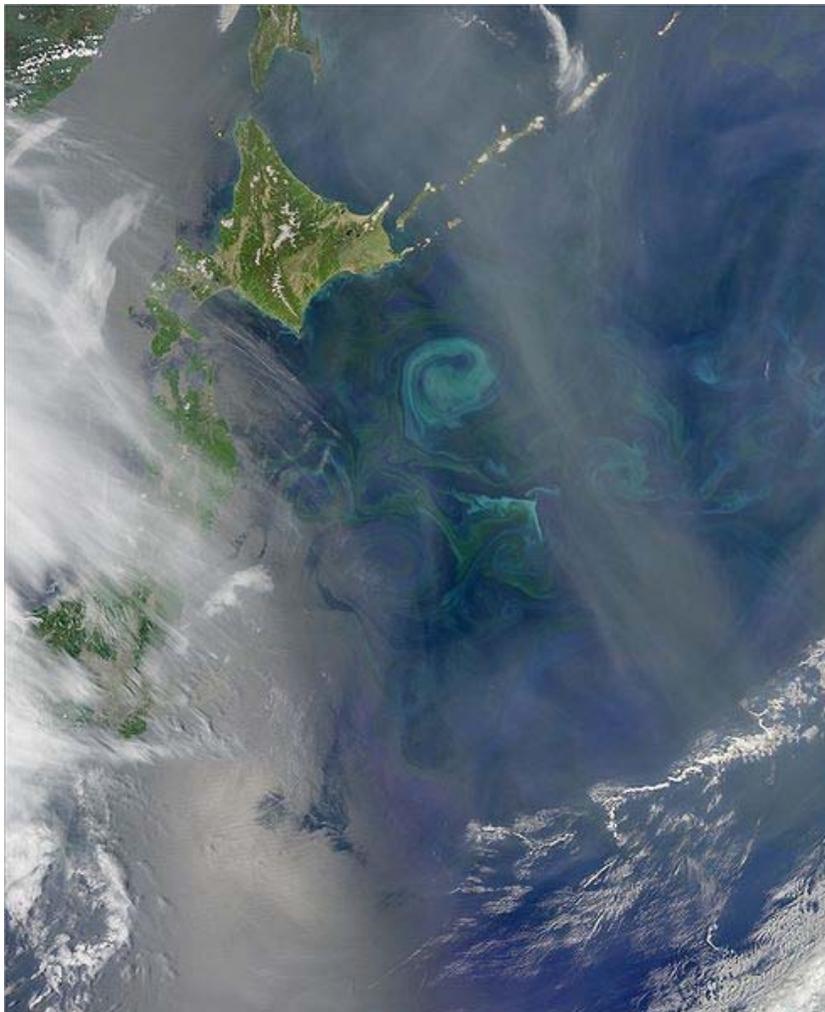
The Oyashio Current colliding with the Kuroshio Current near Hokkaido. When two currents collide, they create eddies. Phytoplankton growing in the surface waters become concentrated along the boundaries of these eddies, tracing out the motions of the water.
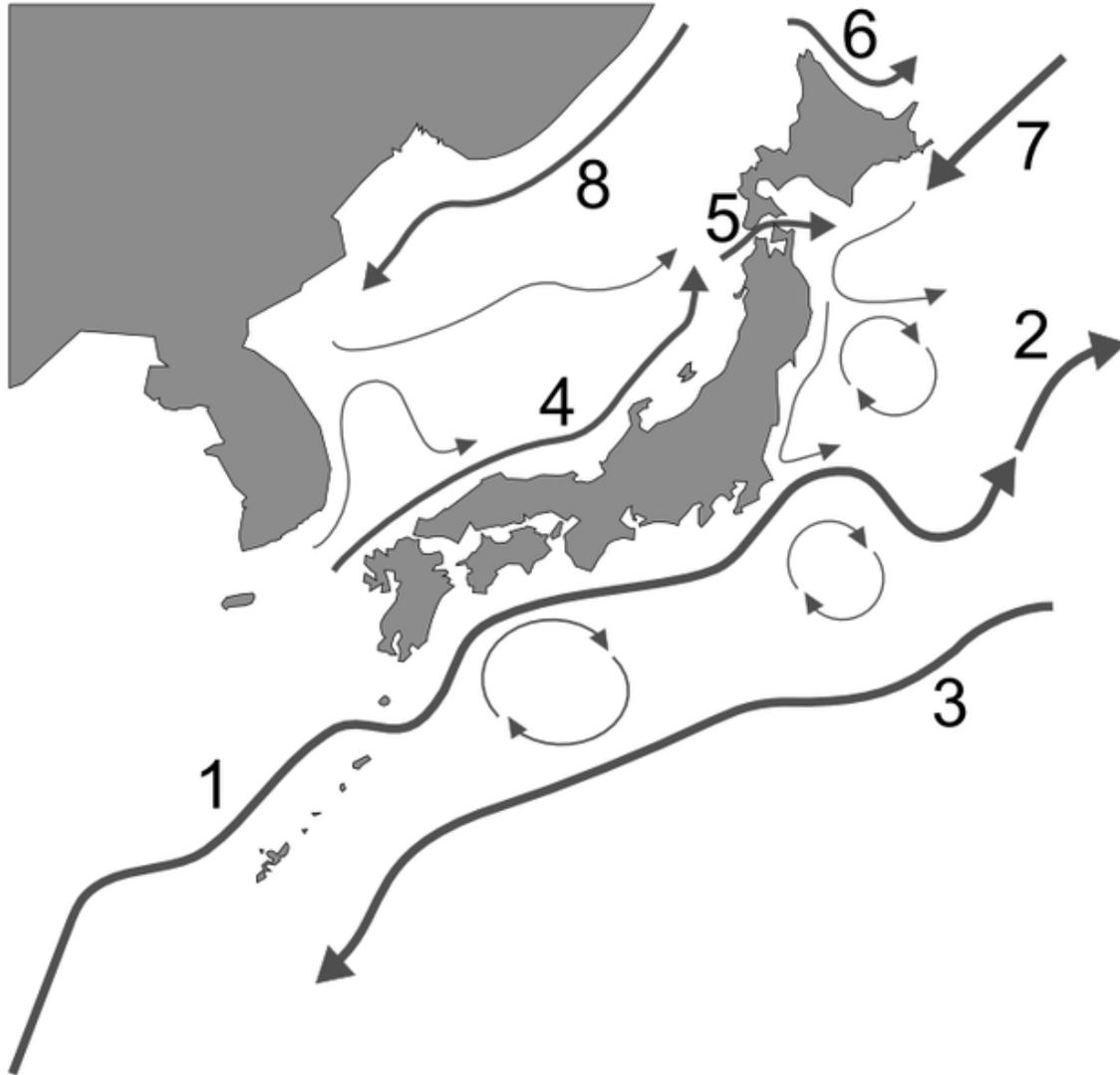
The ocean currents surrounding the Japanese Archipelago: **1. Kuroshio** 2.Kuroshio extension 3. Kuroshio countercurrent 4. The Tsushima Current 5. The Tsugaru Current 6. The Sōya Current 7. Oyashio 8. The Liman Current

Physical properties

The **Kuroshio** is a strong western boundary current in the western north Pacific Ocean. It begins off the east coast of Taiwan and flows northeastward past Japan, where it merges with the easterly drift of the North Pacific Current. It is analogous to the Gulf Stream in the Atlantic Ocean, transporting warm, tropical water northward towards the polar region. It is also sometimes known as the *Black Stream* — the English translation of *kuroshio*, and an allusion to the deep blue of its water—and also as the "Japan Current" (日本海流 *Nihon Kairyū* ˀ).

The path of Kuroshio south of Japan is reported every day. Its counterparts are the North Pacific Current to the north, the California Current to the east, and the North Equatorial Current to the south. The warm waters of the Kuroshio Current sustain the coral reefs of Japan, the northernmost coral reefs in the world. The branch into the Sea of Japan is called **Tsushima Current** (対馬海流 *Tsushima Kairyū* ?). The Japan Current is also responsible for the mild weather experienced around Alaska's southern coast and in British Columbia.

Biological properties

Distribution

Western boundary currents transport organisms long distances rapidly and a variety of commercially important marine organisms migrate in these currents in the course of completing their life histories . Subtropical gyres occupy a large fraction of the world's ocean and are more productive than originally thought. In addition, their fixation of carbon dioxide is an important factor in the global budget for carbon dioxide in the atmosphere.

Satellite images of the **Kuroshio Current** illustrates how the current path meanders and forms isolated rings or eddies on the order of 100–300 km. Eddies retain their unique form for several months and have their own biological characteristics that depend on where they form. If the eddies are formed between the current and coastline of Japan, they may impinge on the continental shelf and their high kinetic energy has the effect of drawing large volumes of water off the shelf on one side of the ring, while adding water to the other side. Eddies size and strength decline with distance from major ocean currents. The amount of energy decreases from the rings associated with the major currents and down to eddies remote from those currents. Cyclonic eddies have the potential to cause upwelling that would affect the global primary-production budget . Upwelling brings cold, nutrient rich water to the surface resulting in an increase in productivity. The biological consequences for young fish populations that inhabit the shelf are quite large.

Production

Impact of eddies

The Kuroshio is a warm current (24°C annual average sea surface temperature), about 100 km wide and produces frequent small to meso-scale eddies. The Kuroshio Current is ranked as a moderately high productivity ecosystem (150-300 $gCm^{-2}y^{-1}$) based on SeaWiFs global primary productivity estimates. The coastal areas are highly productive and the maximum chlorophyll value is found around 100 meters depth .

There are indications that eddies contribute to the preservation and survival of fish larvae transported by the Kuroshio . Plankton biomass fluctuates yearly and is typically highest

in the eddy area of the Kuroshio's edge. Warm-core rings are not known for having high productivity. However, the biology of the warm-core rings from the Kuroshio Current show results of productivity equally distributed throughout for a couple of reasons. One is upwelling at the periphery and two, the convective mixing caused by the cooling of surface water as the ring moves north of the current. The thermostad is the deep mixed layer that has discrete boundaries and uniform temperature. Within this layer, nutrient-rich water is brought to the surface, which generates a burst of primary production. Given that the water in the core of a ring has a different temperature regime than the shelf waters, there are times when a warm-core ring is undergoing its spring bloom while the surrounding shelf waters are not.

There are many complex interactions with the warm-core ring and thus lifetime productivity is not very different from the surrounding shelf water. A study in 1998 found that the primary productivity within a warm-core ring was almost the same as in the cold jet outside it, with evidence of upwelling of nutrients within the ring. In addition, there was discovery of dense populations of phytoplankton at the nutricline within a ring, presumably supported by upward mixing of nutrients. Furthermore, there have been acoustic studies in the warm-core ring, which showed intense sound scattering from zooplankton and fish populations within the ring and very sparse acoustic signals outside of it.

Copepods have been used as indicator-species of water masses. It has been suggested that copepods have been transported from the Kuroshio Current into southwest Taiwan through the Luzon Strait . The Kuroshio intrusion through the Luzon Strait and further into the South China Sea may also explain why copepods show a very high diversity in adjacent waters of the intrusion areas. The Kuroshio Current intrusion has a major influence on *C. sinicus* and *E. concinna*, which are two copepod species with higher index values for winter and originate from the East China Sea. During the SW monsoon, the South China Sea Surface Current moves northwards during the summer towards the Kuroshio Current. As a result of this water circulation, the zooplankton communities in the boundary waters are unique and diverse.

Fish

The biomass of fish stocks depends on the biomass of lower trophic levels, primary production and on oceanic and atmospheric conditions . In the Kuroshio-Oyashio region, the fish catches depend on oceanographic conditions, such as the Oyashio's southward intrusion and the Kuroshio's large meander south of Honshu. The Oyashio Current contains subarctic water that is much colder and fresher than the resident water east of Honshu. Thus, the Oyashio intrusion affects recruitment, biomass, and catch of species such as Pollock, sardine, and anchovy. When the Oyashio is well developed and protrudes southward, the cold waters are favorable for sardine production. The Kuroshio large meander development correlates with sardine recruitment and catch due to the proximity of the Kuroshio meander to the southern spawning grounds of sardine.

Squid

The Japanese squid *Todarodes Pacificus* has three stocks that breed at different seasons: winter, summer, and autumn. The winter spawning group is associated with the Kuroshio Current. After spawning in the period of January to April in the East China Sea, the larvae and juveniles travel north with the Kuroshio Current. They are turned inshore and are caught between the islands of Honshu and Hokkaido during the summer. The summer spawning is in another part of the East China Sea, from which the larvae are entrained into the Tsushima current that flows north between the islands of Japan and the mainland. Afterward, the current meets a southward flowing cold coastal current, the Liman Current, and the summer-spawned squid are fished along the boundary between the two. This illustrates the use of these western boundary currents as a rapid transport that enable the eggs and larvae to develop during winter in warm water, while the adults travel north with minimum energy expenditure to exploit the rich feeding grounds further north. Studies have reported that annual catches in Japan have gradually increased since the late 1980s and it has been proposed that changing environmental conditions have caused the autumn and winter spawning areas in the Tsushima Strait and near the Goto Islands to overlap . In addition, winter spawning sites over the continental shelf and slope in the East China Sea are expanding.

Labrador Current

Photo of edies in the Labrador Current
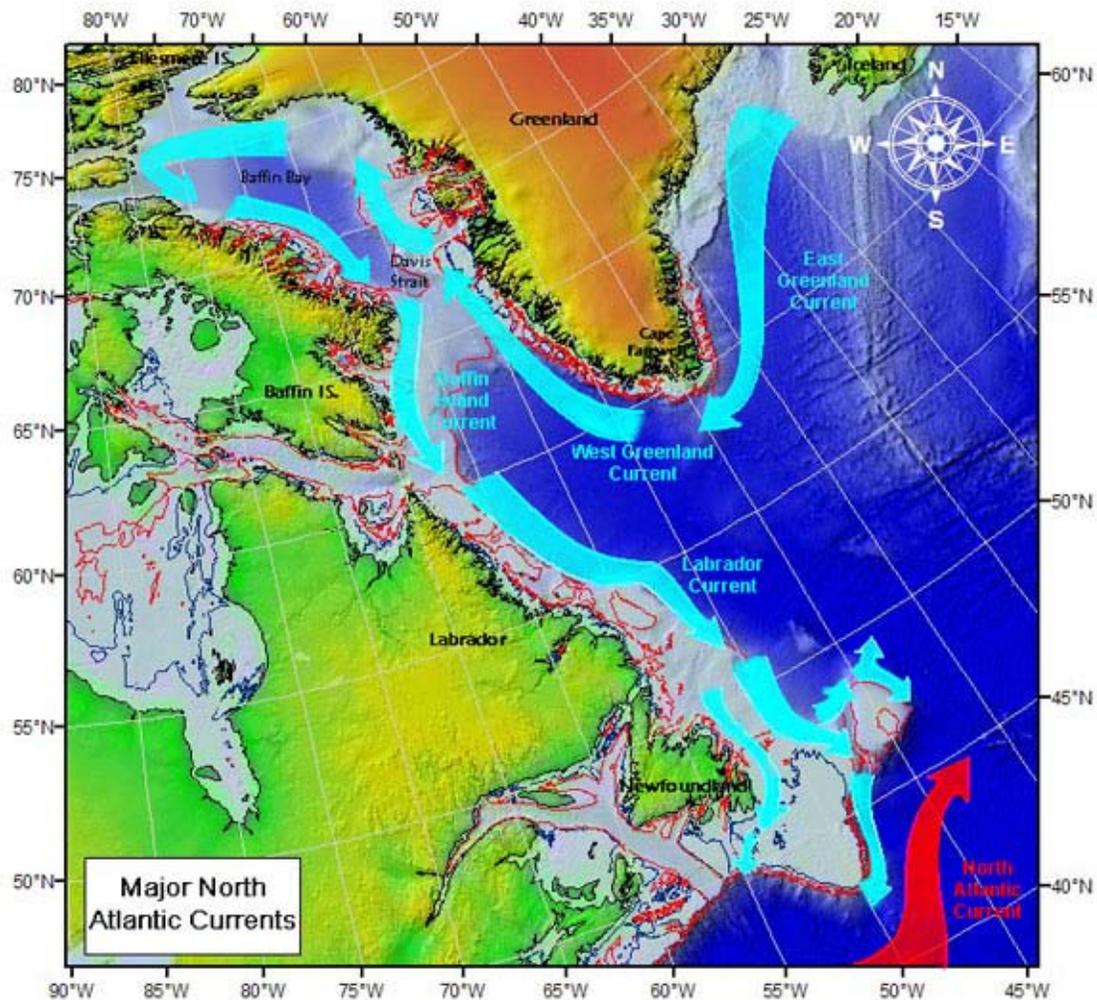
Map of Labrador Current

The **Labrador Current** is a cold current in the North Atlantic Ocean which flows from the Arctic Ocean south along the coast of Labrador and passes around Newfoundland, continuing south along the east coast of Nova Scotia. It is a continuation of the West Greenland Current and the Baffin Island Current.

It meets the warm Gulf Stream at the Grand Banks southeast of Newfoundland and again north of the Outer Banks of North Carolina. The combination of these two currents produces heavy fogs and also created one of the richest fishing grounds in the world.

In spring and early summer, this current transports icebergs from the glaciers of Greenland southwards into the trans-Atlantic shipping lanes.

The waters of the Labrador Current have a cooling effect on the Canadian Atlantic provinces and coastal New England, but rarely have a significant effect on waters south of Cape Cod. This can most clearly be seen in the fact that the northern limit of tree growth can be as much as *fifteen degrees* farther south than in Siberia, Europe or western Canada.

The transport of the Labrador Current is believed to contain a large barotropic component. Early estimates indicated that the current may be 30% stronger than geostrophic calculations indicated as a result of a significant barotropic flow component (Hayes and Robe, 1978). Greenberg and Petrie (1988) calculated a total transport of 7.6 Sverdrup. (One Sverdrup (Sv) is equal to 10^6 cubic meters per second.) The geostrophic transport was calculated to be just 4.1 Sv (based on IIP sections). With a 30% increase (due to barotropic flow) the transport is only 5.3 Sv so, the high transport values are thought to largely from the inclusion of deep currents indicated by a deep water mooring. Speeds for the Labrador Current are about 0.3–0.5 m/s along the shelf edge (Greenbergand Petrie, Reynaud et al., 1985. Current speeds of 0.3–0.5 m/s were found by Reynaud et al. (1995) for the Labrador Current. Including the barotropic component, they estimate a value of 3 Sv for the continental shelf branch of the Labrador Current and 16 Sv transport for the slope branch of the Labrador Current. The inshore branch of the Labrador Current is approximately 100 km wide and 150 m deep and it passes through Avalon Channel and the splitting of the Labrador Current around Flemish Cap can be seen in the tracks of satellite tracked drifters (Petrie and Isenor). Within the Flemish Pass, Petrie and Isenor (1985) report that the width of the Labrador Current is reduced to 50 km with a speed of 0.25 m/s which they believe is actually 0.30 m/s.

The Labrador Current has a tendency to sometimes go farther south and/or east than normal. This can make it very hazardous to ships as it can carry icebergs into an area of the Atlantic where they are not usually found. The current has been known to transport icebergs as far south as Bermuda and as far east as the Azores. The International Ice Patrol was set up to track icebergs, including those found in areas of the ocean where they are rarely located. .

Oyashio Current
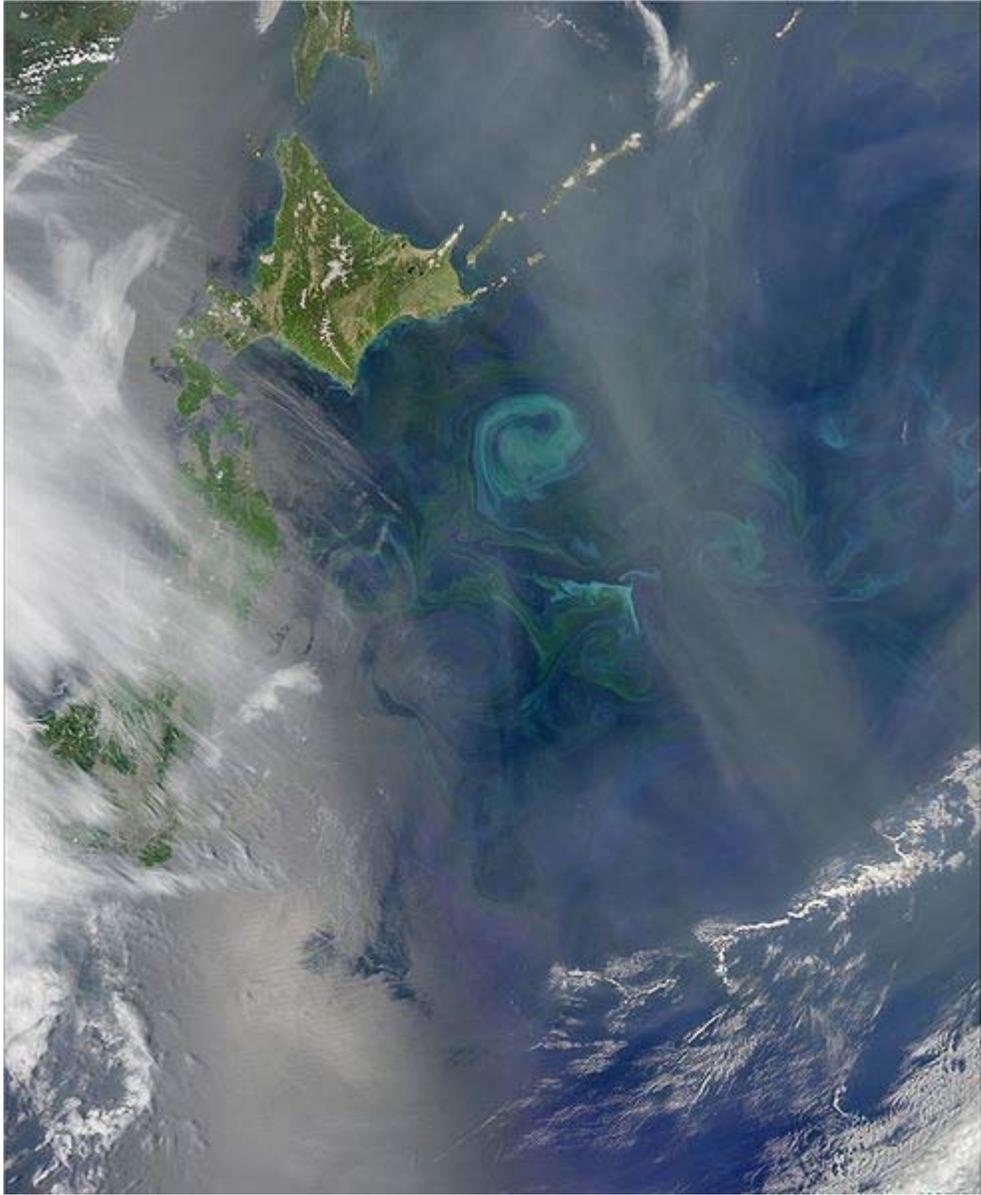
The Oyashio Current colliding with the Kuroshio Current near Hokkaido. When two currents collide, they create eddies. Phytoplankton growing in the surface waters become concentrated along the boundaries of these eddies, tracing out the motions of the water.
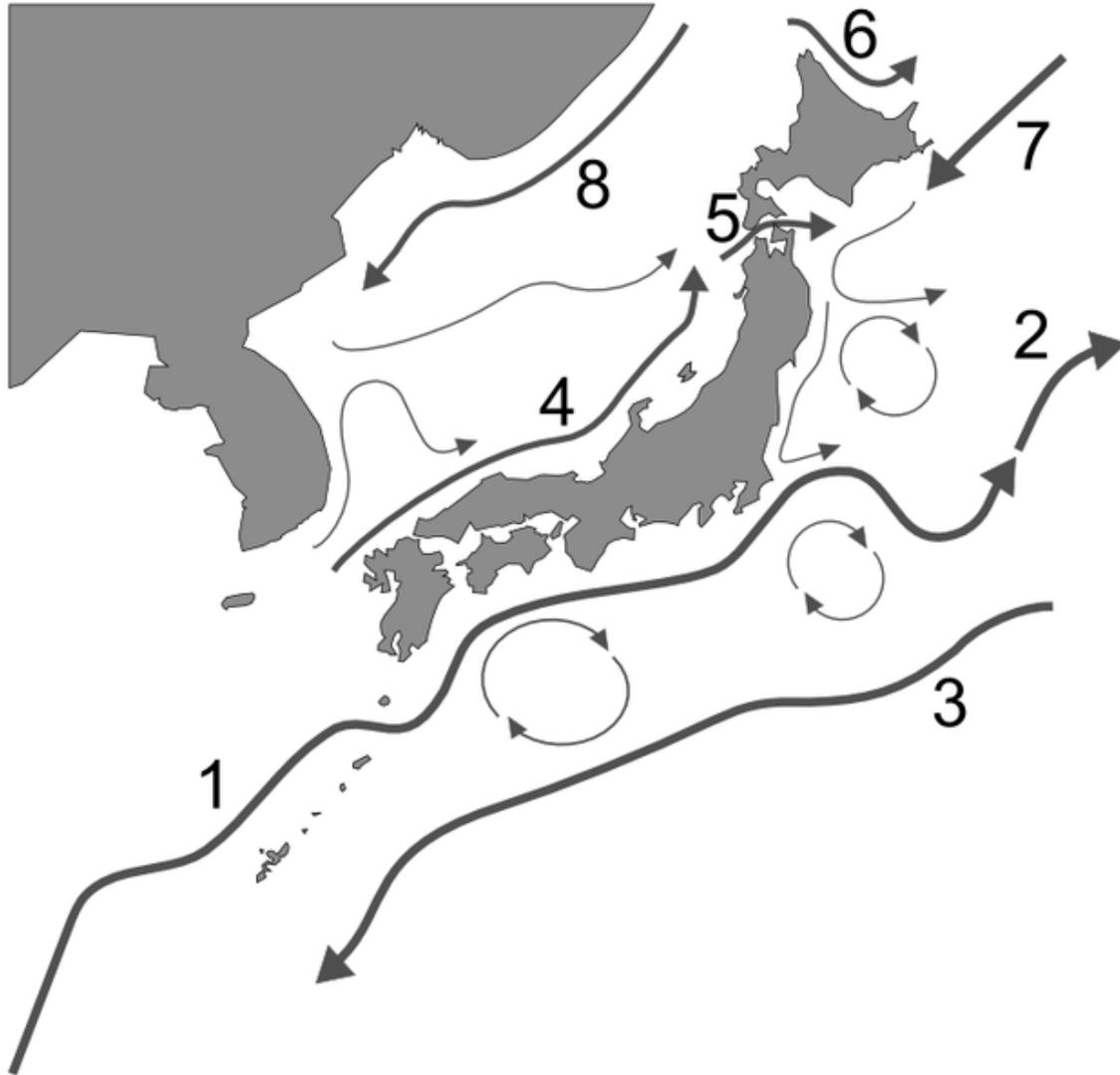
The ocean currents surrounding the Japanese Archipelago: 1.Kuroshio 2. Kuroshio extension 3. Kuroshio countercurrent 4. The Tsushima Current 5. The Tsugaru Current 6. The Sōya Current 7. **Oyashio** 8. The Liman Current

Oyashio (親潮?), also known as **Oya Siwo**, **Okhotsk** or the **Kurile** current, is a cold subarctic ocean current that flows south and circulates counterclockwise in the western North Pacific Ocean. It collides with the Kuroshio Current off the eastern shore of Japan to form the North Pacific Current (or Drift). This cold current flows through Bering Strait in the southern direction and transports cold water of the Arctic Sea into the Pacific ocean. The waters of the Oyashio Current originate in the Arctic Ocean and flow southward via the Bering Sea. The current has an important impact on the climate of the Russian Far East, mainly in Kamchatka and Chukotka, where the northern limit of tree growth is moved up to ten degrees south of the latitude it can reach in inland Siberia. The waters of the Oyashio Current form probably the richest fishery in the world owing to the extremely high nutrient content of the cold water and the very high tides (up to ten metres) in some areas - which further enhances the availability of nutrients. However, the

Oyashio Current also causes Vladivostok to be the most equatorward port to seasonally freeze and require icebreaking ships to remain open in winter. Nonetheless, this has relatively little effect on the fish yield through the Sea of Okhotsk because the large tides mean freezing does not occur so easily.

Another important feature of the Oyashio Current is that during glacial periods, when lower sea level causes the formation of the Bering land bridge, the current cannot flow and in the regions the Oyashio affects today, the level of cooling with the onset of glacial conditions (after an interglacial) is much less than in other areas of the Earth at similar latitudes. This allowed Tōhoku and Hokkaidō, which were the only areas of East Asia that receive enough snowfall to potentially form glaciers, to remain unglaciated except at high elevations during periods when Europe and North America were largely glaciated. This lack of glaciation explains why, despite its present climate being much colder than most of Europe, East Asia has retained 96 percent of Pliocene tree genera, whereas Europe has retained only 27%.

Agulhas Current

The **Agulhas Current** is the Western Boundary Current of the southwest Indian Ocean. It flows down the east coast of Africa from 27°S to 40°S. It is narrow, swift and strong. It is even suggested that the Agulhas is the largest western boundary current in the world ocean, as comparable western boundary currents transport less, ranging from the Brazil Current, 16.2 Sverdrups), to the Kuroshio, 42 Sverdrups.

Physical properties
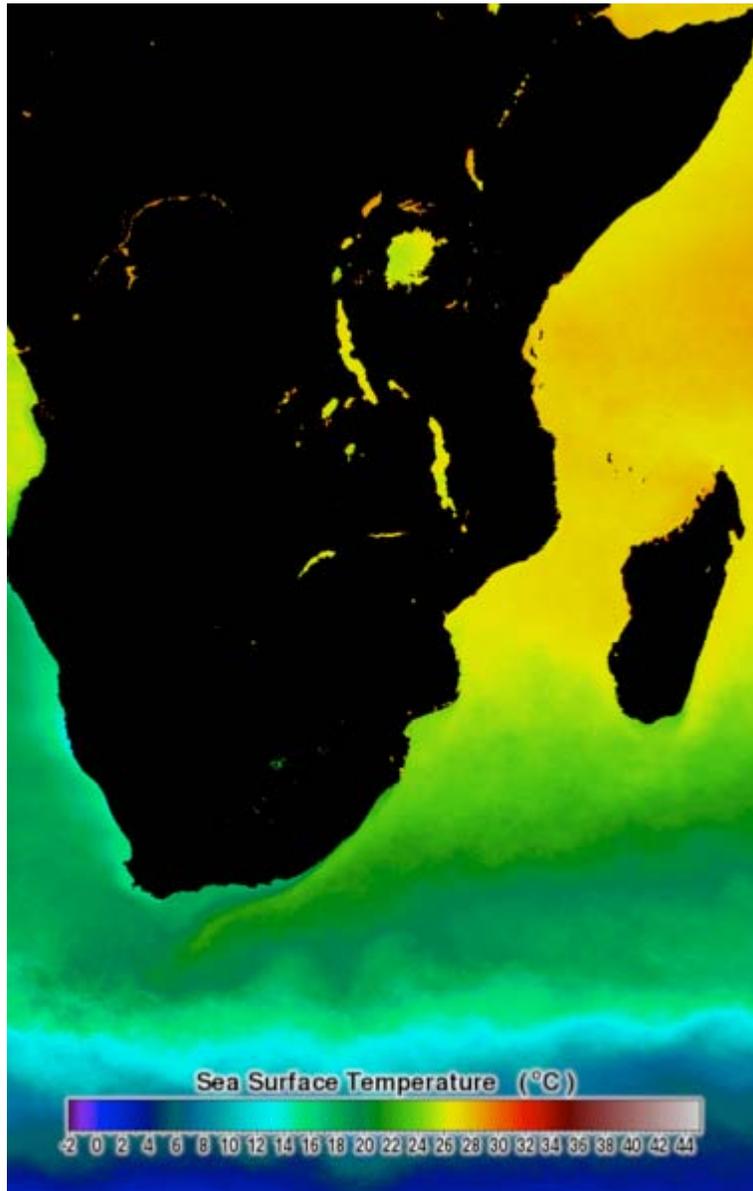
Mean sea surface temperature map of the Agulhas Current for 2009. Note the separation of the current from the African coast as a warm tongue of water south of Cape Agulhas, as it retroflects into the Indian Ocean.

The sources of the Agulhas Current are the East Madagascar Current (25 Sverdrups), the Mozambique Current (5 Sverdrups) and a reticulated part of the Agulhas Current itself (35 Sverdrups). The net transport of the Agulhas Current is estimated as 100 Sv. The flow of the Agulhas Current is directed by the topography. The current follows the continental shelf from Maputo to the tip of the Agulhas Bank (Cape Agulhas). Here the

momentum of the current overcomes the vorticity balance holding the current to the topography and the current leaves the shelf.

Retroflection

In the southeast Atlantic Ocean the current retroflects (turns back on itself) in the Agulhas Retroflection due to shear interactions with the strong Antarctic Circumpolar Current. This water becomes the Agulhas Return Current, rejoining the Indian Ocean Gyre. It is estimated that up to 85 Sv (Sverdrups) of the net transport is returned to the Indian Ocean through the retroflection. The remaining water is transported into the South Atlantic Gyre in the Agulhas Leakage. Along with direct branch currents, this leakage takes place in surface water filaments, and Agulhas Eddies.

Agulhas leakage

It is estimated that as much as 15 Sv of Indian Ocean water is leaked directly into the South Atlantic. 10 Sv of this is relatively warm, salty thermocline water, with the remaining 5 Sv being cold, low salinity Antarctic Intermediate Water. Since Indian Ocean water is significantly warmer (24-26°C) and saltier than South Atlantic water, the Agulhas Leakage is a significant source of salt and heat for the South Atlantic Gyre. This heat flux is believed to contribute to the high rate of evaporation in the South Atlantic, a key mechanism in the Meridional Overturning Circulation. It should be noted that a small amount of the Agulhas Leakage joins the North Brazil Current, carrying Indian Ocean water into the North Atlantic Subtropical Gyre .

Filaments

Surface water filaments are estimated to account for up to 13% of the total salt transport from the Agulhas Current into the Benguela Current and South Atlantic Gyre. Due to surface dissipation, these filaments are not believed to significantly contribute to inter-basin heat flux.

Eddies

Where the Agulhas turns back on itself the loop of the retroflection pinches off periodically, releasing an eddy into the South Atlantic Gyre. This "Agulhas Ring" enters the flow of the Benguela Current or is advected northwestward across the South Atlantic where it joins the South Equatorial Current, where they dissipate into the larger background currents. These anticyclonic warm core rings are estimated to have a transport of 3-9 Sv each, in total injecting salt at a rate of $2.5.10^6$ kg/s and heat at a rate of 0.045 PW .

Biological properties

Mean chlorophyl-a concentration map of the Agulhas Current for 2009. Note the high productivity water in the Agulhas Retroflection.

Primary production

The Agulhas acts as an oceanic convergence zone. Due to mass continuity this drives surface waters down, resulting in the upwelling of cold, nutrient rich water south of the current. Additionally, the convergence tends to increase the concentration of plankton in and around the Agulhas. Both of these factors result in the area being one of enhanced primary productivity as compared to the surrounding waters. This is especially notable in

the Agulhas Retroflection waters, where chl-a concentrations tend to be significantly higher than the surrounding South Indian Ocean and South Atlantic Ocean waters.

Impact of rings

Warm core rings are known to have lower primary productivity than surrounding cold waters. Agulhas Rings are no exception, and have been observed to carry waters with low chlorophyll-a concentration water into the South Atlantic. It can also be noted that the size of phytoplankton in Agulhas Rings tends to be smaller than in the surrounding water (around 20 μm in diameter).

Agulhas Rings have also bee observed as removing larval and juvenile fish from the continental shelf. This removal of young fish can result in a reduced Anchovy catch in the Benguela system if a ring passes through the fishery.

East Australian Current
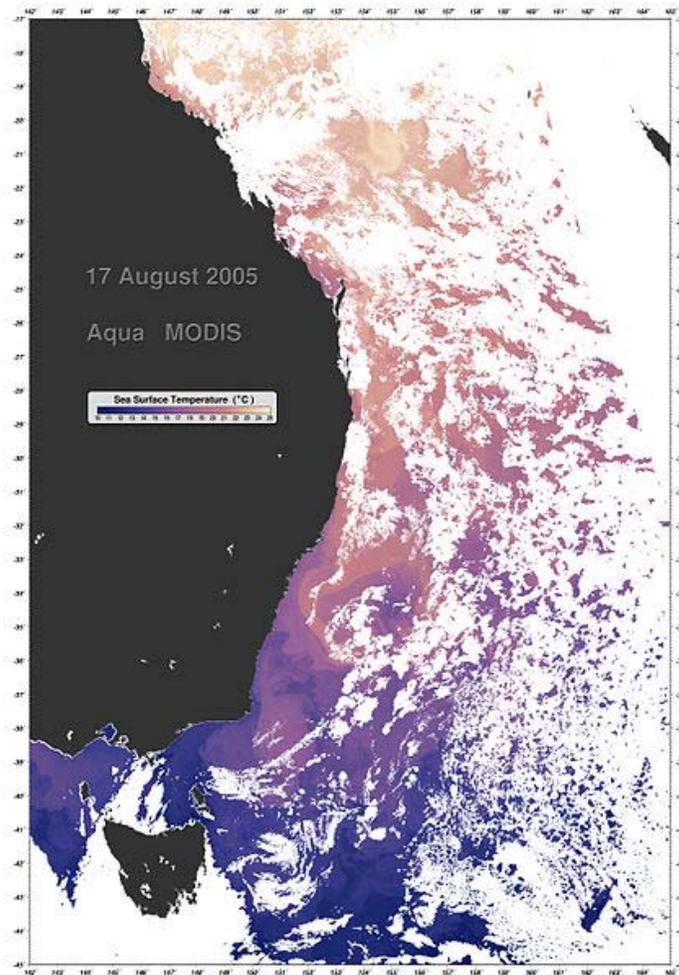
Thermal profile of the East Australian Current

The **East Australian Current** (EAC) is an ocean current that moves warm water in a clockwise fashion down the east coast of Australia. It is the largest ocean current close to the shores of Australia. Its source is the tropical Coral Sea off the north-east coast of Australia. It can reach speeds of up to 7 knots in some of the shallower waters along the Australian continental shelf, but is generally measured at 2 or 3 knots. The EAC results in a current vortex in the Tasman Sea between Australia and New Zealand. The EAC also acts to transport tropical marine fauna to habitats in sub-tropical regions along the south east Australian coast.

Chapter- 5

Eastern Boundary Currents

California Current

The **California Current** is a Pacific Ocean current that moves south along the western coast of North America, beginning off southern British Columbia, and ending off southern Baja California. There are five major coastal currents affiliated with upwelling zones. These are the California Current (located off the coast of Oregon and California), the Humboldt Current (located off the coast of Chile and Peru), the Canary Current (located off the coast of northwest Africa), the Benguela Current (located off the coast of southwest Africa), and the Somali Current (located in the western Indian Ocean) (Mann and Lazier, 2006). The five major coastal currents are parts of the global ocean gyre system and as such, these currents are driven by wind and deflected by landmasses. Each of the major ocean basins has both a western boundary current and an eastern boundary current. The western boundary currents tend to be deep and fast and the eastern boundary currents are mainly shallow, broad, and less-defined (Mann and Lazier, 2006). The California Current is an Eastern boundary current and is part of the North Pacific Gyre, a large swirling current that occupies the northern basin of the Pacific. The movement of northern waters southward makes the coastal waters cooler than the coastal areas of comparable latitude on the east coast of the United States. Additionally, extensive upwelling of colder sub-surface waters occurs, caused by the prevailing northeasterly winds acting through the Ekman Effect. The winds drive surface water to the right of the wind flow, that is offshore, which draws water up from below to replace it. The upwelling further cools the already cool California Current. This is the mechanism that produces California's characteristic coastal fog and the negative temperature anomaly we measure in California's coastal waters during summer (Mann and Lazier, 2006). This translates into cold coastal waters during the summer, stretching from Oregon to Baja California. Note, this does not include the coastal water surrounding San Diego. There is a warm water anomaly off San Diego (Mann and Lazier, 2006).

The cold water is highly productive due to the upwelling, which brings to the surface nutrient-rich sediments, supporting large populations of whales, seabirds and important fisheries. Winds of the appropriate direction and strength to induce upwelling are more prevalent in the presence of Eastern boundary currents, such as the California Current (Mann and Lazier, 2006). Phytoplankton production is dramatically increased in these areas because the nutrient-rich water lying below the pycnocline is relatively close to the

surface and is thus easily upwelled (Mann and Lazier, 2006). A narrower, weaker counter current, the Davidson Current, occasionally moves somewhat warmer water northwards during the winter months. During El Niño events, the California Current is disrupted, leading to declines in phytoplankton, resulting in cascading effects up the food chain, such as declines in fisheries, seabird breeding failures and marine mammal mortality (Schwing et al., 2003). In 2005, a failure in the otherwise predictable upwelling events, unassociated with El Niño, caused a collapse in krill in the current, leading to similar effects (Schwing et al., 2003).

Bakun (1973) calculated a 20-year average of the monthly mean Ekman transport for different regions off the California coast. His 'Bakun upwelling index' ranges from 300 meters-cubed/second (in the offshore direction) to -212 meters-cubed/second (toward the coast, or onshore direction) (Mann and Lazier,2006). Bakun's index showed there is year-round upwelling off Southern California's coast, but it is strongest in the summer months. Bakun's work also shows that off the coast of Oregon and Washington, there is forceful downwelling in the winter months, and upwelling in the region is restricted to the months of April through September (Mann and Lazier, 2006).

Primary Production in the California Current

Primary production is a topic of interest among those who study the California Current. In their study, Hayward and Venrick (1982) found great variability in both biomass and the productivity of phytoplankton in the California Current. The differences observed by Hayward and Venrick in carbon-fixation rates (0.2-2.0 grams Carbon/(meter-squared x day)) show the heterogeneous nature of the California Current, with its combination of advected and upwelled water. Several studies have investigated the carbon flow from primary production to the pelagic fish stocks which depend on the California Current. Lasker (1988) described powerful 'jets and squirts' off northern and central California. These 'jets and squirts' move large quantities of cold, nutrient rich water offshore. This water then gets carried by the southward bound California Current and adds significant primary production to the sardine population (Mann and Lazier, 2006).

Physical Properties of the California Current

The Southern California Bight is a sub-region of the California Current and has unique physical properties. Upwelling is fairly weak in the California Bight and Smith and Eppley (1982) stated that the 16-year average for primary production was 0.402 grams Carbon/(meter-squared x day),or approximately 150 grams Carbon/(meter-squared x year). Further, Smith and Eppley (1982) found that the highest daily rates of temperature decrease were correlated with the maximum amount of upwelling (Mann and Lazier, 2006). Digiacomo and Holt (2001) used satellite images to study the mesoscale and sub-mesoscale eddies in the Southern California Bight. Their work showed that all eddies were less than 50 km in diameter and 70 % of all eddies measured less than 10 km (Mann and Lazier, 2006). The eddies appeared to be caused mostly by topography (particularly islands), wind, and instabilities in the current. The location of these eddies was mainly

between the California Current (flowing toward the equator) and the coastline (Mann and Lazier, 2006). The majority of these eddies were cyclonic and had the ability to induce the upwelling of nutrient-rich water. Small scale topographic features such as headlands have been shown to cause substantial effects on the population dynamics of benthic invertebrates, such a change in the settlement patterns of crabs and sea urchin (Mann and Lazier, 2006).

Fish Production and Growth in the California Current

The California Current produces an abundance of sardines, anchovies, hake, jack mackerel, and mackerel (Mann and Lazier, 2006). An abundance of these fish species is a common feature of eastern boundary currents. Sardines in particular were heavily fished from 1916 - 1967. This lead to the California state legislature to impose a suspension on sardine fishing in 1967 (Mann and Lazier, 2006). The largest stocks of both sardine and anchovy spawn in the Southern California Bight. Sardines in the California Current are divisible into four stocks and anchovies in this current have several subpopulations as well (Mann and Lazier, 2006). The largest stocks of both sardines and anchovies spawn in the Southern California Bight. The California Bight is a region of relatively weak upwelling (and thus weak phytoplankton production)compared to the greater California Current. From these observations, we see that fish often choose to spawn in areas where Ekman transport will not carry their eggs too far offshore. Many fish species avoid spawning in areas of strong upwelling. Although upwelling and the subsequent high biological productivity produces optimal conditions for the growth of juvenile and adult sardines, the absence of strong upwelling in late winter and early spring (such as that found in the California Bight) is what creates optimum conditions for the survival of fish larvae (Mann and Lazier, 2006). Once anchovy and sardine larvae have spent a significant amount of time in waters free of strong upwelling and mixing (i.e. The California Bight), they migrate (as juveniles) toward areas of great upwelling (i.e. The California Current proper). There the juveniles can take advantage of the high biological productivity and maximize their growth rate.

Canary Current

The **Canary Current** is a wind driven surface current that is part of the North Atlantic Gyre. This eastern Boundary current branches south from the North Atlantic Current and flows southwest about as far as Senegal where it turns west and later joins the Atlantic North Equatorial Current. The current is named after the Canary Islands. The archipelago partially blocks the flow of the Canary Current (Gyory, 2007).

This wide and slow moving current is thought to have been exploited in the early Phoenician navigation and settlement along the coast of western Morocco. The ancient Phoenicians not only exploited numerous fisheries within this current zone, but also

established a factory at Iles Purpuraires off of present day Essaouira for extracting a Tyrian purple dye from a marine gastropod murex species (Hogan, 2007).

Upwelling

A prominent feature of Eastern Boundary Currents is the presence of upwelling. Ekman drift causes offshore transport of surface waters, which are then replaced with deep water from below. Deep waters are cold and Nutrient-rich and have a key role in stimulating Primary productivity. Upwelling has led to the enhancement of coastal fisheries in western Morocco (Hance, 1975).

Major upwelling occurs between 23 and 25 degrees northern latitude (Canary Current, 2002). Upwelling occurs year-round at Cap Blanc (Ras Nouadhibou) and northward. South of Cap Blanc, upwelling is limited to winter and spring due to the northward migration of the Azores high during summer, which is responsible for driving equatorward winds. Minas et al (1982) showed that at the latitude of Cap Blanc, a front exists that separates North Atlantic Central Water (NACW) and South Atlantic Central Water (SACW). SACW, to the south of Cap Blanc, is richer in nutrients than NACW. A poleward subsurface counter-current is responsible for bringing SACW to the Cap Blanc region resulting in maximal primary production. Primary production to the north is limited by nutrient availability in NACW. Primary production to the south of Cap Blanc is limited by the occurrence of upwelling events.

Upwelling and primary production

Huntsman and Barber (1977) hypothesized that high productivity results from alternating upwelling events and relatively calm periods. Upwelling is necessary to bring the nutrients to the surface but if the event is sustained for a long period of time, it is tough for phytoplankton to remain in the euphotic zone. Calm periods allow for stratification to develop, which means that phytoplankton can grow and multiply while held in the shallow mixed layer. In other words, there is a miniature spring bloom during each calm period (Mann & Lazier, 1996).

Upwelling and zooplankton

Upwelling and primary production follow the onset of a strong wind within a few days (Mann & Lazier, 1996). Zooplankton, such as copepods, take longer to respond to the abundance of food available because they have life cycles of weeks rather than days. Zooplankton in the Canary Current reach their peak density in autumn when upwelling intensity decreases. The decrease in upwelling allows the zooplankton to stay over the shelf where their food supply exists. Due to the rapid response of phytoplankton to upwelled nutrients, zooplankton are seldom food-limited.

Upwelling and fish

Four types of fish comprise 75% of total catch in the Cap Blanc region (Mann & Lazier, 1996). Clupeids (*Sardina pilchardus*, the sardine, and *Sardinella aurita*) were the most abundant. *S. pilchards* dominate in the cooler northern waters while *S. aurita* are dominate in warmer southern waters. Next most abundant were Jack mackerel (*Trachurus* spp.) and Redfish (Sparidae). Ansa-Emmin (1982) found that in 1974, the total fish landings reached 2.68 million tons. Nearly 1 million tons were Clupeidae with .67 million tons being sardines.

Nutrient recycling

Phytoplankton over the shelf area face two fates: They sink to the bottom or are consumed by zooplankton. If they settle to the bottom, phytoplankton release ammonia during their decomposition, which returns nitrogen to the waters. Consequently, the phytoplankton remains could be consumed by benthic dwellers, which also excrete ammonia. If consumed by zooplankton, nitrogen from the phytoplankton will be returned to the environment via excreted ammonia or fecal pellets, which settle to the bottom. Regardless of the mechanism, a high proportion of phytoplankton nitrogen ends up being released in the shoreward-moving lower layer of the water column (Mann & Lazier, 1996). This water will later be upwelled and can stimulate further primary production. Barber and Smith (1981) estimated that on the shelf off Cap Blanc, regenerated nitrogen accounted for 72% of total nitrogen.
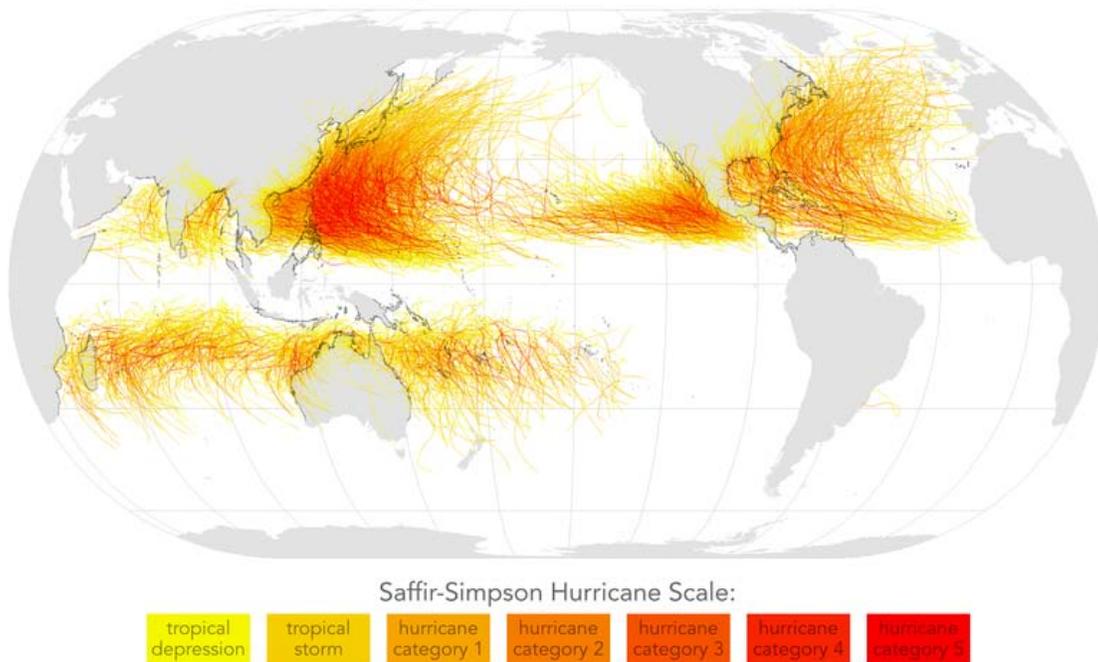
Humboldt Current
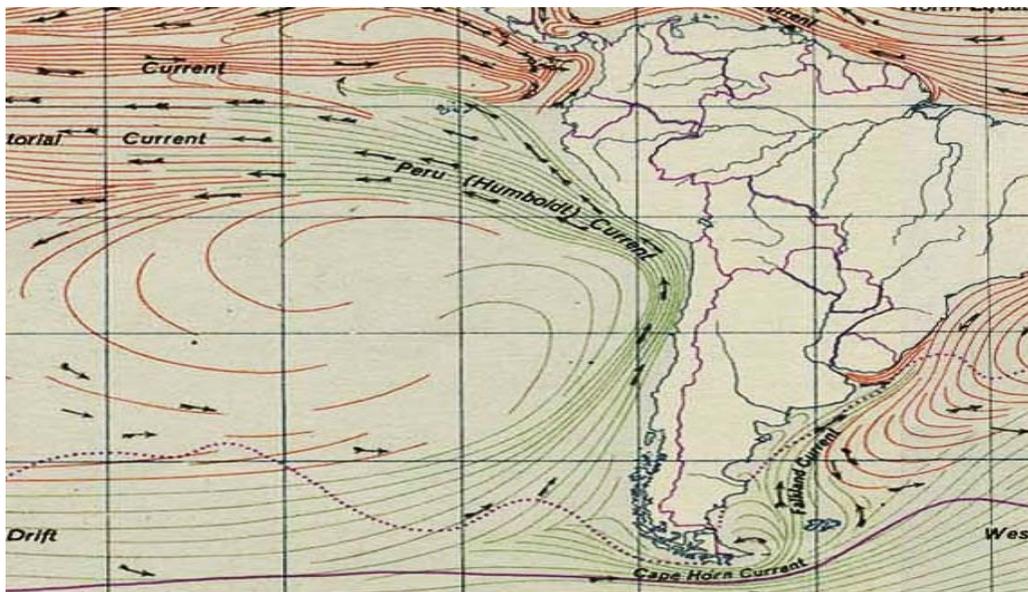
Humboldt Current

The **Humboldt Current** is a cold, low-salinity ocean current that flows north-westward along the west coast of South America from the southern tip of Chile to northern Peru. It is an eastern boundary current flowing in the direction of the equator, and can extend 1,000 kilometers offshore. The Humboldt Current Large Marine Ecosystem (**LME**), named after the Prussian naturalist Alexander von Humboldt, is one of the major upwelling systems of the world, supporting an extraordinary abundance of marine life. Upwelling occurs off Peru year-round but off Chile only during the spring and summer, because of the displacement of the subtropical center of high pressure during the summer.

The Humboldt Current LME is considered a Class I, highly productive (>300 gC/m2-yr), ecosystem. It is the most productive marine ecosystem in the world, as well as the largest upwelling system. The Humboldt's high rates of primary and secondary productivity support the world's largest fisheries. Approximately 18-20% of the world's fish catch comes from the Humboldt Current LME. The species are mostly pelagic: sardines, anchovies and jack mackerel. The LME's high productivity supports other important fishery resources as well as marine mammals. The cold, nutrient-rich water brought to the surface by upwelling drives the system's extraordinary productivity.


The presence of the Humboldt Current and its associated wind shear prevents the formation of tropical cyclones in the area (The same effect occurs in the South Atlantic with the Benguela Current).
(Worldwide tropical cyclone tracks, 1945–2006.)

Periodically, the upwelling that drives the system's productivity is disrupted by the El Niño-Southern Oscillation (ENSO) event. When this occurs, fish abundance and distribution are significantly affected, often leading to stock crashes and cascading social and economic impacts. These events have led to sequential changes, where sardines and anchovies have replaced each other periodically as the dominant species in the ecosystem. These species changes can have negative consequences for the fishing industry and the economies of the countries that fish the system.

The Humboldt has a considerable cooling influence on the climate of Chile, the climate of Peru and the climate of Ecuador. It is also largely responsible for the aridity that prevails in northern Chile and coastal areas of Peru and southern Ecuador. Marine air is cooled by the current and thus is not conducive to generating precipitation (although clouds and fog are produced).

Benguela Current
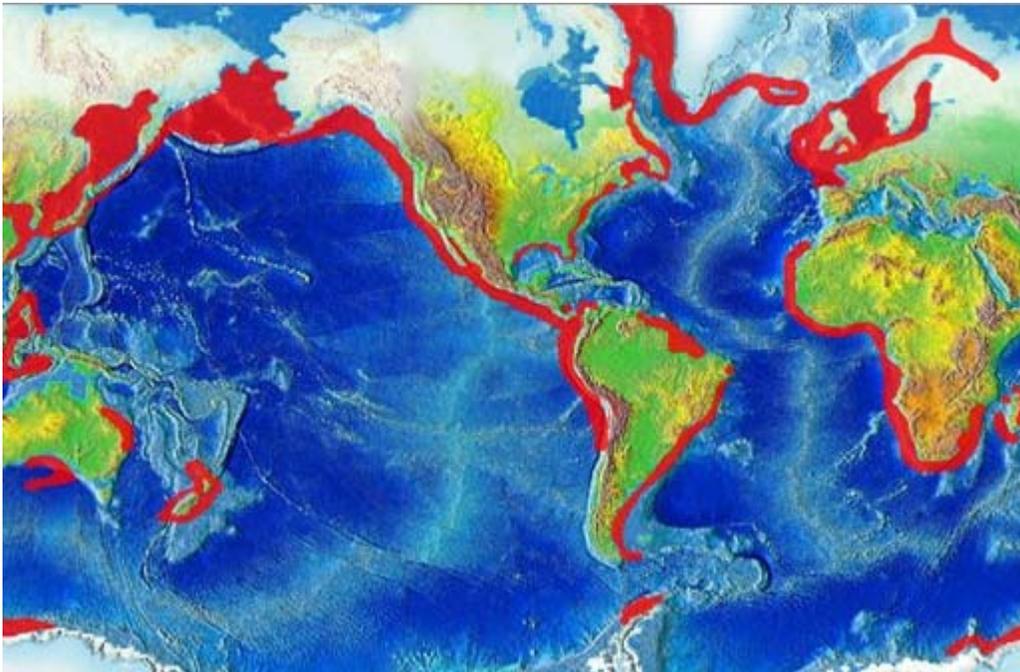
The red areas show major upwelling areas. The Benguela Current is on the southwest coast of Africa.

The **Benguela Current** is the broad, northward flowing ocean current that forms the eastern portion of the South Atlantic Ocean gyre. The current extends from roughly Cape Point in the south, to the position of the Angola-Benguela Front in the north, at around 16°S. The current is driven by the prevailing South Easterly Trade winds. Inshore of the

Benguela Current proper, the south easterly winds drive coastal upwelling, forming the Benguela Upwelling System. The cold, nutrient rich waters that upwell from around 200-300 m depth in turn fuel high rates of phytoplankton growth, and sustain the productive Benguela ecosystem.

Boundaries

Source waters for the Benguela include Indian and South Atlantic subtropical thermocline water; saline, low-oxygen tropical Atlantic water; and cooler, fresher deep water. The Benguela current is 200 to 300 km wide and widens further as it flows north and northwest. Its western, seaward edge is ill-defined, with many temporary and seasonal eddies and meanders. There is however a well defined thermal front between the waters associated with the Benguela Upwelling System and those of the south east Atlantic.

Where the icy Benguela and the warm, south-flowing Agulhas current mix, there is a richly productive marine ecosystem off the Cape of Good Hope but storms and turbulence above.

Upwelling and Primary Production

Northward winds along the coast result in Ekman transport offshore and upwelling of nutrient rich deep water to the euphotic zone. The intensity of the upwelling event is determined by wind strength. Variations in wind strength cause pulses of upwelling, which propagate to the south along the coast with speeds of 5 to 8 m/s. The pulses are similar to a Kelvin wave, except on a scale of 30 to 60 km instead of 1000 km, and can propagate around the cape depending on wind systems.

Pulses of upwelling induce biological production. In the Benguela system, phytoplankton growth requires a period of upwelling followed by a period of stratification and relatively calm waters. The phytoplankton bloom usually lags the upwelling event by 1 to 4 days and blooms for 4 to 10 days. In order for zooplankton to have a continuous food supply, the phytoplankton blooms must not occur too far apart. Pulses of upwelling in the Benguela system regularly have a duration of 10 days, an optimal period for biological production. It is estimated that the annual new production in the Benguela system is 4.7×10^{13} gC/y, making the Benguela system 30 to 65 times more productive per unit area than the global ocean average.

While upwelling promotes abundant primary and secondary production in the upper parts of the water column and near the coast, deeper waters with limited oxygen exchange create hypoxic areas called oxygen minimum zones at the coastal shelf and upper coastal slope. The Benguela oxygen minimum zone starts around a depth of 100 m and is a few hundred meters thick. Bacteria that use sulpher rather than oxygen reside in the oxygen minimum zone.

The most abundant fishes in the Benguela system are *Sardinops* and *Engraulis*. *Sardinops ocelata* (pilchard) was intensely fished beginning in the 1950s and peaking in 1968 with landings over 1.3 million tons. Since then, the *Sardinops* fishery has declined and the *Engraulis capensis* (anchovy) fishery has taken over.

Benguela Niño

Similar to the Pacific El Niño, a thick slab of warm, nutrient poor water enters the northern part of the Benguela upwelling system off the Namibia coast about once per decade. During the Benguela Niño, warm, salty waters from the Angola Current move southward, from 15°S to as far as 25°S. This slab of warm salty water extends to 150 km offshore and to 50 m depth. Heavy rains, changes in fish abundance, and temporal proximity to the Pacific El Niño have been observed; however, the causes and effects of the Benguela Niño are not well understood. One research team has shown that the Benguela Niño is caused by winds in the west-central equatorial Atlantic Ocean that propagate as subsurface sea temperature anomalies to the African coast.

Chapter- 6

Kelvin Wave and Rossby Wave

Kelvin wave

A **Kelvin wave** is a wave in the ocean or atmosphere that balances the Earth's Coriolis force against a topographic boundary such as a coastline, or a waveguide such as the equator. A feature of a Kelvin wave is that it is non-dispersive, i.e., the phase speed of the wave crests is equal to the group speed of the wave energy for all frequencies. This means that it retains its shape in the alongshore direction over time.

A Kelvin wave (fluid dynamics) is also a long scale perturbation mode of a vortex in superfluid dynamics; in terms of the meteorological or oceanographical derivation, one may assume that the meridional velocity component vanishes (i.e. there is no flow in the north–south direction, thus making the momentum and continuity equations much simpler).

Coastal Kelvin wave

In a stratified ocean of mean depth *H*, free waves propagate along coastal boundaries (and hence become trapped in the vicinity of the coast itself) in the form of internal Kelvin waves on a scale of about 30 km. These waves are called coastal Kelvin waves, and have propagation speeds of approximately 2 m/s in the ocean. Utilizing the assumption that the cross-shore velocity *v* is zero at the coast, *v* = 0, one may solve a frequency relation for the phase speed of coastal Kelvin waves, which are among the class of waves called boundary waves, edge waves, trapped waves, or surface waves (similar to the Lamb waves). The (linearised) primitive equations then become the following:

- the continuity equation (accounting for the effects of horizontal convergence and divergence):

$$\frac{\partial u}{\partial x} + \frac{\partial v}{\partial y} = \frac{-1}{H}\frac{\partial \eta}{\partial t}$$

- the *u*-momentum equation (zonal wind component):

$$\frac{\partial u}{\partial t} = -g\frac{\partial \eta}{\partial x} + fv$$

- the *v*-momentum equation (meridional wind component):

$$\frac{\partial v}{\partial t} = -g\frac{\partial \eta}{\partial y} - fu.$$

If one assumes that the Coriolis coefficient *f* is constant along the right boundary conditions and the zonal wind speed is set equal to zero, then the primitive equations become the following:

- the continuity equation:

$$\frac{\partial v}{\partial y} = \frac{-1}{H}\frac{\partial \eta}{\partial t}$$

- the *u*-momentum equation:

$$g\frac{\partial \eta}{\partial x} = fv$$

- the *v*-momentum equation:

$$\frac{\partial v}{\partial t} = -g\frac{\partial \eta}{\partial y}.$$

The solution to these equations yields the following phase speed: $c^2 = gH$, which is the same speed as for shallow-water gravity waves without the effect of Earth's rotation. It is important to note that for an observer traveling with the wave, the coastal boundary (maximum amplitude) is always to the right in the northern hemisphere and to the left in the southern hemisphere (i.e. these waves move equatorward/southward – negative phase speed – on a western boundary and poleward/northward – positive phase speed – on an eastern boundary; the waves move cyclonically around an ocean basin).

Equatorial Kelvin wave

The equatorial zone essentially acts as a waveguide, causing disturbances to be trapped in the vicinity of the equator, and the equatorial Kelvin wave illustrates this fact because the equator acts analogously to a topographic boundary for both the Northern and Southern Hemispheres, making this wave very similar to the coastally-trapped Kelvin wave. The primitive equations are identical to those used to develop the coastal Kelvin wave phase speed solution (U-momentum, V-momentum, and continuity equations) and the motion is

unidirectional and parallel to the equator. Because these waves are equatorial, the Coriolis parameter vanishes at 0 degrees; therefore, it is necessary to use the equatorial beta plane approximation that states:

$$f = \beta y,$$

where β is the variation of the Coriolis parameter with latitude. This equatorial Beta plane assumption requires a geostrophic balance between the eastward velocity and the north-south pressure gradient. The phase speed is identical to that of coastal Kelvin waves, indicating that the equatorial Kelvin waves propagate toward the east without dispersion (as if the earth were a non-rotating planet). For the first baroclinic mode in the ocean, a typical phase speed would be about 2.8 m/s, causing an equatorial Kelvin wave to take 2 months to cross the Pacific Ocean between New Guinea and South America; for higher ocean and atmospheric modes, the phase speeds are comparable to fluid flow speeds.

When the motion at the equator is to the east, any deviation toward the north is brought back toward the equator because the Coriolis force acts to the right of the direction of motion in the Northern Hemisphere, and any deviation to the south is brought back toward the equator because the Coriolis force acts to the left of the direction of motion in the Southern Hemisphere. Note that for motion toward the west, the Coriolis force would not restore a northward or southward deviation back toward the equator; thus, equatorial Kelvin waves are only possible for eastward motion (as noted above). Both atmospheric and oceanic equatorial Kelvin waves play an important role in the dynamics of El Nino-Southern Oscillation, by transmitting changes in conditions in the Western Pacific to the Eastern Pacific.

There have been studies that connect equatorial Kelvin waves to coastal Kelvin waves. Moore (1968) found that as an equatorial Kelvin wave strikes an "eastern boundary," part of the energy is reflected in the form of planetary and gravity waves; and the remainder of the energy is carried poleward along the eastern boundary as coastal Kelvin waves. This process indicates that some energy may be lost from the equatorial region and transported to the poleward region.

Equatorial Kelvin waves are often associated with anomalies in surface wind stress. For example, positive (eastward) anomalies in wind stress in the central Pacific excite positive anomalies in 20°C isotherm depth which propagate to the east as equatorial Kelvin waves.

Rossby wave

Atmospheric Rossby waves are giant meanders in high-altitude winds that are a major influence on weather. They are not to be confused with **oceanic Rossby waves**, which move along the thermocline: that is, the boundary between the warm upper layer of the ocean and the cold deeper part of the ocean.

Rossby waves are a subset of inertial waves.

Atmospheric waves

The emergence of atmospheric Rossby waves is due to shear in rotating fluids, so that the Coriolis force changes along the sheared coordinate. In planetary atmospheres, they are due to the variation in the Coriolis effect with latitude. The waves were first identified in the Earth's atmosphere in 1939 by Carl-Gustaf Arvid Rossby who went on to explain their motion.

The special identifying feature of the Rossby wave is its phase velocity (that of the wave crests) always has a westward component. However, the wave's group velocity (associated with the energy flux) can be in any direction. In general: shorter waves have an eastward group velocity and long waves a westward group velocity.

The terms "barotropic" and "baroclinic" Rossby waves are used to distinguish their vertical structure. Barotropic Rossby waves do not vary in the vertical, and have the fastest propagation speeds. The baroclinic wave modes are slower, with speeds of only a few centimetres per second or less.
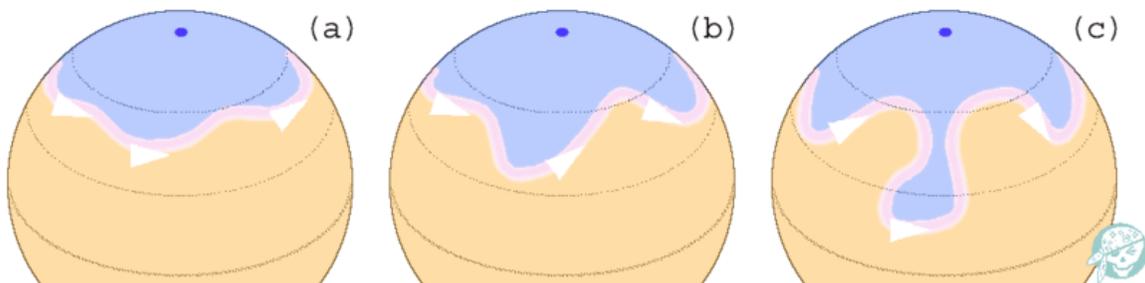
Meanders of the northern hemisphere's jet stream developing (a, b) and finally detaching a "drop" of cold air (c). Orange: warmer masses of air; pink: jet stream.

Most work on Rossby waves has been done on those in Earth's atmosphere. Rossby waves in the Earth's atmosphere are easy to observe as (usually 4-6) large-scale meanders of the jet stream. When these loops become very pronounced, they detach the masses of cold, or warm, air that become cyclones and anticyclones and are responsible for day-to-day weather patterns at mid-latitudes.

Free Barotropic Rossby Waves under a zonal flow with linearized vorticity equation

Let us start with perturbing a flow that with only a time and spatially invariant zonal flow U with no meridional component.

$$u = U + u'(t, x, y)$$
$$v = v'(t, x, y)$$

We assume the perturbation to be much smaller than the mean zonal flow.

$$U \gg u', v'$$

Relative Vorticity η, U and V can be written in the form stream function (ψ) (assuming non-divergent flow which stream function completely describes the flow):

$$u = \frac{\partial \psi}{\partial y}$$
$$v = -\frac{\partial \psi}{\partial x}$$
$$\eta = \nabla \times (u\hat{\boldsymbol{i}} + v\hat{\boldsymbol{j}}) = \nabla^2 \psi$$

Considering a parcel of air that has no relative vorticity before perturbation (uniform U has no vorticity) but with planetary vorticity f as a function of the latitude, perturbation will lead to a slight change of latitude, so the perturbed relative vorticity must change in order to conserve potential vorticity. Also we make the approximation that $U >> u'$, so the perturbation flow does not advect relative vorticity.

$$\frac{d(\eta + f)}{dt} = 0 = \frac{\partial \eta}{\partial t} + U\frac{\partial \eta}{\partial x} + \beta v'$$

which $\beta = \dfrac{\partial f}{\partial y}$, and plug in the definition of stream function to obtain:

$$0 = \frac{\partial \nabla^2 \psi}{\partial t} + U\frac{\partial \nabla^2 \psi}{\partial x} + \beta\frac{\partial \psi}{\partial x}$$

Guess a traveling wave solution with wave numbers k and l, and frequency omega:

$$\psi = \psi_0 e^{i(kx + ly - \omega t)}$$

We obtain the dispersion relation of:

$$\omega = Uk - \beta \frac{k}{k^2 + l^2}$$

The zonal phase speed and group speed are given by

$$c \equiv \frac{\omega}{k} = U - \frac{\beta}{(k^2 + l^2)},$$

$$c_g \equiv \frac{\partial \omega}{\partial k} = U - \frac{\beta(l^2 - k^2)}{(k^2 + l^2)^2},$$

where c is the phase speed, c_g is the group speed, u is the mean westerly flow, β is the Rossby parameter, and k is the zonal wave number. The above proves that phase speed is always westward relative to mean flow, but group speed can travel both ways depending on the wave number; large zonal wave number waves (short waves) leads the mean flow, and small zonal wave number waves (long wave) retrogrades. The meaning of large and small only depends on the value of l, if $l = k$, then the group speed is the same as the mean zonal flow.

Meaning of Beta

The Rossby parameter is defined:

$$\beta = \frac{\partial f}{\partial y} = \frac{1}{a}\frac{d}{d\phi}(2\omega \sin \phi) = \frac{2\omega \cos \phi}{a}$$

φ is the latitude, ω is the angular speed of the Earth's rotation, and a is the mean radius of the Earth.

If $\beta = 0$, there will be no Rossby Waves; Rossby Waves owe their origin to the gradient of the tangential speed of the planetary rotation (planetary vorticity). A "cylinder" planet has no Rossby Waves. It also means that near the equator on Earth where $f = 0$ but $\beta > 0$ except at the poles, one can still have Rossby Waves (Equatorial Rossby wave).

Oceanic waves

Oceanic Rossby waves are thought to communicate climatic changes due to variability in forcing, due to both the wind and buoyancy. Both barotropic and baroclinic waves cause variations of the sea surface height, although the length of the waves made them difficult to detect until the advent of satellite altimetry. Observations by the NASA/CNES TOPEX/Poseidon satellite confirmed the existence of oceanic Rossby waves.

Baroclinic waves also generate significant displacements of the oceanic thermocline, often of tens of meters. Satellite observations have revealed the stately progression of

Rossby waves across all the ocean basins, particularly at low- and mid-latitudes. These waves can take months or even years to cross a basin like the Pacific.

Rossby waves have been suggested as an important mechanism to account for the heating of Europa's ocean.

Rossby-gravity waves

Rossby-gravity waves are equatorially-trapped waves (much like Kelvin waves), meaning that they rapidly decay as their distance increases away from the equator (along as the Brunt–Vaisala frequency does not remain constant). These waves have the same trapping scale as Kelvin waves, more commonly known as the equatorial Rossby deformation radius. They always carry energy eastward, but, oddly, their 'crests' and 'troughs' may propagate westward if their periods are long enough. The eastward speed of propagation of these waves can be derived for an inviscid slowly moving layer of fluid of uniform depth H . Because the Coriolis parameter ($f = 2\Omega \sin(\theta)$ where Ω is the angular velocity of the earth, 7.2921×10^{-5} rad/s, and θ is latitude) vanishes at 0 degrees latitude (equator), the "equatorial beta plane" approximation must be made. This approximation states that "f" is approximately equal to βy, where "y" is the distance from the equator

and "β" is the variation of the coriolis parameter with latitude, $\dfrac{\partial f}{\partial y} = \beta$. With the inclusion of this approximation, the primitive equations become (neglecting friction):

- the continuity equation (accounting for the effects of horizontal convergence and divergence and written with geopotential height):

$$\frac{\partial \phi}{\partial t} + c^2 \left(\frac{\partial v}{\partial y} + \frac{\partial u}{\partial x} \right) = 0$$

- the U-momentum equation (zonal wind component):

$$\frac{\partial u}{\partial t} - v\beta y = -\frac{\partial \phi}{\partial x}$$

- the V-momentum equation (meridional wind component):

$$\frac{\partial v}{\partial t} + u\beta y = -\frac{\partial \phi}{\partial y}.$$

These three equations can be separated and solved using solutions in the form of zonally-propagating waves, which are analogous to exponential solutions with a dependence on x and t and the inclusion of structure functions that vary in the y-direction:

$$\{u, v, \phi\} = \{\hat{u}(y), \hat{v}(y), \hat{\phi}(y)\} e^{i(kx - \omega t)}$$

Once the frequency relation is formulated in terms of ω, the angular frequency, the problem can be solved with 3 distinct solutions. These three solutions correspond to the equatorially-trapped gravity wave, the equatorially-trapped Rossby wave and the mixed Rossby-gravity wave (which has some of the characteristics of the former two) . It is important to note that equatorial gravity waves can be either westward- or eastward-propagating and correspond to n=1 (same as for the equatorially-trapped Rossby wave) on a dispersion relation diagram ("w-k" diagram). At $n = 0$ on a dispersion relation diagram, the mixed Rossby-gravity waves can be found where for large, positive zonal wave numbers (+k), the solution behaves like a gravity wave; but for large, negative zonal wave numbers (−k), the solution appears to be a Rossby wave (hence the term Rossby-gravity waves). As mentioned earlier, the group velocity (or energy packet/dispersion) is always directed toward the east with a maximum for short waves (gravity waves).

Vertically-propagating Rossby-gravity waves

As previously stated, the mixed Rossby-gravity waves are equatorially-trapped waves unless the buoyancy frequency remains constant, introducing an additional vertical wave number to complement the zonal wave number and angular frequency. If this Brunt–Vaisala frequency does not change, then these waves become vertically-propagating solutions. On a typical "m,k" dispersion diagram, the group velocity (energy) would be directed at right angles to the $n = 0$ (mixed Rossby-gravity waves) and $n = 1$ (gravity or Rossby waves) curves and would increase in the direction of increasing angular frequency. Typical group velocities for each component are the following: 1 cm/s for gravity waves and 2 mm/s for planetary (Rossby) waves.

These vertically-propagating mixed Rossby-gravity waves were first observed in the stratosphere as westward-propagating mixed waves by M. Yanai. They had the following characteristics: 4–5 days, horizontal wavenumbers of 4 (four waves circling the earth, corresponding to wavelengths of 10,000 km), vertical wavelengths of 4–8 km, and upward group velocity. Similarly, westward-propagating mixed waves were also found in the Atlantic Ocean by Weisberg et al. (1979) with periods of 31 days, horizontal wavelengths of 1200 km, vertical wavelengths of 1 km, and downward group velocity. Also, the vertically-propagating gravity wave component was found in the stratosphere with periods of 35 hours, horizontal wavelengths of 2400 km, and vertical wavelengths of 5 km.

Chapter- 7

Tsunami

Tsunami striking Thailand on December 26, 2004

A **tsunami** or **tidal wave** is a series of water waves (called a **tsunami wave train**) caused by the displacement of a large volume of a body of water, usually an ocean, but can occur in large lakes. Tsunamis are a frequent occurrence in Japan; approximately 195 events have been recorded. Due to the immense volumes of water and energy involved, tsunamis can devastate coastal regions.

Earthquakes, volcanic eruptions and other underwater explosions (including detonations of underwater nuclear devices), landslides and other mass movements, meteorite ocean

impacts or similar impact events, and other disturbances above or below water all have the potential to generate a tsunami.

The Greek historian Thucydides was the first to relate tsunami to submarine earthquakes, but understanding of tsunami's nature remained slim until the 20th century and is the subject of ongoing research. Many early geological, geographical, and oceanographic texts refer to tsunamis as "**seismic sea waves**."

Some meteorological conditions, such as deep depressions that cause tropical cyclones, can generate a storm surge, called a meteotsunami, which can raise tides several metres above normal levels. The displacement comes from low atmospheric pressure within the centre of the depression. As these storm surges reach shore, they may resemble (though are not) tsunamis, inundating vast areas of land. Such a storm surge inundated Burma in May 2008.

Etymology

The term *tsunami* comes from the Japanese, meaning "**harbor**" (*tsu*, 津) and "**wave**" (*nami*, 波). (For the plural, one can either follow ordinary English practice and add an *s*, or use an invariable plural as in the Japanese.)

Tsunami are sometimes referred to as **tidal waves**. In recent years, this term has fallen out of favor, especially in the scientific community, because tsunami actually have nothing to do with tides. The once-popular term derives from their most common appearance, which is that of an extraordinarily high tidal bore. Tsunami and tides both produce waves of water that move inland, but in the case of tsunami the inland movement of water is much greater and lasts for a longer period, giving the impression of an incredibly high tide. Although the meanings of "tidal" include "resembling" or "having the form or character of" the tides, and the term *tsunami* is no more accurate because tsunami are not limited to harbours, use of the term *tidal wave* is discouraged by geologists and oceanographers.

There are only a few other languages that have a native word for this disastrous wave. In the Tamil language, the word is *aazhi peralai*. In the Acehnese language, it is *ië beuna* or *alôn buluëk* (Depending on the dialect. Note that in the fellow Austronesian language of Tagalog, a major language in the Philippines, *alon* means "wave".) On Simeulue island, off the western coast of Sumatra in Indonesia, in the Defayan language the word is *smong*, while in the Sigulai language it is *emong*.

Generation mechanisms

The principal generation mechanism (or cause) of a tsunami is the displacement of a substantial volume of water or perturbation of the sea. This displacement of water is usually attributed to either earthquakes, landslides, volcanic eruptions, or more rarely by meteorites and nuclear tests. The waves formed in this way are then sustained by gravity.

It is important to note that tides do not play any part in the generation of tsunamis, hence referring to tsunamis as 'tidal waves' is inaccurate.

Seismicity generated tsunamis

Tsunamis can be generated when the sea floor abruptly deforms and vertically displaces the overlying water. Tectonic earthquakes are a particular kind of earthquake that are associated with the earth's crustal deformation; when these earthquakes occur beneath the sea, the water above the deformed area is displaced from its equilibrium position. More specifically, a tsunami can be generated when thrust faults associated with convergent or destructive plate boundaries move abruptly, resulting in water displacement, due to the vertical component of movement involved. Movement on normal faults will also cause displacement of the seabed, but the size of the largest of such events is normally too small to give rise to a significant tsunami.
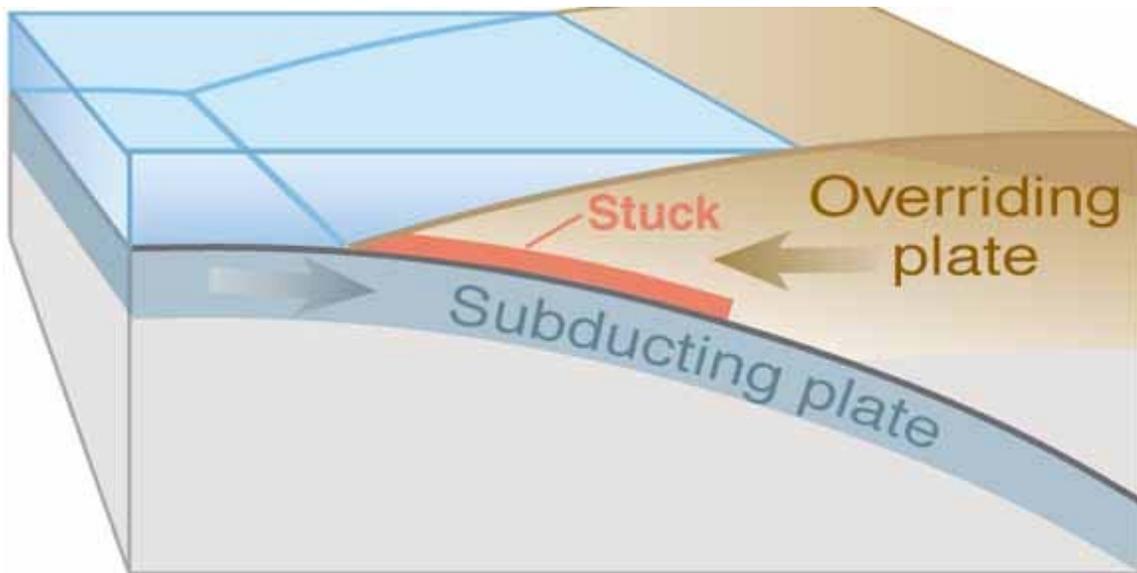
Drawing of tectonic plate boundary before earthquake.
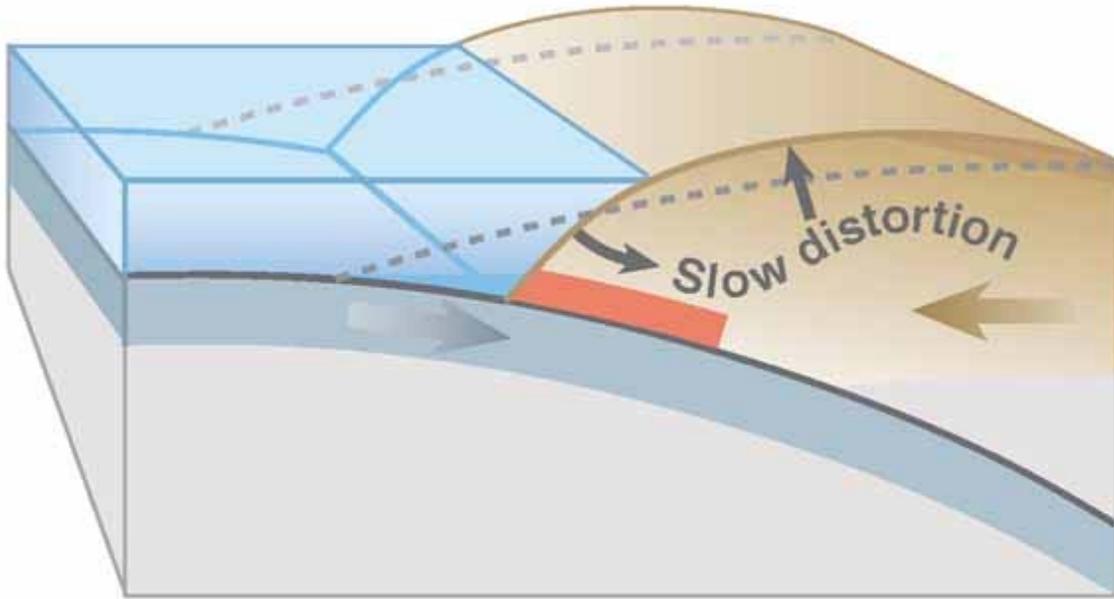
Overriding plate bulges under strain, causing tectonic uplift.

Earthquake starts tsunami

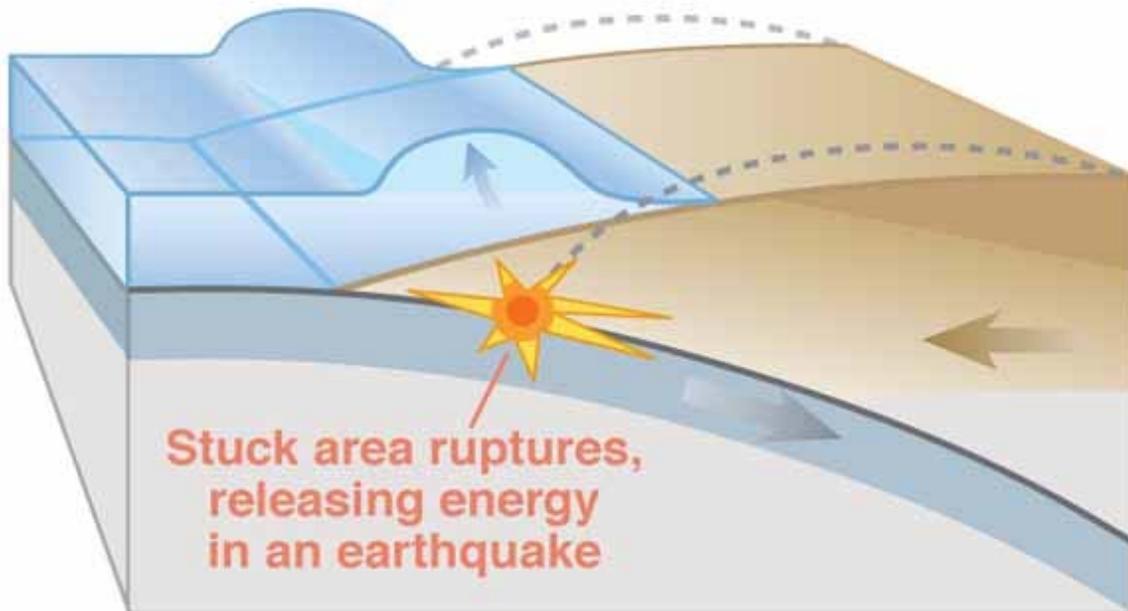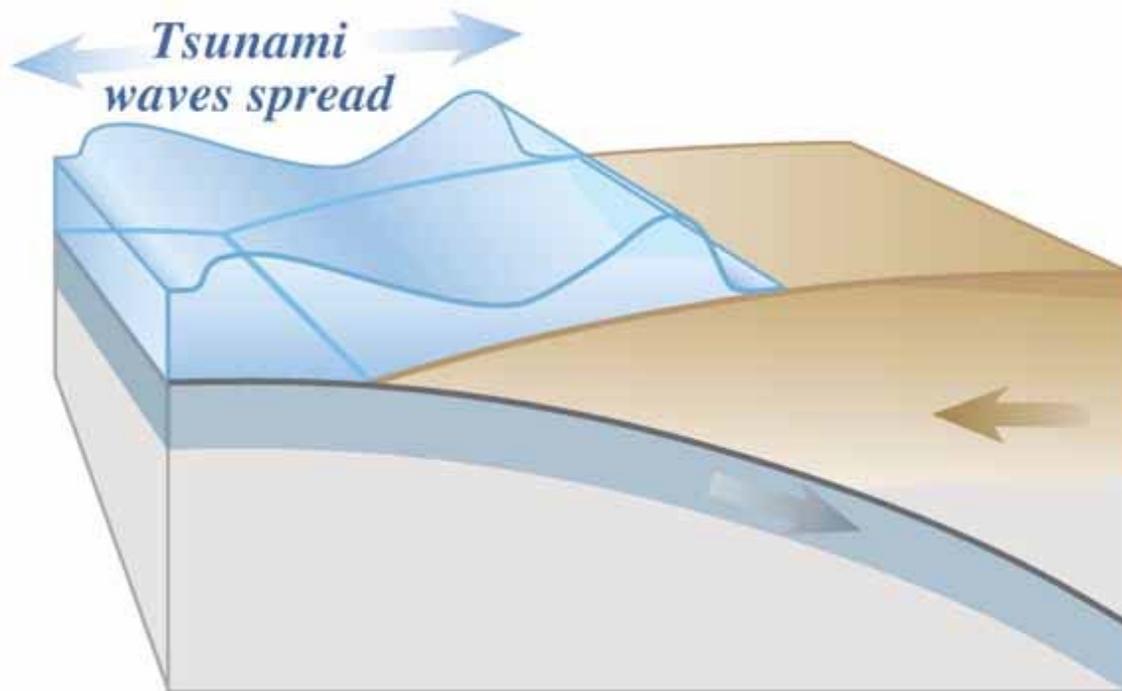Stuck area ruptures, releasing energy in an earthquake

Plate slips, causing subsidence and releasing energy into water.

The energy released produces tsunami waves.

Tsunamis have a small amplitude (wave height) offshore, and a very long wavelength (often hundreds of kilometers long), which is why they generally pass unnoticed at sea, forming only a slight swell usually about 300 millimetres (12 in) above the normal sea surface. They grow in height when they reach shallower water, in a wave shoaling process described below. A tsunami can occur in any tidal state and even at low tide can still inundate coastal areas.

On April 1, 1946, a magnitude-7.8 (Richter Scale) earthquake occurred near the Aleutian Islands, Alaska. It generated a tsunami which inundated Hilo on the island of Hawai'i with a 14 metres (46 ft) high surge. The area where the earthquake occurred is where the Pacific Ocean floor is subducting (or being pushed downwards) under Alaska.

Examples of tsunami at locations away from convergent boundaries include Storegga about 8,000 years ago, Grand Banks 1929, Papua New Guinea 1998 (Tappin, 2001). The Grand Banks and Papua New Guinea tsunamis came from earthquakes which destabilized sediments, causing them to flow into the ocean and generate a tsunami. They dissipated before traveling transoceanic distances.

The cause of the Storegga sediment failure is unknown. Possibilities include an overloading of the sediments, an earthquake or a release of gas hydrates (methane etc.)

The 1960 Valdivia earthquake (M_w 9.5) (19:11 hrs UTC), 1964 Alaska earthquake (M_w 9.2), and 2004 Indian Ocean earthquake (M_w 9.2) (00:58:53 UTC) are recent examples of

powerful megathrust earthquakes that generated tsunamis (known as teletsunamis) that can cross entire oceans. Smaller (M_w 4.2) earthquakes in Japan can trigger tsunamis (called **local** and **regional tsunamis**) that can only devastate nearby coasts, but can do so in only a few minutes.

In the 1950s, it was discovered that larger tsunamis than had previously been believed possible could be caused by giant landslides. These phenomena rapidly displace large water volumes, as energy from falling debris or expansion transfers to the water at a rate faster than the water can absorb. Their existence was confirmed in 1958, when a giant landslide in Lituya Bay, Alaska, caused the highest wave ever recorded, which had a height of 524 metres (over 1700 feet). The wave didn't travel far, as it struck land almost immediately. Two people fishing in the bay were killed, but another boat amazingly managed to ride the wave. Scientists named these waves megatsunami.

Scientists discovered that extremely large landslides from volcanic island collapses can generate megatsunami, that can travel trans-oceanic distances.

Characteristics
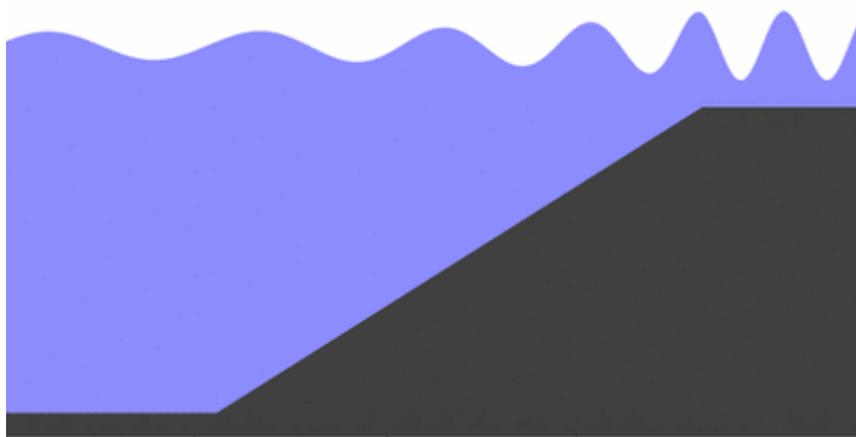
When the wave enters shallow water, it slows down and its amplitude (height) increases.
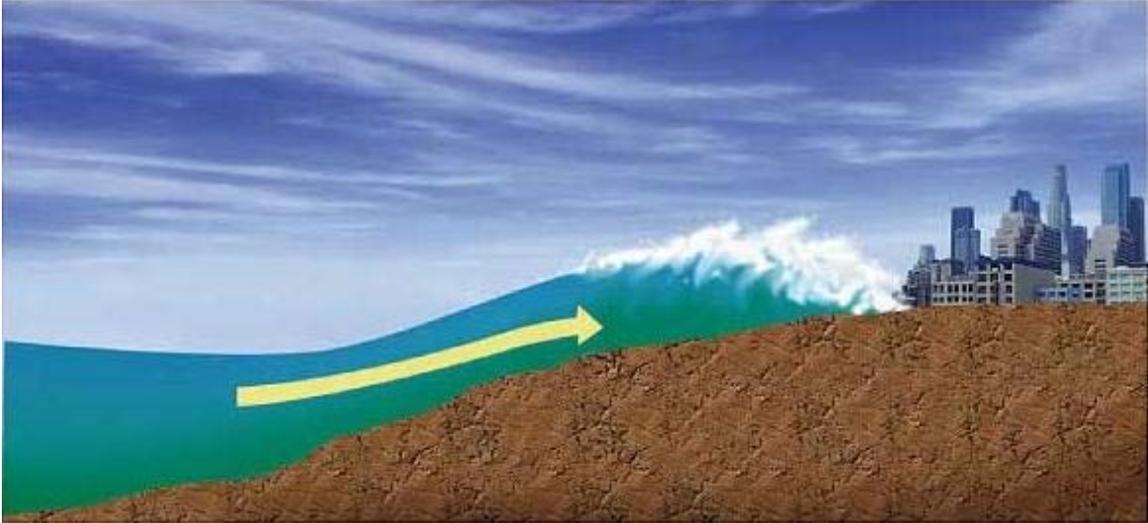
The wave further slows and amplifies as it hits land. Only the largest waves crest.

While everyday wind waves have a wavelength (from crest to crest) of about 100 metres (330 ft) and a height of roughly 2 metres (6.6 ft), a tsunami in the deep ocean has a wavelength of about 200 kilometres (120 mi). Such a wave travels at well over 800 kilometres per hour (500 mph), but due to the enormous wavelength the wave oscillation at any given point takes 20 or 30 minutes to complete a cycle and has an amplitude of only about 1 metre (3.3 ft). This makes tsunamis difficult to detect over deep water. Ships rarely notice their passage.

As the tsunami approaches the coast and the waters become shallow, wave shoaling compresses the wave and its velocity slows below 80 kilometres per hour (50 mph). Its wavelength diminishes to less than 20 kilometres (12 mi) and its amplitude grows enormously, producing a distinctly visible wave. Since the wave still has such a long wavelength, the tsunami may take minutes to reach full height. Except for the very largest tsunamis, the approaching wave does not break (like a surf break), but rather appears like a fast moving tidal bore. Open bays and coastlines adjacent to very deep water may shape the tsunami further into a step-like wave with a steep-breaking front.

When the tsunami's wave peak reaches the shore, the resulting temporary rise in sea level is termed 'run up'. Run up is measured in metres above a reference sea level. A large tsunami may feature multiple waves arriving over a period of hours, with significant time between the wave crests. The first wave to reach the shore may not have the highest run up.

About 80% of tsunamis occur in the Pacific Ocean, but are possible wherever there are large bodies of water, including lakes. They are caused by earthquakes, landslides, volcanic explosions, and bolides.

Drawback

If the first part of a tsunami to reach land is a trough—called a **drawback**—rather than a wave crest, the water along the shoreline recedes dramatically, exposing normally submerged areas.

A drawback occurs because the water propagates outwards with the trough of the wave at its front. Drawback begins before the wave arrives at an interval equal to half of the wave's period. Drawback can exceed hundreds of metres, and people unaware of the danger sometimes remain near the shore to satisfy their curiosity or to collect fish from the exposed seabed. During the Indian Ocean tsunami, the sea withdrew and many people went onto the exposed sea bed to investigate. Photos show people walking on the normally submerged areas with the advancing wave in the background. Few survived.

Scales of intensity and magnitude

As with earthquakes, several attempts have been made to set up scales of tsunami intensity or magnitude to allow comparison between different events.

Intensity scales

The first scales used routinely to measure the intensity of tsunami were the *Sieberg-Ambraseys scale*, used in the Mediterranean Sea and the *Imamura-Iida intensity scale*, used in the Pacific Ocean. The latter scale was modified by Soloviev, who calculated the Tsunami intensity I according to the formula

$$I = \frac{1}{2} + \log_2 H_{av}$$

where H_{av} is the average wave height along the nearest coast. This scale, known as the *Soloviev-Imamura tsunami intensity scale*, is used in the global tsunami catalogues compiled by the NGDC/NOAA and the Novosibirsk Tsunami Laboratory as the main parameter for the size of the tsunami.

Magnitude scales

The first scale that genuinely calculated a magnitude for a tsunami, rather than an intensity at a particular location was the ML scale proposed by Murty & Loomis based on the potential energy. Difficulties in calculating the potential energy of the tsunami mean that this scale is rarely used. Abe introduced the *tsunami magnitude scale M_t*, calculated from,

$$M_t = a \log h + b \log R = D$$

where *h* is the maximum tsunami-wave amplitude (in m) measured by a tide gauge at a distance *R* from the epicenter, *a*, *b* & *D* are constants used to make the M_t scale match as closely as possible with the moment magnitude scale.

Warnings and predictions

One of the deep water buoys used in the DART tsunami warning system

Drawbacks can serve as a brief warning. People who observe drawback (many survivors report an accompanying sucking sound), can survive only if they immediately run for high ground or seek the upper floors of nearby buildings. In 2004, ten-year old Tilly Smith of Surrey, England, was on Maikhao beach in Phuket, Thailand with her parents and sister, and having learned about tsunamis recently in school, told her family that a tsunami might be imminent. Her parents warned others minutes before the wave arrived, saving dozens of lives. She credited her geography teacher, Andrew Kearney.

In the 2004 Indian Ocean tsunami drawback was not reported on the African coast or any other eastern coasts it reached. This was because the wave moved downwards on the eastern side of the fault line and upwards on the western side. The western pulse hit coastal Africa and other western areas.

A tsunami cannot be precisely predicted, even if the magnitude and location of an earthquake is known. Geologists, oceanographers, and seismologists analyse each earthquake and based on many factors may or may not issue a tsunami warning. However, there are some warning signs of an impending tsunami, and automated systems can provide warnings immediately after an earthquake in time to save lives. One of the most successful systems uses bottom pressure sensors that are attached to buoys. The sensors constantly monitor the pressure of the overlying water column. This is deduced through the calculation:

$$P = \rho g h$$

where
P = the overlying pressure in newtons per metre square,
ρ = the density of the seawater= 1.1×10^3 kg/m^3,
g = the acceleration due to gravity= 9.8 m/s^2 and
h = the height of the water column in metres.

Hence for a water column of 5,000 m depth the overlying pressure is equal to

$$P = \rho g h = \left(1.1 \times 10^3 \, \frac{\text{kg}}{\text{m}^3}\right) \left(9.8 \, \frac{\text{m}}{\text{s}^2}\right) \left(5.0 \times 10^3 \, \text{m}\right) = 5.4 \times 10^7 \, \frac{\text{N}}{\text{m}^2} = 54 \, \text{MPa}$$

or about 5500 tonnes-force per square metre.

Regions with a high tsunami risk typically use tsunami warning systems to warn the population before the wave reaches land. On the west coast of the United States, which is prone to Pacific Ocean tsunami, warning signs indicate evacuation routes. In Japan, the community is well-educated about earthquakes and tsunamis, and along the Japanese shorelines the tsunami warning signs are reminders of the natural hazards together with a network of warning sirens, typically at the top of the cliff of surroundings hills.

The Pacific Tsunami Warning System is based in Honolulu, Hawai'i. It monitors Pacific Ocean seismic activity. A sufficiently large earthquake magnitude and other information triggers a tsunami warning. While the subduction zones around the Pacific are seismically active, not all earthquakes generate tsunami. Computers assist in analysing the tsunami risk of every earthquake that occurs in the Pacific Ocean and the adjoining land masses.

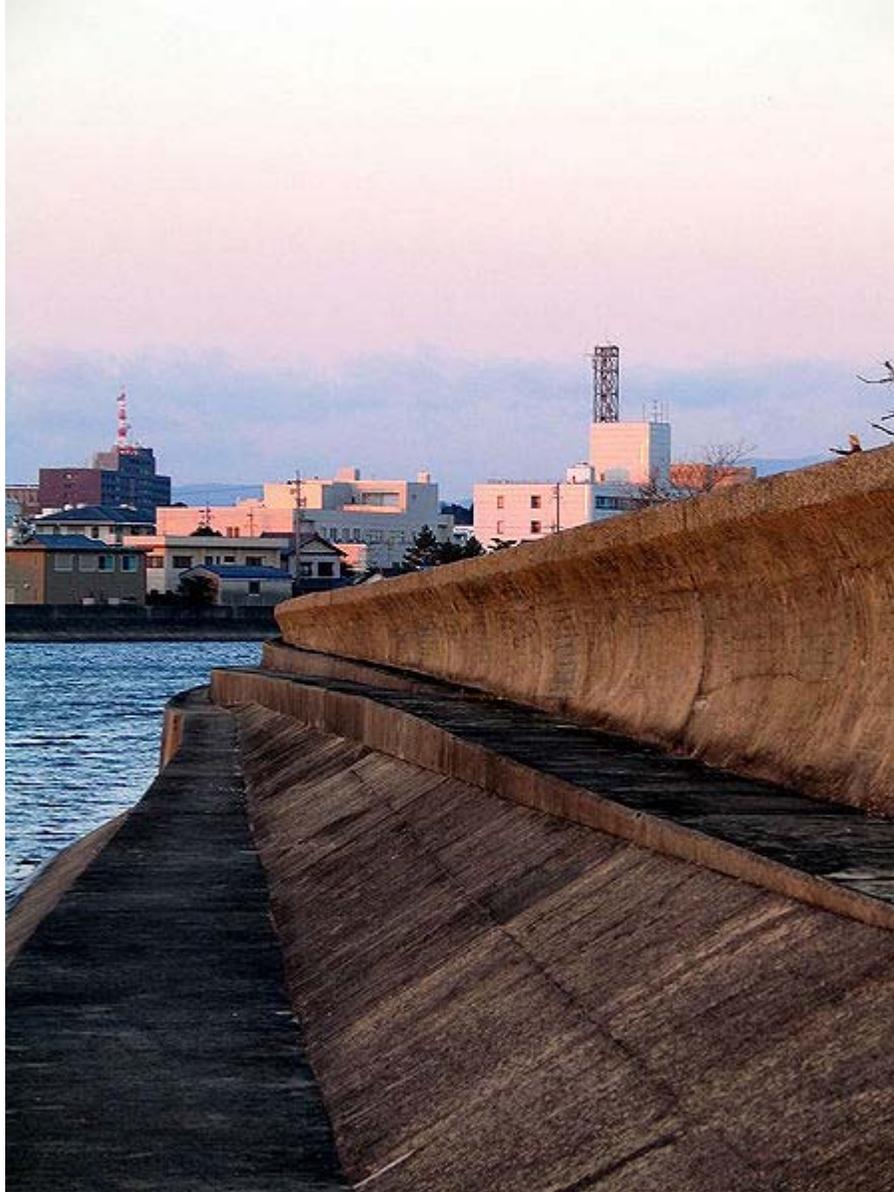Tsunami hazard sign at Bamfield, British Columbia

A tsunami warning sign on a seawall in Kamakura, Japan, 2004.

The monument to the victims of tsunami at Laupahoehoe, Hawaii

Tsunami memorial in Kanyakumari beach

A seawall at Tsu, Japan

Tsunami Evacuation Route signage along U.S. Route 101, in Washington

As a direct result of the Indian Ocean tsunami, a re-appraisal of the tsunami threat for all coastal areas is being undertaken by national governments and the United Nations Disaster Mitigation Committee. A tsunami warning system is being installed in the Indian Ocean.

Computer models can predict tsunami arrival, usually within minutes of the arrival time. Bottom pressure sensors relay information in real time. Based on these pressure readings and other seismic information and the seafloor's shape (bathymetry) and coastal topography, the models estimate the amplitude and surge height of the approaching tsunami. All Pacific Rim countries collaborate in the Tsunami Warning System and most regularly practice evacuation and other procedures. In Japan, such preparation is mandatory for government, local authorities, emergency services and the population.

Some zoologists hypothesise that some animal species have an ability to sense subsonic Rayleigh waves from an earthquake or a tsunami. If correct, monitoring their behavior could provide advance warning of earthquakes, tsunami etc. However, the evidence is controversial and is not widely accepted. There are unsubstantiated claims about the Lisbon quake that some animals escaped to higher ground, while many other animals in the same areas drowned. The phenomenon was also noted by media sources in Sri Lanka in the 2004 Indian Ocean earthquake. It is possible that certain animals (e.g., elephants) may have heard the sounds of the tsunami as it approached the coast. The elephants' reaction was to move away from the approaching noise. By contrast, some humans went to the shore to investigate and many drowned as a result.

It is not possible to prevent a tsunami. However, in some tsunami-prone countries some earthquake engineering measures have been taken to reduce the damage caused on shore. Japan built many tsunami walls of up to 4.5 metres (15 ft) to protect populated coastal areas. Other localities have built floodgates and channels to redirect the water from incoming tsunami. However, their effectiveness has been questioned, as tsunami often overtop the barriers. For instance, the Okushiri, Hokkaidō tsunami which struck Okushiri Island of Hokkaidō within two to five minutes of the earthquake on July 12, 1993 created waves as much as 30 metres (100 ft) tall—as high as a 10-story building. The port town of Aonae was completely surrounded by a tsunami wall, but the waves washed right over the wall and destroyed all the wood-framed structures in the area. The wall may have succeeded in slowing down and moderating the height of the tsunami, but it did not prevent major destruction and loss of life.

Natural factors such as shoreline tree cover can mitigate tsunami effects. Some locations in the path of the 2004 Indian Ocean tsunami escaped almost unscathed because trees such as coconut palms and mangroves absorbed the tsunami's energy. In one striking example, the village of Naluvedapathy in India's Tamil Nadu region suffered only minimal damage and few deaths because the wave broke against a forest of 80,244 trees planted along the shoreline in 2002 in a bid to enter the Guinness Book of Records. Environmentalists have suggested tree planting along tsunami-prone seacoasts. Trees require years to grow to a useful size, but such plantations could offer a much cheaper and longer-lasting means of tsunami mitigation than artificial barriers.

Mitigation

Natural barriers

A report published by the United Nations Environment Programme (UNEP) suggests that the tsunami of 26th December 2004 caused less damage in the areas where natural barriers were present, such as mangroves, coral reefs or coastal vegetation. A Japanese study of this tsunami in Sri Lanka used satellite imagery modelling to establish the parameters of coastal resistance as a function of different types of trees.

History
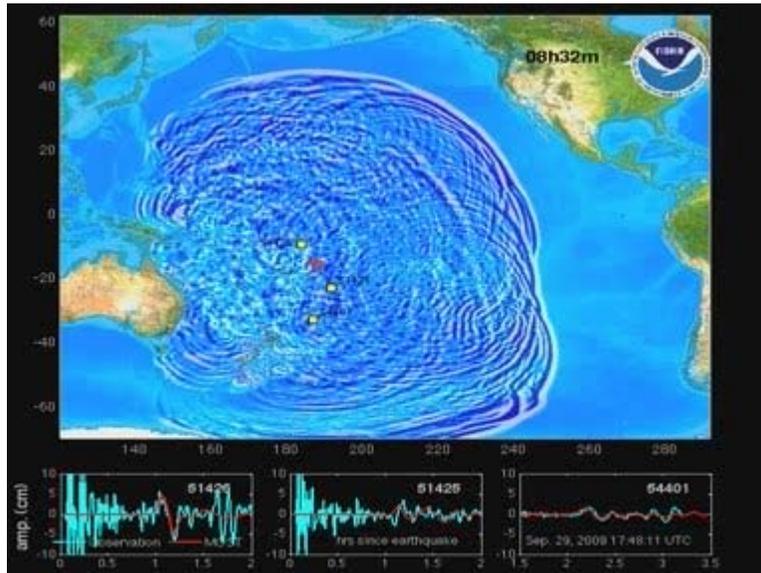
The Samoan tsunami of September 2009

A devastated Marina beach in Chennai after the Indian Ocean Tsunami

Destructive tsunamis have been recorded throughout history, for example there were 26 that caused 200 or more deaths in the last century alone. Of these, many were recorded in the Asia–Pacific region, particularly around Japan and Indonesia.

Ancient history

As early as 426 B.C. the Greek historian Thucydides inquired in his book *History of the Peloponnesian War* about the causes of tsunami, and was the first to argue that ocean earthquakes must be the cause.

The cause, in my opinion, of this phenomenon must be sought in the earthquake. At the point where its shock has been the most violent the sea is driven back, and suddenly recoiling with redoubled force, causes the inundation. Without an earthquake I do not see how such an accident could happen.

The Roman historian Ammianus Marcellinus (*Res Gestae* 26.10.15-19) described the typical sequence of a tsunami, including an incipient earthquake, the sudden retreat of the sea and a following gigantic wave, after the 365 A.D. tsunami devastated Alexandria.

2004 Indian Ocean tsunami

The 2004 Indian Ocean earthquake and tsunami killed over 200,000 people with many bodies either being lost to the sea or unidentified.

According to an article in *Geographical* magazine (April 2008), the Indian Ocean tsunami of December 26, 2004 was not the worst that the region could expect. Professor Costas Synolakis of the Tsunami Research Center at the University of Southern California co-authored a paper in *Geophysical Journal International* which suggests that a future tsunami in the Indian Ocean basin could affect locations such as Madagascar, Singapore, Somalia, Western Australia, and many others.

As a weapon

There have been studies and some attempt to create tsunami waves as a weapon. In World War II, the army in New Zealand trialled explosives in the area of today's Shakespeare Regional Park to create small tsunamis, an attempt which failed.

Chapter- 8

Internal Tide

Internal tides are generated as the surface tides move stratified water up and down sloping topography, which produces a wave in the ocean interior. So internal tides are internal waves at a tidal frequency. The other major source of internal waves is the wind which produces internal waves near the inertial frequency. When a small water parcel is displaced from its equilibrium position, it will return either downwards due to gravity or upwards due to buoyancy. The water parcel will overshoot its original equilibrium position and this disturbance will set off an internal gravity wave. Munk (1981) notes, "Gravity waves in the ocean's interior are as common as waves at the sea surface-perhaps even more so, for no one has ever reported an interior calm."

Simple explanation

Simple interfacial internal wave

Barotropic Wave

$2\pi/k = $ one wavelength

$$h = -h_0\cos(kx - \omega t)$$

$$U_1 = \frac{\omega h_0}{H_1 k}\cos(kx - \omega t)$$

$$U_2 = -\frac{\omega h_0}{H_2 k}\cos(kx - \omega t)$$

Baroclinic Wave
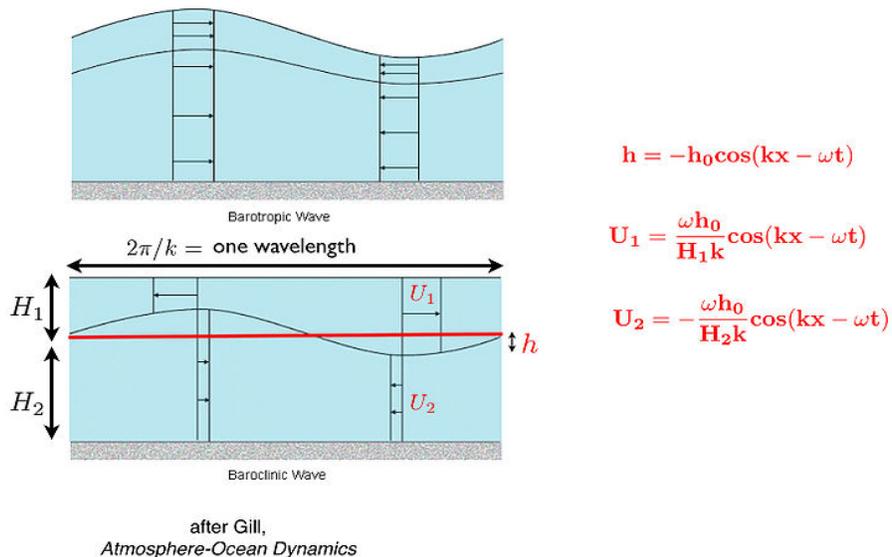
after Gill,
Atmosphere-Ocean Dynamics

Figure 1: Water parcels in the whole water column move together with the surface tide (top), while shallow and deep waters move in opposite directions in an internal tide

(bottom). The surface displacement and interface displacement are the same for a surface wave (top), while for an internal wave the surface displacements are very small, while the interface displacements are large (bottom). This figure is a modified version of one appearing in Gill (1982).

The surface tide propagates as a wave, in which water parcels in the whole water column oscillate in the same direction at a given phase (i.e, in the trough or at the crest, Fig. 1, top). At the simplest level, an internal wave can be thought of as an interfacial wave (Fig. 1, bottom). If there are two levels in the ocean, such as a warm surface layer and cold deep layer separated by a thermocline,then motions on the interface are possible. The interface movement is large compared to surface movement. The restoring force for internal waves and tides is still gravity but its effect is reduced because the densities of the 2 layers are relatively similar compared to the large density difference at the air-sea interface. Thus larger displacements are possible inside the ocean than at the sea surface.

Tides occur mainly at diurnal and semidiurnal periods. The principal lunar semidiurnal constituent is known as M2 and generally has the largest amplitudes.

Where are internal tides found?

The largest internal tides are generated at steep, midocean topography such as the Hawaiian Ridge, Tahiti, the Macquarie Ridge, and submarine ridges in the Luzon Strait. Continental slopes such as the Australian North West Shelf also generate large internal tides. These internal tide may propagate onshore and dissipate much like surface waves. Or internal tides may propagate away from the topography into the open ocean. For tall, steep, midocean topography, such as the Hawaiian Ridge, it is estimated that about 85% of the energy in the internal tide propagates away into the deep ocean with about 15% of its energy being lost within about 50 km of the generation site. The lost energy contributes to turbulence and mixing near the generation sites.   It is not clear where the energy that leaves the generation site is dissipated, but there are 3 possible processes: 1) the internal tides scatter and/or break at distant midocean topography, 2) interactions with other internal waves remove energy from the internal tide, or 3) the internal tides shoal and break on continental shelves.

Where do internal tides go and what happens to them along the way?

Briscoe (1975) succinctly noted that "We cannot yet answer satisfactorily the questions: 'where does the internal wave energy come from, where does it go, and what happens to it along the way?'" Although technological advances in instrumentation and modeling have produced greater knowledge of internal tide and near-inertial wave generation, Garrett and Kunze (2007) observed 33 years later that "The fate of the radiated [large-scale internal tides] is still uncertain. They may scatter into [smaller scale waves] on further encounter with islands or the rough seafloor , or transfer their energy to smaller-scale internal waves in the ocean interior " or "break on distant continental slopes ". It is

now known that most of the internal tide energy generated at tall, steep midocean topography radiates away as large-scale internal waves. This radiated internal tide energy is one of the main sources of energy into the deep ocean, roughly half of the wind energy input . Broader interest in internal tides is spurred by their impact on the magnitude and spatial inhomogeneity of mixing, which in turn has first order effect on the meridional overturning circulation   .

The internal tidal energy in one tidal period going through an area perpendicular to the direction of propagation is called the energy flux and is measured in Watts/m^2. The energy flux at one point can be summed over depth- this is the depth-integrated energy flux and is measured in Watts/m. The Hawaiian Ridge produces depth-integrated energy fluxes as large as 10 kW/m. The longest wavelength waves are the fastest and thus carry most of the energy flux. Near Hawaii, the typical wavelength of the longest internal tide is about 150 km while the next longest is about 75 km. These waves are called mode 1 and mode 2, respectively. Although Fig. 1 shows there is no sea surface expression of the internal tide, there actually is a displacement of a few centimeters. These sea surface expressions of the internal tide at different wavelengths can be detected with the Topex/Poseidon or Jason-1 satellites (Fig. 2). Near 15 N, 175 W on the Line Islands Ridge, the mode-1 internal tides scatter off the topography, possibly creating turbulence and mixing, and producing smaller wavelength mode 2 internal tides.
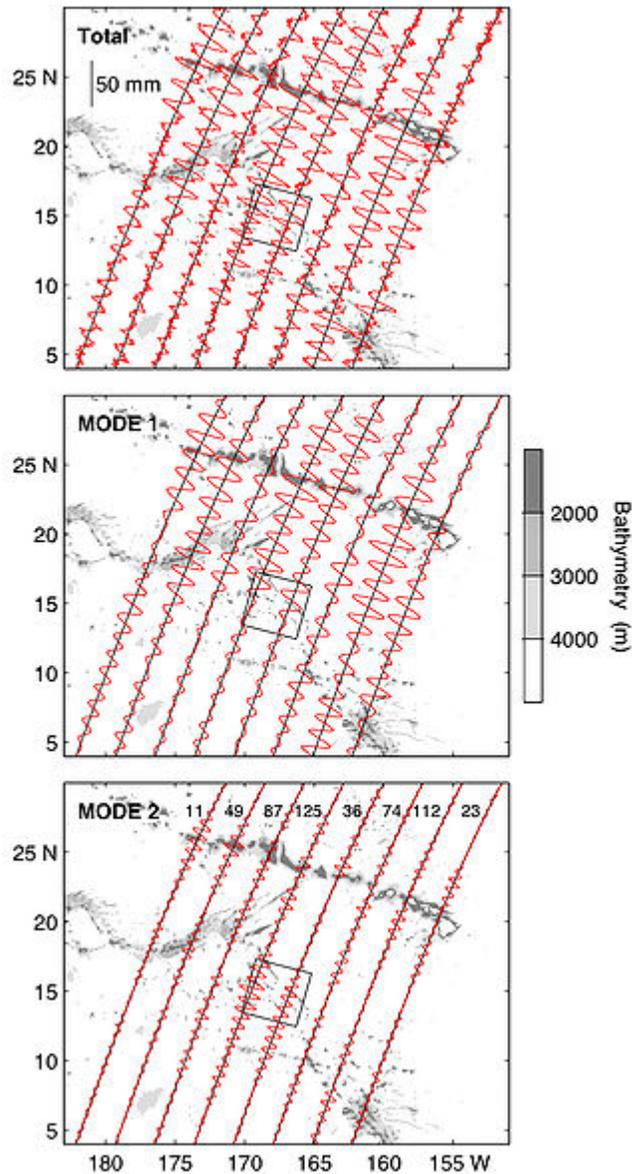
Figure 2: The internal tide sea surface elevation that is in phase with the surface tide (i.e., crests occur in a certain spot at a certain time that are both the same relative to the surface tide) can be detected by satellite (top). (The satellite track is repeated about every 10 days and so M2 tidal signals are shifted to longer periods due to aliasing.) The longest internal tide wavelengths are about 150 km near Hawaii and the next longest waves are about 75 km long. The surface displacements due to the internal tide are plotted as wiggly red lines with amplitudes plotted perpendicular to the satellite groundtracks (black lines). Figure is adapted from Johnston et al. (2003).

The inescapable conclusion is that energy is lost from the surface tide to the internal tide at midocean topography and continental shelves, but the energy in the internal tide is not necessarily lost in the same place. Internal tides may propagate thousands of kilometers or more before breaking and mixing the abyssal ocean.

Their importance to abyssal mixing and the meridional overturning circulation

The importance of internal tides and internal waves in general relates to their breaking, energy dissipation, and mixing of the deep ocean. If there were no mixing in the ocean, the deep ocean would be a cold stagnant pool with a thin warm surface layer. While the meridional overturning circulation (also referred to as the thermohaline circulation) redistributes about 2 PW of heat from the tropics to polar regions, the energy source for this flow is the interior mixing which is comparatively much smaller- about 2 TW. Sandstrom (1908) showed a fluid which is both heated and cooled at its surface cannot develop a deep overturning circulation. Most global models have incorporated uniform mixing throughout the ocean because they do not include or resolve internal tidal flows.

However, models are now beginning to include spatially variable mixing related to internal tides and the rough topography where they are generated and distant topography where they may break. Wunsch and Ferrari (2004) describe the global impact of spatially inhomogeneous mixing near midocean topography: "A number of lines of evidence, none complete, suggest that the oceanic general circulation, far from being a heat engine, is almost wholly governed by the forcing of the wind field and secondarily by deep water tides... The now inescapable conclusion that over most of the ocean significant 'vertical' mixing is confined to topographically complex boundary areas implies a potentially radically different interior circulation than is possible with uniform mixing. Whether ocean circulation models... neither explicitly accounting for the energy input into the system nor providing for spatial variability in the mixing, have any physical relevance under changed climate conditions is at issue." There is a limited understanding of "the sources controlling the internal wave energy in the ocean and the rate at which it is dissipated" and are only now developing some "parameterizations of the mixing generated by the interaction of internal waves, mesoscale eddies, high-frequency barotropic fluctuations, and other motions over sloping topography."

Internal tides at the beach

Internal tides may also dissipate on continental slopes and shelves or even reach within 100 m of the beach (Fig. 3). Internal tides bring pulses of cold water shoreward and produce large vertical temperature differences. When surface waves break, the cold water is mixed upwards making the water cold for surfers, swimmers, and other beachgoers. Surface waters in the surf zone can change by about 10°C in about an hour.
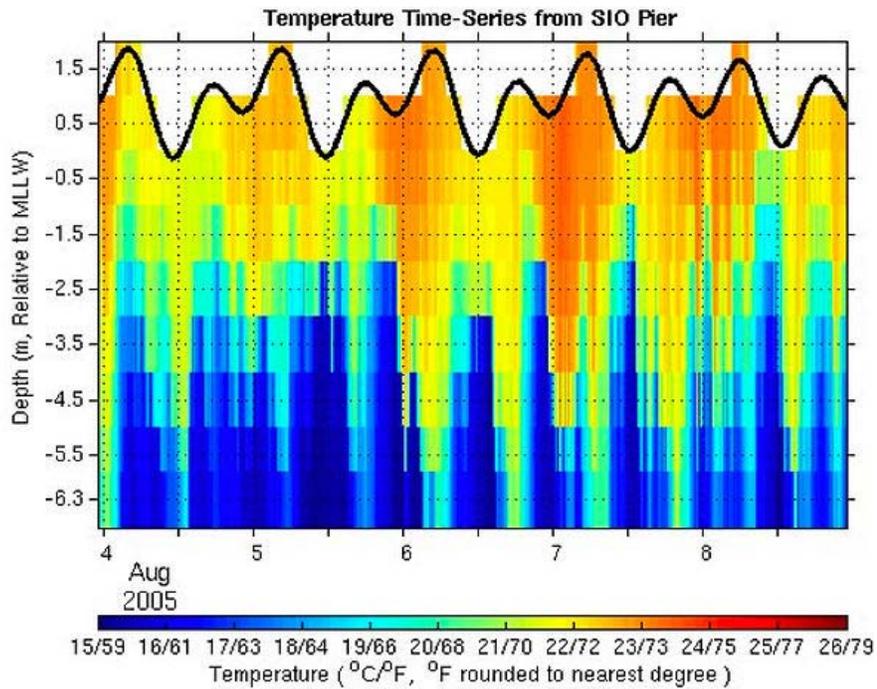
Figure 3: The internal tide produces large vertical differences in temperature at the research pier at the Scripps Institution of Oceanography. The black line shows the surface tide elevation relative to mean lower low water (MLLW). Figure provided by Eric Terrill, Scripps Institution of Oceanography with funding from the U.S. Office of Naval Research

Chapter- 9

Earth Tide

Earth tide is the sub-meter motion of the Earth of about 12 hours or longer caused by Moon and Sun gravitation, also called *body tide* which is the largest contribution globally. The largest body tide contribution is from the semidiurnal constituents, but there are also significant diurnal constituents. There also semi-annual and fortnightly contributions due to the axial tilt. The use of the word *tide* is by analogy, and although the forcing is quite similar, the responses are quite different.

Tidal forcing
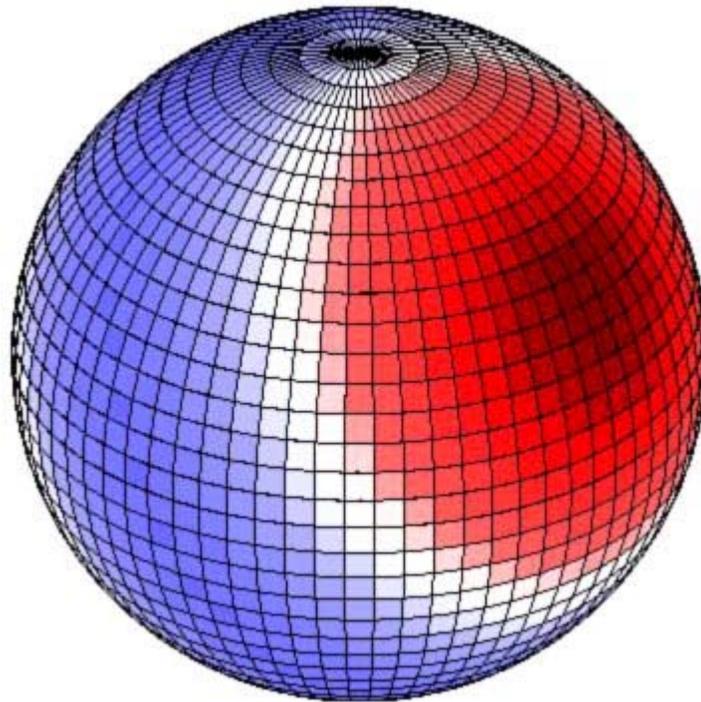
*A*. Lunar tidal forcing: this depicts the Moon directly over 30° N (or 30° S) viewed from above the Northern Hemisphere.
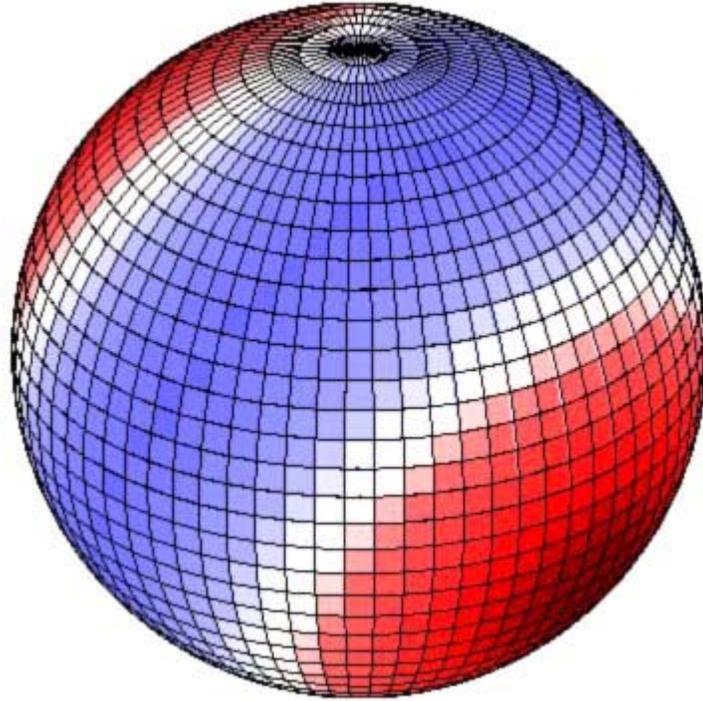
B. This view shows same forcing from 180° from view *A*. Viewed from above the Northern Hemisphere. Red up, blue down.

The larger of the periodic gravitational forcings is from the Moon but that of the Sun is also important. The images here show lunar tidal forcing when the Moon appears directly over 30° N (or 30° S). This pattern remains fixed with the red area directed toward (or directly away from) the Moon. Red indicates upward pull, blue downward. If, for example the Moon is directly over 90° W (or 90° E), the center of the red areas are centered on the western northern hemisphere, on upper right. Red up, blue down. If for example the Moon is directly over 90° W (90° E), the center of the red area is 30° N, 90° W and 30° S, 90° E, and the center of the bluish band follows the great circle equidistant from those points. At 30° latitude a strong peak occurs once per lunar day, giving significant diurnal forcing at that latitude. Along the equator two equally sized peaks (and depressions) are equally sized, giving semi-diurnal forcing there.

Body tide
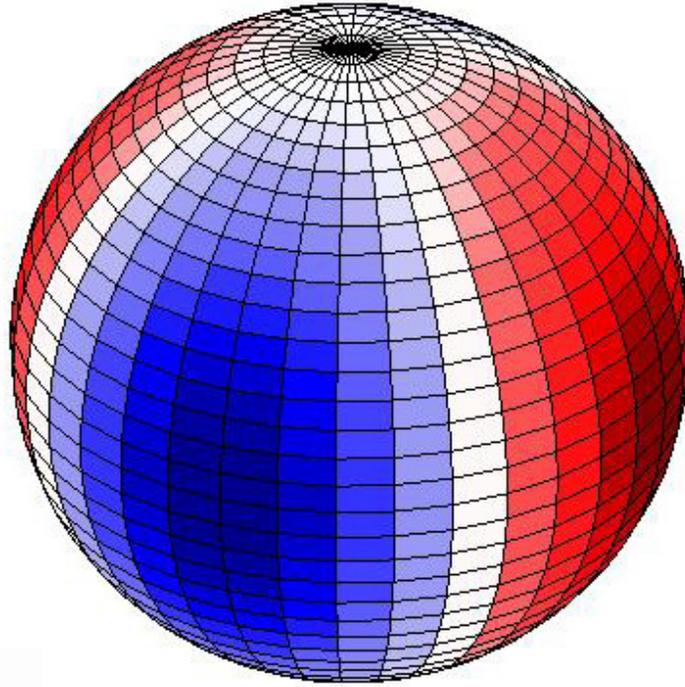
Vertical displacements of sectorial movement. Red up, blue down
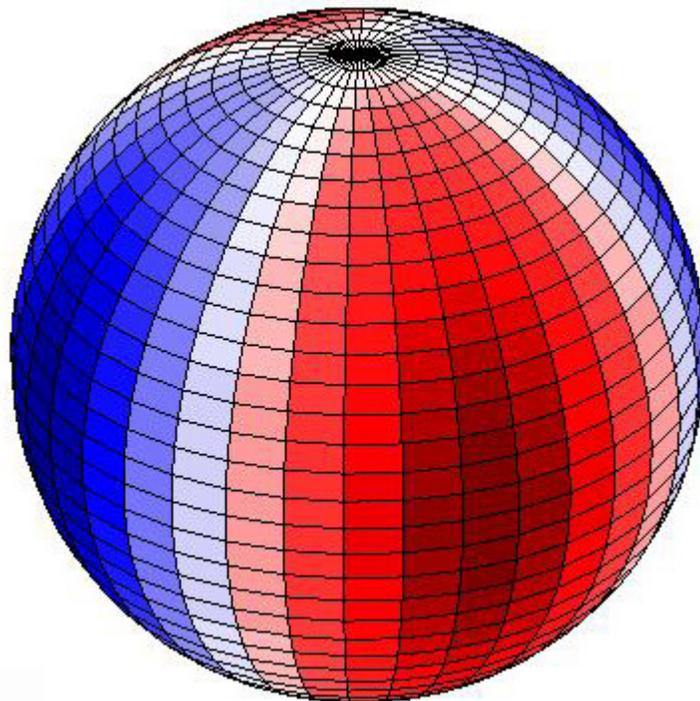
East-west displacements of sectorial movement. Red east, blue west.

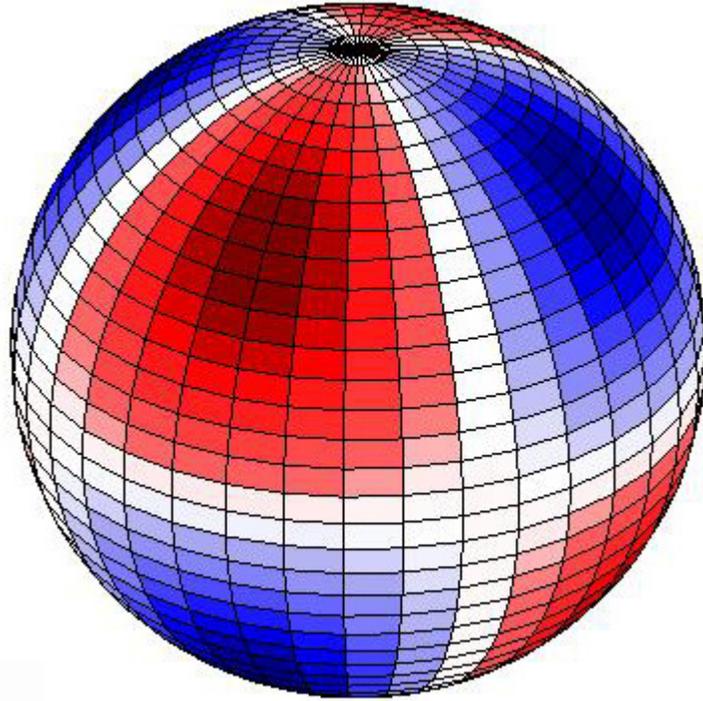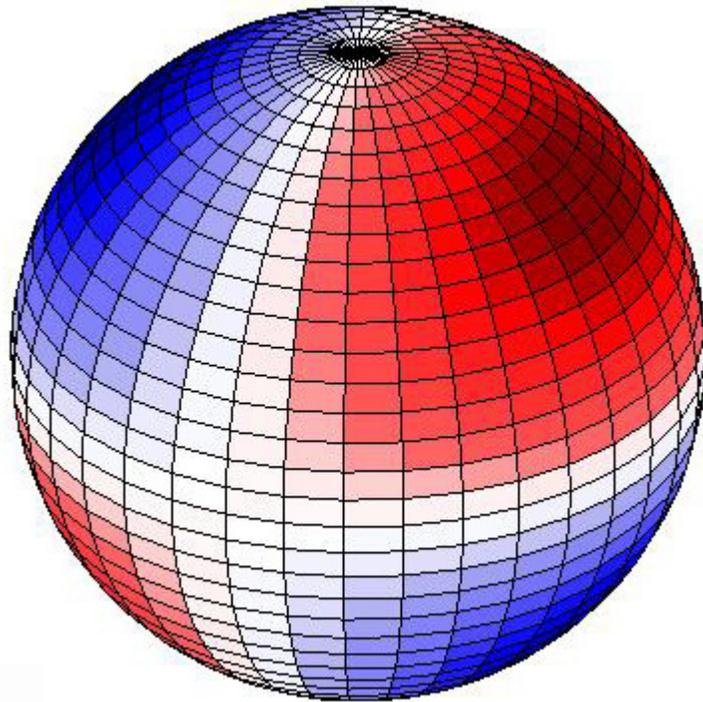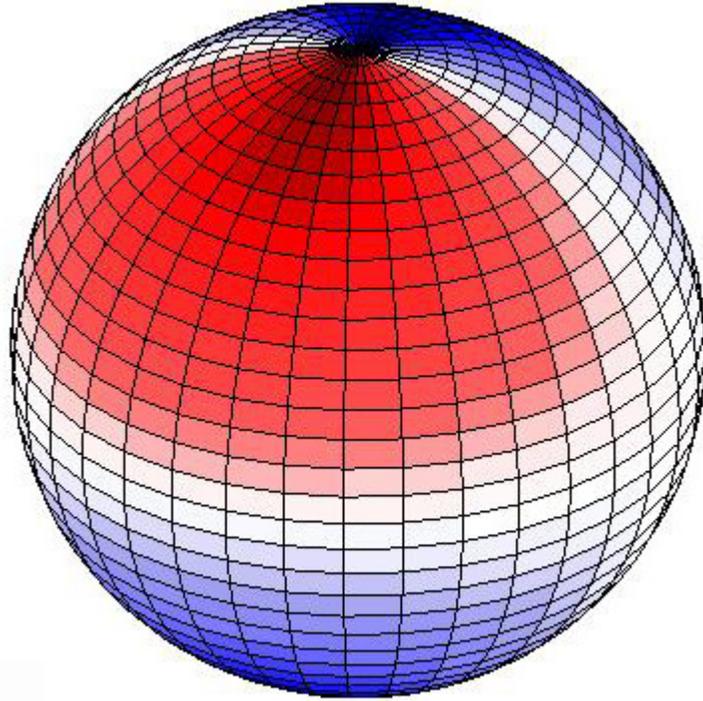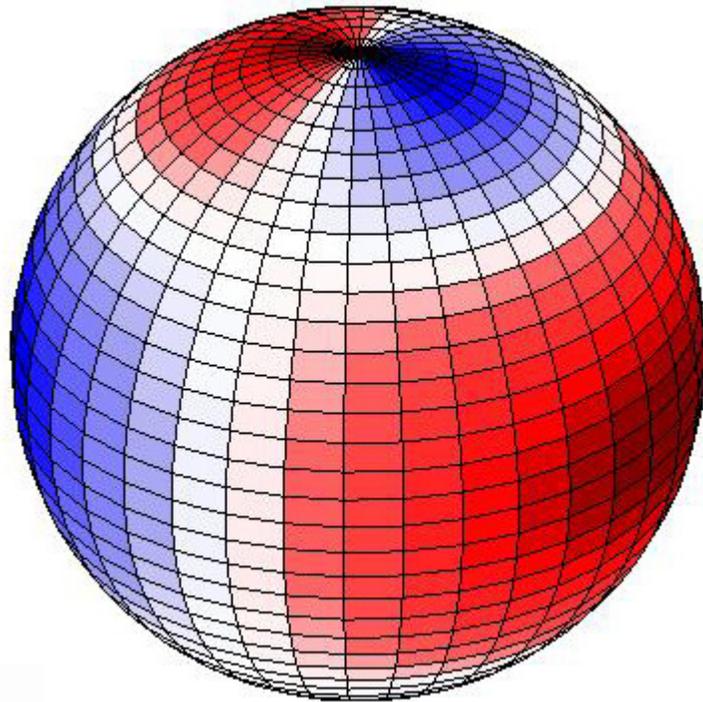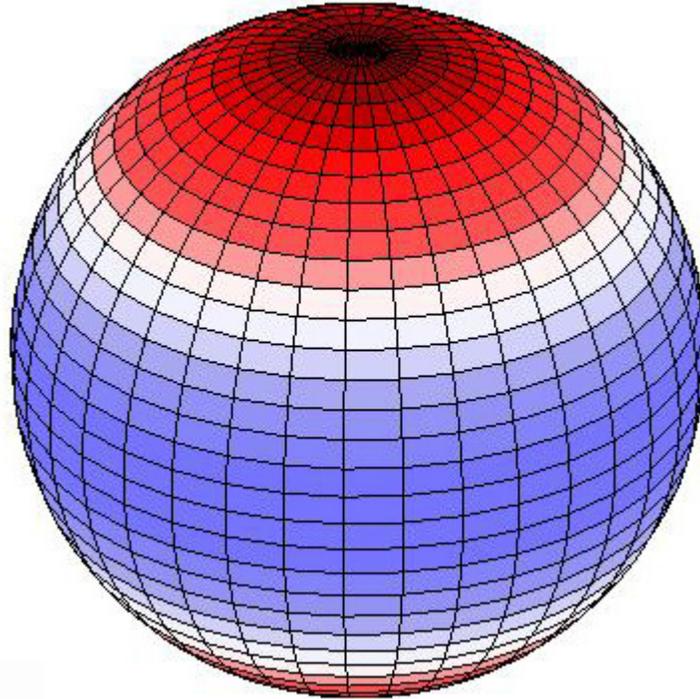North-south displacements of sectorial movement. Red north, blue south

Vertical displacements of tessearal movement. Red up, blue down.

East-West displacements of tessearal movement. Red east, blue west

North-South displacements of tessearal movement. Red north, blue south.

Vertical displacements of zonal movement. Red up, blue down.

The Earth tide encompasses the entire body of the Earth and is unhindered by the thin crust and land masses of the surface, on scales that make the rigidity of rock irrelevant. Ocean tides are a consequence of the resonance of the same driving forces with water movement periods in ocean basins accumulated over many days, so that their amplitude and timing are quite different and vary over short distances of just a few hundred kilometres. The oscillation periods of the earth as a whole are not near the astronomical periods, so its flexing is due to the forces of the moment.

The tide components with a period near twelve hours have a lunar amplitude (earth bulge/depression distances) that are a little more than twice the height of the solar amplitudes, as tabulated below. At new and full moon, the Sun and the Moon are aligned, and the lunar and the solar tidal maxima and minima (bulges and depressions) add together for the greatest tidal range at particular latitudes. At first- and third-quarter phases of the moon, lunar and solar tides are in opposition, and the tidal range is at a minimum. The semi-diurnal tides go through one full cycle (a high and low tide) about once every 12 hours and one full cycle of maximum height (a spring and neap tide) about once every 14 days.

The classical theory of Earth tides first became established in 1905. , primarily to explain nutations, but are also used in Earth rotation predictions. The semi-diurnal tide (one maximum every 12 or so hours) is primarily Lunar (only S_2 is purely solar) and gives rise to *sectorial* deformations which rise and fall at the same time along the same longitude. Sectorial variations of vertical and east-west displacements are maximum at the equator and vanish at the poles. There are two cycles along each latitude, the bulges opposite one

another, and the depressions similarly opposed. The diurnal tide is Lunisolar, and gives rise to *tesseral* deformations. The vertical and east-west movement is maximum at 45° latitude and is zero on the equator and at the poles. Tesseral variation have one cycle per latitude, one bulge and one depression; the bulge are opposed (antipodal), that is to say the western part of the northern hemisphere and the eastern part of the southern hemisphere, for example, and similarly the depressions are opposed,the western part of the northern hemisphere and the western part of the southern hemisphere, in this case. Finally, fortnightly and semi-annual tides have 'zonal'deformations (constant along a circle of latitude), as the Moon or Sun gravitation is directed alternately away from the Northern and Southern hemispheres due to tilt. There is zero vertical displacement at 35°16' latitude.

Since these displacements affect the vertical direction east-west and north-south variations are often tabulated in milliarc seconds for astronomical use. The vertical displacement is frequent tabulated in µgal, since the gradient of gravity is location dependent so that the distance conversion is only approximately 3 µgal per cm

Other Earth tide contributors

In coastal areas because the ocean tide is quite out of step with the earth tide, at high ocean tide there is an excess (or at low tide a deficit) of water about what would be the gravitational equilibrium level and the adjacent ground falls (or rises) in response to the resulting differences in weight. Displacements caused by ocean tidal loading can exceed the displacements due to the earth body tide. Sensitive instruments far inland often have to make similar corrections. Atmospheric loading and storm events may also be measurable, though the masses in movement are less weighty.

Tidal constituents

Principal body tide constituents. The amplitudes may vary from those listed within several per cent.

Semi-diurnal			
Tidal constituent	Period	Vertical amplitude (mm)	Horizontal amplitude(mm)
M_2	12.421 hr	384.83	53.84
S_2 (Solar Semi-diurnal)	12.000 hr	179.05	25.05
N_2	12.658 hr	73.69	10.31
K_2	11.967 hr	48.72	6.82
Diurnal			
Tidal constituent	Period	Vertical amplitude (mm)	Horizontal amplitude(mm)

K_1	23.934 hr	191.78	32.01
O_1	25.819 hr	158.11	22.05
P_1	24.066 hr	70.88	10.36
φ_1	23.804 hr	3.44	0.43
ψ_1	23.869 hr	2.72	0.21
S_1 (Solar diurnal)	24.000 hr	1.65	0.25

Long term

Tidal constituent	Period	Vertical amplitude (mm)	Horizontal amplitude(mm)
M_f	13.661 days	40.36	5.59
M_m (Moon Monthly)	27.555 days	21.33	2.96
S_{sa} (Solar semi-Annual)	0.50000 yr	18.79	2.60
lunar node	18.613 yr	16.92	2.34
S_a (Solar Annual)	1.0000 yr	2.97	0.41

Earth tide effects

Volcanologists use the regular, predictable Earth tide movements to calibrate and test sensitive volcano deformation monitoring instruments. The tides may also trigger volcanic events. Seismologists have determined that microseismic events are correlated to tidal variations in Central Asia (north of the Himalayas). The semidiurnal amplitude of terrestrial tides can reach about 55 cm at the equator which is important in GPS calibration and VLBI measurements. Also to make precise astronomical angular measurements requires knowledge of the Earth's rate of rotation and nutation, both of which are influenced by earth tides. It is a matter of conjecture at present but there is some correlation between terrestrial tides and earthquake activity.

Terrestrial tides also need to be taken in account in the case of some particle physics experiments. For instance, at the CERN or SLAC, the very large particle accelerators were designed while taking terrestrial tides into account for proper operation. Among the effects that need to be taken into account are circumference deformation for circular accelerators and particle beam energy.

Since tidal forces generate currents of conducting fluids within the interior of the Earth, they affect in turn the Earth's magnetic field itself.

Chapter- 10

Tidal Force
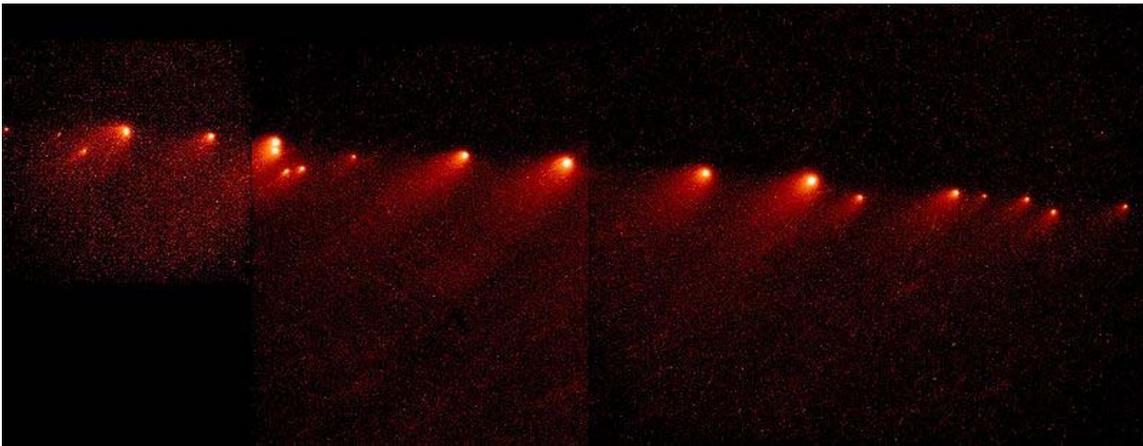
Figure 1: Comet Shoemaker-Levy 9 in 1994 after breaking up under the influence of Jupiter's tidal forces during a previous pass in 1992.

The **tidal force** is a secondary effect of the force of gravity and is responsible for the tides. It arises because the gravitational force per unit mass exerted on one body by a second body is not constant across its diameter, the side nearest to the second being more attracted by it than the side farther away.

In a more general usage in celestial mechanics, the expression 'tidal force' can refer to a situation in which a body or material (for example, tidal water, or the Moon) is mainly under the gravitational influence of a second body (for example, the Earth), but is also perturbed by the gravitational effects of a third body (for example, by the Moon in the case of tidal water, or by the Sun in the case of the Moon). The perturbing force is sometimes in such cases called a tidal force (for example, the perturbing force on the Moon): it is the difference between the force exerted by the third body on the second and the force exerted by the third body on the first.

Explanation

Figure 2: The Moon's gravity differential field at the surface of the Earth is known (along with another and weaker differential effect due to the Sun) as the Tide Generating Force. This is the primary mechanism driving tidal action, explaining two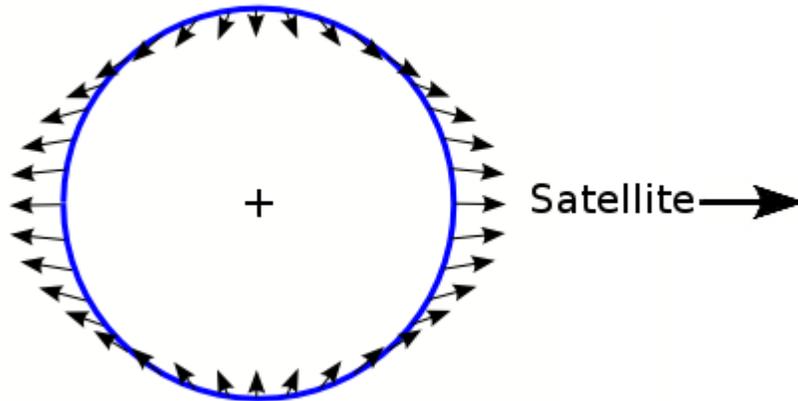 tidal equipotential bulges, and accounting for two high tides per day. In this figure, the Moon is either on the right side or on the left side of the Earth (at center). The **outward** direction of the arrows on the right and left indicates that where the Moon is overhead (or at the nadir) its perturbing force opposes and weakens the Earth's net attraction; and the **inward** direction of the arrows at top and bottom indicates that where the Moon is 90 degrees away from overhead, its perturbing effect reinforces and strengthens the Earth's net attraction.

When a body (body 1) is acted on by the gravity of another body (body 2), the field can vary significantly on body 1 between the side of the body facing body 2 and the side facing away from body 2. Figure 2 shows the differential force of gravity on a spherical body (body 1) exerted by another body (body 2). These so called *tidal forces* cause strains on both bodies and may distort them or even, in extreme cases, break one or the other apart. The Roche limit is the distance from a planet at which tidal effects would cause an object to disintegrate because the differential force of gravity from the planet overcomes the attraction of the parts of the object for one another. These strains would not occur if the gravitational field were uniform, because a uniform field only causes the entire body to accelerate together in the same direction and at the same rate.

Effects of tidal forces
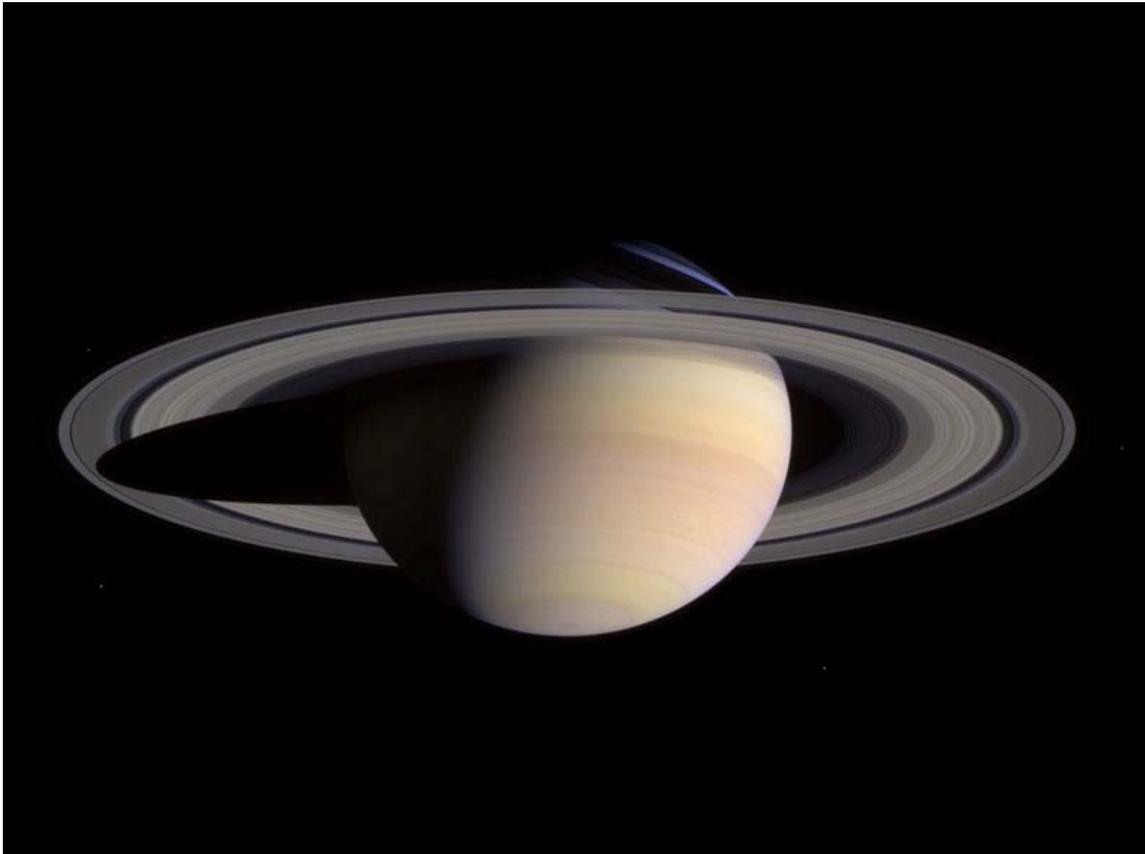
Figure 3: Saturn's rings are inside the orbits of its moons. Tidal forces prevented the material in the rings from coalescing gravitationally to form moons.

In the case of an infinitesimally small elastic sphere, the effect of a tidal force is to distort the shape of the body without any change in volume. The sphere becomes an ellipsoid with two bulges, pointing towards and away from the other body. Larger objects distort into an ovoid, and are slightly compressed, this is approximately what happens to the Earth's oceans under the action of the Moon. The Earth and Moon rotate about their common center of mass or barycenter, and their gravitational attraction provides the centripetal force necessary to maintain this motion. To an observer on the Earth, very close to this barycenter, the situation is one of the Earth as body 1 acted upon by the gravity of the Moon as body 2. All parts of the Earth are subject to the Moon's gravitational forces, causing the water in the oceans to redistribute, forming bulges on the sides near the Moon and far from the Moon.

When a body rotates while subject to tidal forces, internal friction results in the gradual dissipation of its rotational kinetic energy as heat. If the body is close enough to its primary, this can result in a rotation which is tidally locked to the orbital motion, as in the case of the Earth's moon. Tidal heating produces dramatic volcanic effects on Jupiter's

moon Io. Stresses caused by tidal forces also cause a regular monthly pattern of moonquakes on Earth's Moon.

Tidal forces contribute to ocean currents, which moderate global temperatures by transporting heat energy toward the poles. It has been suggested that in addition to other factors, harmonic beat variations in tidal forcing may contribute to climate changes.

Tidal effects become particularly pronounced near small bodies of high mass, such as neutron stars or black holes, where they are responsible for the "spaghettification" of infalling matter. Tidal forces create the oceanic tide of Earth's oceans, where the attracting bodies are the Moon and, to a lesser extent, the Sun.

Tidal forces are also responsible for tidal locking and tidal acceleration.

Mathematical treatment

For a given (externally-generated) gravitational field, the **tidal acceleration** at a point with respect to a body is obtained by vectorially subtracting the gravitational acceleration at the center of the body (due to the given externally-generated field) from the gravitational acceleration (due to the same field) at the given point. Correspondingly, the term *tidal force* is used to describe the forces due to tidal acceleration. Note that for these purposes the only gravitational field considered is the external one; the gravitational field of the body (as shown in the graphic) is not relevant. (In other words the comparison is with the conditions at the given point as they would be if there were no externally-generated field acting unequally at the given point and at the center of the reference body. The externally-generated field is usually that produced by a perturbing third body, often the Sun or the Moon in the frequent example-cases of points on or above the Earth's surface in a geocentric reference frame.).
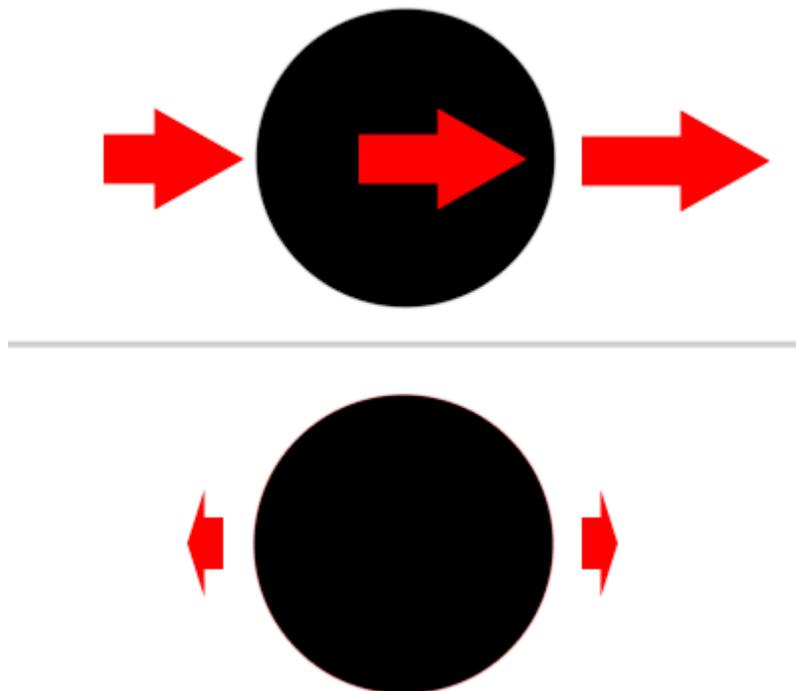
Figure 4: Graphic of tidal forces; the gravity field is generated by a body to the right. The top picture shows the gravitational forces; the bottom shows their residual once the field of the sphere is subtracted; this is the tidal force.

Tidal acceleration does not require rotation or orbiting bodies; for example, the body may be freefalling in a straight line under the influence of a gravitational field while still being influenced by (changing) tidal acceleration.

By Newton's law of universal gravitation and laws of motion, a body of mass m a distance R from the center of a sphere of mass M feels a force $\vec{F}_g$ equivalent to an acceleration $\vec{a}_g$, where:

$$\vec{F}_g = -\hat{r}\ G\ \frac{Mm}{R^2}\ \ldots, \text{ and } \ldots\ \vec{a}_g = -\hat{r}\ G\ \frac{M}{R^2}\ldots,$$

where $\hat{r}$ is a unit vector pointing from the body M to the body m (here, acceleration from m towards M has negative sign).

Consider now the acceleration due to the sphere of mass M experienced by a particle in the vicinity of the body of mass m. With R as the distance from the center of M to the center of m, let Δr be the (relatively small) distance of this other particle from the center of the body of mass m. For simplicity, distances are first considered only in the direction

pointing towards or away from the sphere of mass M. If the body of mass m is itself a sphere of radius Δr, then the new particle considered may be located on its surface, at a distance $(R \pm \Delta r)$ from the centre of the sphere of mass M, and Δr may be taken as positive where the particle's distance from M is greater than R. Leaving aside whatever gravitational acceleration may be experienced by the particle towards m on account of m's own mass, we have the acceleration on the particle due to gravitational force towards M as:

$$\vec{a}_g = -\hat{r} \; G \; \frac{M}{(R \pm \Delta r)^2}$$

Pulling out the R^2 term from the denominator gives:

$$\vec{a}_g = -\hat{r} \; G \; \frac{M}{R^2} \; \frac{1}{(1 \pm \Delta r / R)^2}$$

The Maclaurin series of $1/(1 + x)^2$ is $1 - 2x + 3x^2 - ...$, which gives a series expansion of:

$$\vec{a}_g = -\hat{r} \; G \; \frac{M}{R^2} \pm \hat{r} \; G \; \frac{2M}{R^2} \; \frac{\Delta r}{R} \mp \cdots$$

The first term is the gravitational acceleration due to M at the center of the reference body m, i.e. at the point where Δr is zero. This term does not affect the observed acceleration of particles on the surface of m because with respect to M, m (and everything on its surface) is in free fall. Effectively, this first term cancels. The remaining (residual) terms represent the difference mentioned above and are tidal force (acceleration) terms. Where Δr, is small compared to R, the first of the tidal acceleration terms is usually much more significant than the others, giving for the tidal acceleration $\vec{a}_t$(axial) for the distances Δr considered, along the axis joining the centers of m and M:

$$\vec{a}_{t\text{(axial)}} \approx \pm \; \hat{r} \; 2\Delta r \; G \; \frac{M}{R^3}$$

When calculated in this way for the case where Δr is a distance along the axis joining the centers of m and M, $\vec{a}_t$ is directed outwards, relative to the center of m where Δr is zero. Tidal accelerations can also be calculated away from the axis connecting the bodies m and M, requiring a vector calculation. In the plane perpendicular to that axis, the tidal acceleration is directed inwards (towards the center where Δr is zero), and its magnitude is $|\vec{a}_{t\text{(axial)}}| / 2$ in linear approximation as in Figure 2.

The tidal accelerations at the surface of planets in the Solar System are generally very small. For example, the lunar tidal acceleration at the Earth's surface along the Moon-Earth axis is about 1.1×10^{-7} g, while the solar tidal acceleration at the Earth's surface along the Sun-Earth axis is about 0.52×10^{-7} g, where g is the gravitational acceleration

at the Earth's surface. Modern estimates put the size of the tide-raising force (acceleration) due to the Sun at about 45% of that due to the Moon. The solar tidal acceleration at the Earth's surface was first given by Newton in the 'Principia'

Chapter- 11

Tidal Locking

Tidal locking (or **captured rotation**) occurs when the gravitational gradient makes one side of an astronomical body always face another; for example, one side of the Earth's Moon always faces the Earth. A tidally locked body takes just as long to rotate around its own axis as it does to revolve around its partner. This synchronous rotation causes one hemisphere constantly to face the partner body. Usually, at any given time only the satellite is tidally locked around the larger body, but if the difference in mass between the two bodies and their physical separation is small, *each* may be tidally locked to the other, as is the case between Pluto and Charon. This effect is employed to stabilize some artificial satellites.

Mechanism

The change in rotation rate necessary to tidally lock a body B to a larger body A is caused by the torque applied by A's gravity on bulges it has induced on B by tidal forces.

Tidal bulges

A's gravity produces a tidal force on B which distorts its gravitational equilibrium shape slightly so that it becomes elongated along the axis oriented toward A, and conversely, is slightly reduced in dimension in directions perpendicular to this axis. These distortions are known as tidal bulges. When B is not yet tidally locked, the bulges travel over its surface, with one of the two "high" tidal bulges traveling close to the point where body A is overhead. For large astronomical bodies which are near-spherical due to self-gravitation, the tidal distortion produces a slightly prolate spheroid - i.e., an axially symmetric ellipsoid that is elongated along its major axis. Smaller bodies also experience distortion, but this distortion is less regular.

Bulge dragging

The material of B exerts resistance to this periodic reshaping caused by the tidal force. In effect, some time is required to reshape B to the gravitational equilibrium shape, by which time the forming bulges have already been carried some distance away from the A-B axis by B's rotation. Seen from a vantage point in space, the points of maximum bulge extension are displaced from the axis oriented towards A. If B's rotation period is shorter

than its orbital period, the bulges are carried forward of the axis oriented towards A in the direction of rotation, whereas if B's rotation period is longer the bulges lag behind instead.

Resulting torque

Since the bulges are now displaced from the A-B axis, A's gravitational pull on the mass in them exerts a torque on B. The torque on the A-facing bulge acts to bring B's rotation in line with its orbital period, while the "back" bulge which faces away from A acts in the opposite sense. However, the bulge on the A-facing side is closer to A than the back bulge by a distance of approximately B's diameter, and so experiences a slightly stronger gravitational force and torque. The net resulting torque from both bulges, then, is always in the direction which acts to synchronize B's rotation with its orbital period, leading eventually to tidal locking.

Orbital changes
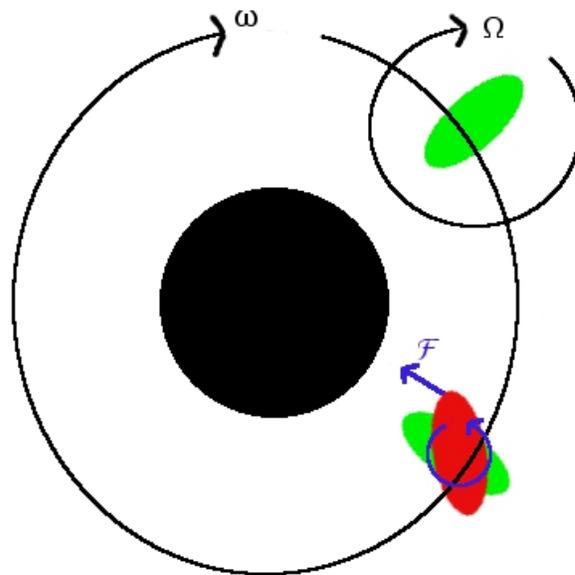
If rotational frequency is larger than orbital frequency, a small torque counteracting the rotation arises, eventually locking the frequencies (situation depicted in green)

The angular momentum of the whole A-B system is conserved in this process, so that when B slows down and loses rotational angular momentum, its *orbital* angular momentum is boosted by a similar amount (there are also some smaller effects on A's rotation). This results in a raising of B's orbit about A in tandem with its rotational slowdown. For the other case where B starts off rotating too slowly, tidal locking both speeds up its rotation, and *lowers* its orbit.

Locking of the larger body

The tidal locking effect is also experienced by the larger body A, but at a slower rate because B's gravitational effect is weaker due to B's smaller size. For example, the Earth's rotation is gradually slowing down because of the Moon, by an amount that becomes noticeable over geological time in some fossils. For similar sized bodies the effect may be of comparable size for both, and both may become tidally locked to each other. The dwarf planet Pluto and its satellite Charon are good examples of this—Charon is only visible from one hemisphere of Pluto and vice versa.

Rotation-orbit resonance

Finally, in some cases where the orbit is eccentric and the tidal effect is relatively weak, the smaller body may end up in an orbital resonance, rather than tidally locked. Here the ratio of rotation period to orbital period is some well-defined fraction different from 1:1. A well known case is the rotation of Mercury—locked to its orbit around the Sun in a 3:2 resonance.

Occurrence

Moons
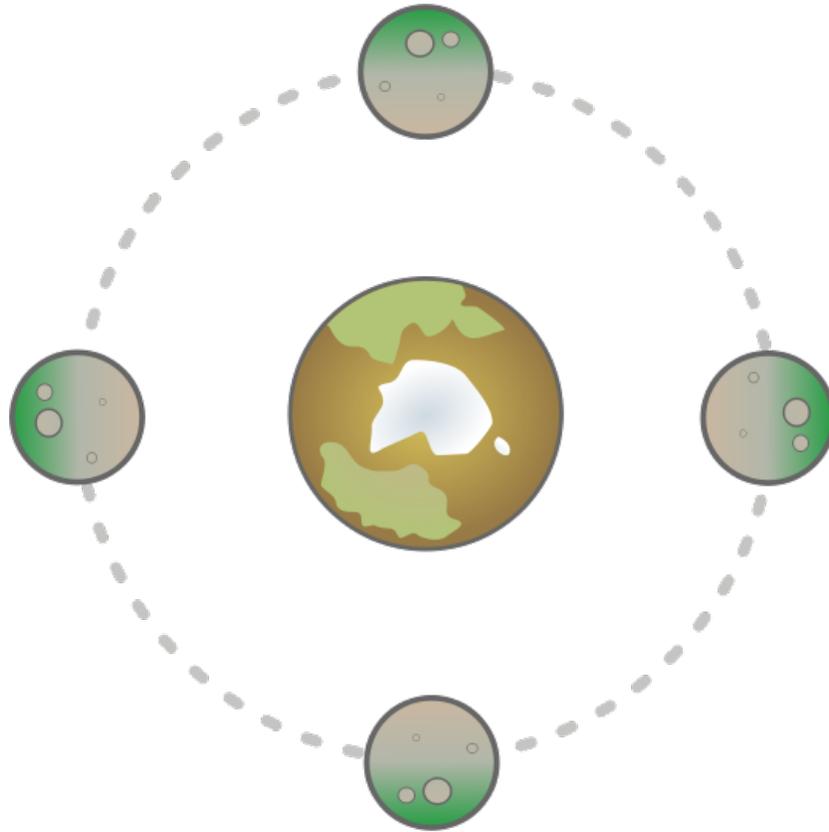
Due to tidal locking, the inhabitants of the central body will never be able to see its side marked with green.

Most significant moons in the Solar System are tidally locked with their primaries, since they orbit very closely and tidal force increases rapidly (as a cubic) with decreasing distance. Notable exceptions are the irregular outer satellites of the gas giant planets, which orbit much farther away than the large well-known moons.

Pluto and Charon are an extreme example of a tidal lock. Charon is a relatively large moon in comparison to its primary and also has a very close orbit. This has made Pluto also tidally locked to Charon. In effect, these two celestial bodies revolve around each other (their barycenter lies outside of Pluto) as if joined with a rod connecting two opposite points on their surfaces.

The tidal locking situation for asteroid moons is largely unknown, but closely-orbiting binaries are expected to be tidally locked, as well as contact binaries.

Earth's Moon

Since the Moon is 1:1 tidally locked, only one side is visible from Earth.

The Moon's rotation and orbital periods are both just under four weeks, so no matter when the Moon is observed from the Earth the same hemisphere of the Moon is always seen. The far side of the Moon was not seen in its entirety until 1959, when photographs were transmitted from the Soviet spacecraft Luna 3.

Despite the Moon's rotational and orbital periods being exactly locked, about 59% of the moon's total surface may be seen with repeated observations from earth due to the phenomena of librations and parallax. Librations are primarily caused by the Moon's varying orbital speed due to the eccentricity of its orbit: this allows us to see up to about 6° more along its perimeter. Parallax is a geometric effect: at the surface of the Earth we are offset from the line through the centers of Earth and Moon, and because of this we can observe a bit (about 1°) more around the side of the Moon when it is on our local horizon.

Planets

Until radar observations in 1965 proved otherwise, it was thought that Mercury was tidally locked with the Sun. Instead, it turned out that Mercury has a 3:2 spin-orbit resonance, rotating three times for every two revolutions around the Sun; the eccentricity of Mercury's orbit makes this resonance stable. The original reason astronomers thought it was tidally locked was because whenever Mercury was best placed for observation, it was always at the same point in its 3:2 resonance, so showing the same face, which would also be the case if it were tidally locked.

Venus' 583.92-day interval between successive close approaches to the Earth is almost exactly equal to 5 Venusian solar days (precisely, 5.001444 of these), making approximately the same face visible from Earth at each close approach. Whether this relationship arose by chance or is the result of some kind of tidal locking with the Earth is unknown.

Stars

Close binary stars throughout the universe are expected to be tidally locked with each other, and extrasolar planets that have been found to orbit their primaries extremely closely are also thought to be tidally locked to them. An unusual example, confirmed by MOST, is Tau Boötis, a star tidally locked by a planet. The tidal locking is almost certainly mutual.

Timescale

An estimate of the time for a body to become tidally locked can be obtained using the following formula:

$$t_{\text{lock}} \approx \frac{w a^6 I Q}{3 G m_p^2 k_2 R^5}$$

where

- w is the initial spin rate (radians per second)
- a is the semi-major axis of the motion of the satellite around the planet
- $I \approx 0.4 m_s R^2$ is the moment of inertia of the satellite.
- Q is the dissipation function of the satellite.
- G is the gravitational constant
- m_p is the mass of the planet
- m_s is the mass of the satellite
- k_2 is the tidal Love number of the satellite
- R is the radius of the satellite.

Q and k_2 are generally very poorly known except for the Earth's Moon which has $k_2 / Q =$ 0.0011. However, for a really rough estimate one can take $Q \approx 100$ (perhaps conservatively, giving overestimated locking times), and

$$k_2 \approx \frac{1.5}{1 + \frac{19\mu}{2\rho g R}},$$

where

- ρ is the density of the satellite
- $g \approx G m_s / R^2$ is the surface gravity of the satellite
- μ is rigidity of the satellite. This can be roughly taken as 3×10^{10} Nm^{-2} for rocky objects and 4×10^9 Nm^{-2} for icy ones.

As can be seen, even knowing the size and density of the satellite leaves many parameters that must be estimated (especially w, Q, and μ), so that any calculated locking times obtained are expected to be inaccurate, to even factors of ten. Further, during the tidal locking phase the orbital radius a may have been significantly different from that observed nowadays due to subsequent tidal acceleration, and the locking time is extremely sensitive to this value.

Since the uncertainty is so high, the above formulas can be simplified to give a somewhat less cumbersome one. By assuming that the satellite is spherical, $k_2 \ll 1$, $Q = 100$, and it is sensible to guess one revolution every 12 hours in the initial non-locked state (most asteroids have rotational periods between about 2 hours and about 2 days)

$$t_{\text{lock}} \quad \approx \quad 6 \, \frac{a^6 R \mu}{m_s m_p^2} \quad \times 10^{10} \text{ years,}$$

with masses in kg, distances in meters, and μ in Nm^{-2}. μ can be roughly taken as 3×10^{10} Nm^{-2} for rocky objects and 4×10^9 Nm^{-2} for icy ones.

Note the extremely strong dependence on orbital radius a.

For the locking of a primary body to its moon as in the case of Pluto, satellite and primary body parameters can be interchanged.

One conclusion is that *other things being equal* (such as Q and μ), a large moon will lock faster than a smaller moon at the same orbital radius from the planet because m_s grows much faster with satellite radius than R. A possible example of this is in the Saturn system, where Hyperion is not tidally locked, while the larger Iapetus, which orbits at a greater distance, is. It must be noted, however, that this is not clear cut because Hyperion also experiences strong driving from the nearby Titan, which forces its rotation to be chaotic.

List of known tidally locked bodies

Solar System

Locked to the Sun

- Mercury (in a 3:2 rotation:orbit resonance)

Locked to the Earth

- Moon

Locked to Mars

- Phobos
- Deimos

Locked to Jupiter

- Metis
- Adrastea
- Amalthea
- Thebe
- Io
- Europa
- Ganymede
- Callisto

Locked to Saturn

- Pan
- Atlas
- Prometheus
- Pandora
- Epimetheus
- Janus
- Mimas
- Enceladus
- Telesto
- Tethys
- Calypso
- Dione
- Rhea
- Titan
- Iapetus

Locked to Uranus

- Miranda
- Ariel
- Umbriel
- Titania
- Oberon

Locked to Neptune

- Proteus
- Triton

Locked to Pluto

- Charon (Pluto is itself locked to Charon)

Extra-solar

- Tau Boötis is known to be locked to the close-orbiting giant planet Tau Boötis b.

Bodies likely to be locked

Solar System

Based on comparison between the likely time needed to lock a body to its primary, and the time it has been in its present orbit (comparable with the age of the Solar System for most planetary moons), a number of moons are thought to be locked. However their rotations are not known or not known enough. These are:

Probably locked to Saturn

- Daphnis
- S/2004 S 6
- S/2004 S 4
- S/2004 S 3
- Methone
- Pallene
- Helene
- Polydeuces

Probably locked to Uranus

- Cordelia
- Ophelia
- Bianca

- Cressida
- Desdemona
- Juliet
- Portia
- Rosalind
- Cupid
- Belinda
- Perdita
- Puck
- Mab
- Oberon

Probably locked to Neptune

- Naiad
- Thalassa
- Despina
- Galatea
- Larissa

Extra-solar

- Gliese 581 c may be tidally locked to its parent star Gliese 581.
- Gliese 581 g may be tidally locked to its parent star Gliese 581.
- Gliese 581 b, Gliese 581 d, and Gliese 581 e may be tidally locked to their parent star Gliese 581.

Chapter- 12

Tide

High Tide, Alma, New Brunswick in the Bay of Fundy

Low Tide at the same fishing port in Bay of Fundy

Tides are the rise and fall of sea levels caused by the combined effects of the gravitational forces exerted by the Moon and the Sun and the rotation of the Earth.

Most places in the ocean usually experience two high tides and two low tides each day (semidiurnal tide), but some locations experience only one high and one low tide each day (diurnal tide). The times and amplitude of the tides at the coast are influenced by the alignment of the Sun and Moon, by the pattern of tides in the deep ocean (see figure 4) and by the shape of the coastline and near-shore bathymetry.

Because the gravitational field created by the Moon weakens with distance from the moon, it exerts a slightly harder pull on the side of the Earth facing the Moon than on the opposite side. The Moon thus tends to "stretch" the Earth slightly along the line connecting the two bodies. The solid Earth deforms a bit, but ocean water, being fluid, is free to move much more in response to the tidal force, particularly horizontally. As the Earth rotates, the magnitude and direction of the tidal force at any particular point on the Earth's surface change constantly; although the ocean never reaches equilibrium--there is never time for the fluid to "catch up" to the state it would eventually reach if the tidal force were constant--the changing tidal force nonetheless causes rhythmic changes in sea surface height.

The Moon orbits the Earth in the same direction as the Earth rotates on its axis, so it takes slightly more than a day—about 24 hours and 50 minutes—for the Moon to return to the same location in the sky. During this time, it has passed overhead once and underfoot once, so in many places the period of strongest tidal forcing is 12 hours and 25 minutes. The high tides do not necessarily occur when the Moon is overhead or underfoot, but the period of the forcing still determines the time between high tides.

The Sun also exerts on the Earth a gravitational attraction which results in a (less powerful) secondary tidal effect. When the Earth, Moon and Sun are approximately aligned, these two tidal effects reinforce one another, resulting in higher highs and lower lows. This alignment occurs approximately twice a month (at the full moon and new moon). These recurring extreme tides are termed spring tides. Tides with the smallest range are termed neap tides (occurring around the first and last quarter moons).

The tidal forces affect the entire earth, but the movement of the solid Earth is only centimetres. The atmosphere is much more fluid and compressible so its surface moves kilometres, in the sense of the contour level of a particular low pressure in the outer atmosphere.

Tides vary on timescales ranging from hours to years due to numerous influences. To make accurate records, tide gauges at fixed stations measure the water level over time. Gauges ignore variations caused by waves with periods shorter than minutes. These data are compared to the reference (or datum) level usually called mean sea level.

While tides are usually the largest source of short-term sea-level fluctuations, sea levels are also subject to forces such as wind and barometric pressure changes, resulting in storm surges, especially in shallow seas and near coasts.

Tidal phenomena are not limited to the oceans, but can occur in other systems whenever a gravitational field that varies in time and space is present. For example, the solid part of the Earth is affected by tides.

Characteristics

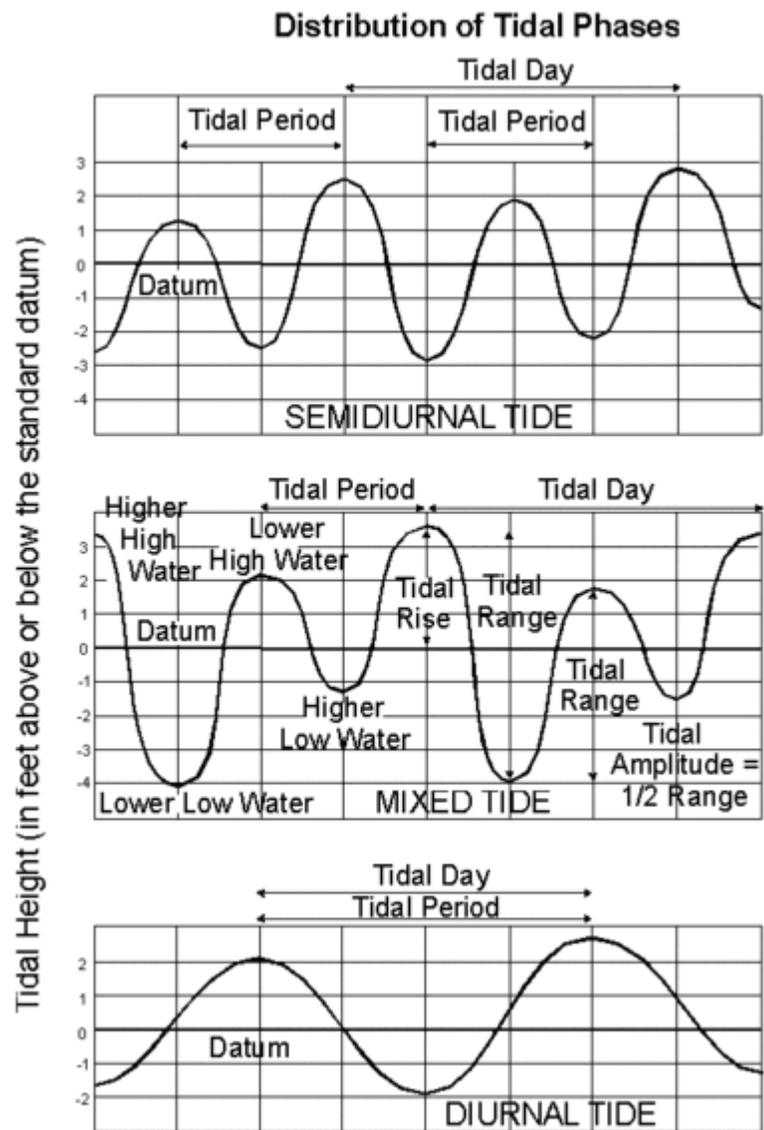## Distribution of Tidal Phases

Fig. 1: Types of tides

Tide changes proceed via the following stages:

- Sea level rises over several hours, covering the intertidal zone; flood tide.
- The water rises to its highest level, reaching high tide.
- Sea level falls over several hours, revealing the intertidal zone; ebb tide.
- The water stops falling, reaching low tide.

Tides produce oscillating currents known as tidal streams. The moment that the tidal current ceases is called slack water or slack tide. The tide then reverses direction and is said to be turning. Slack water usually occurs near high water and low water. But there are locations where the moments of slack tide differ significantly from those of high and low water.

Tides are most commonly *semidiurnal* (two high waters and two low waters each day), or *diurnal* (one tidal cycle per day). The two high waters on a given day are typically not the same height (the daily inequality); these are the *higher high water* and the *lower high water* in tide tables. Similarly, the two low waters each day are the *higher low water* and the *lower low water*. The daily inequality is not consistent and is generally small when the Moon is over the equator.

Tidal constituents

Tidal changes are the net result of multiple influences that act over varying periods. These influences are called tidal constituents. The primary constituents are the Earth's rotation, the positions of Moon and the Sun relative to Earth, the Moon's altitude above the Earth, and bathymetry.

Variations with periods of less than half a day are called *harmonic constituents*. Conversely, *long period* constituents cycle over days, months, or years.

Principal lunar semidiurnal constituent

In most locations, the largest constituent is the "principal lunar semidiurnal", also known as the *M2* (or M_2) tidal constituent. Its period is about 12 hours and 25.2 minutes, exactly half a *tidal lunar day*, which is the average time separating one lunar zenith from the next, and thus is the time required for the Earth to rotate once relative to the Moon. Simple tide clocks track this constituent. The lunar day is longer than the Earth day because the Moon orbits in the same direction the Earth spins. This is analogous to the minute hand on a watch crossing the hour hand at 12:00 and then again at about 1:05 (not at 1:00).

Semidiurnal range differences

When there are two high tides each day with different heights (and two low tides also of different heights), the pattern is called a *mixed semidiurnal tide*.

Range variation: springs and neaps
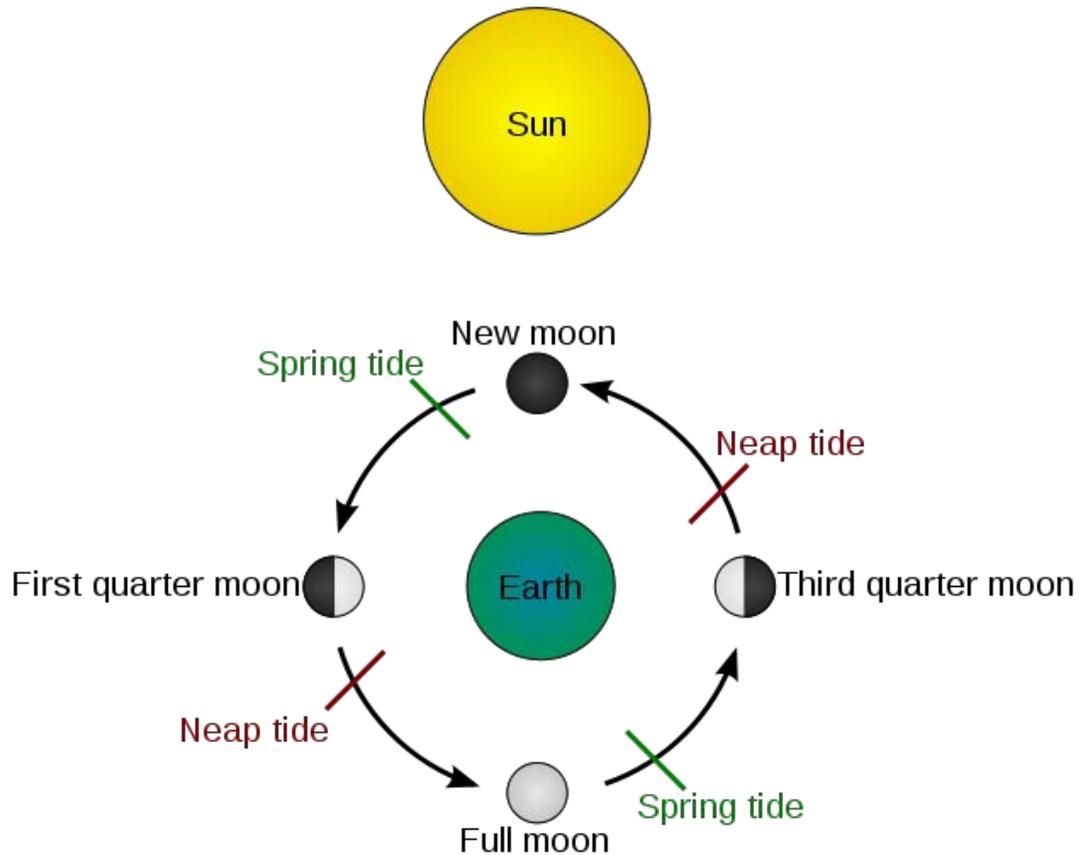
The types of tides

The semidiurnal range (the difference in height between high and low waters over about a half day) varies in a two-week cycle. Around new moon and full moon when the Sun, Moon and Earth form a line (a condition known as syzygy) the tidal force due to the Sun reinforces that due to the Moon. The tide's range is then at its maximum: this is called the *spring tide*, or just *springs*. It is not named after the season but, like that word, derives from an earlier meaning of "jump, burst forth, rise" as in a natural spring. When the Moon is at first quarter or third quarter, the Sun and Moon are separated by 90° when viewed from the Earth, and the solar gravitational force partially cancels the Moon's. At these points in the lunar cycle, the tide's range is at its minimum: this is called the *neap tide*, or *neaps* (a word of uncertain origin). Spring tides result in high waters that are higher than average, low waters that are lower than average, *slack water* time that is shorter than average and stronger tidal currents than average. Neaps result in less extreme tidal conditions. There is about a seven-day interval between springs and neaps.

Lunar altitude

Negative low tide at Ocean Beach in San Francisco

The changing distance separating the Moon and Earth also affects tide heights. When the Moon is at perigee, the range increases, and when it is at apogee, the range shrinks. Every 7½ lunations (the full cycles from full moon to new to full), perigee coincides with either a new or full moon causing perigean spring tides with the largest *tidal range*. If a storm happens to be moving onshore at this time, the consequences (property damage, etc.) can be severe.

Bathymetry

The shape of the shoreline and the ocean floor changes the way that tides propagate, so there is no simple, general rule that predicts the time of high water from the Moon's position in the sky. Coastal characteristics such as underwater bathymetry and coastline shape mean that individual location characteristics affect tide forecasting; actual high water time and height may differ from model predictions due to the coastal morphology's effects on tidal flow. However, for a given location the relationship between lunar altitude and the time of high or low tide (the lunitidal interval) is relatively constant and predictable, as is the time of high or low tide relative to other points on the same coast. For example, the high tide at Norfolk, Virginia, predictably occurs approximately two and a half hours before the Moon passes directly overhead.

Land masses and ocean basins act as barriers against water moving freely around the globe, and their varied shapes and sizes affect the size of tidal frequencies. As a result, tidal patterns vary. For example, in the U.S., the East coast has predominantly semi-diurnal tides, as do Europe's Atlantic coasts, while the West coast predominantly has mixed tides.

Other constituents

These include solar gravitational effects, the obliquity (tilt) of the Earth's equator and rotational axis, the inclination of the plane of the lunar orbit and the elliptical shape of the Earth's orbit of the Sun.

A compound tide (or overtide) results from the shallow-water interaction of its two parent waves.

Phase and amplitude
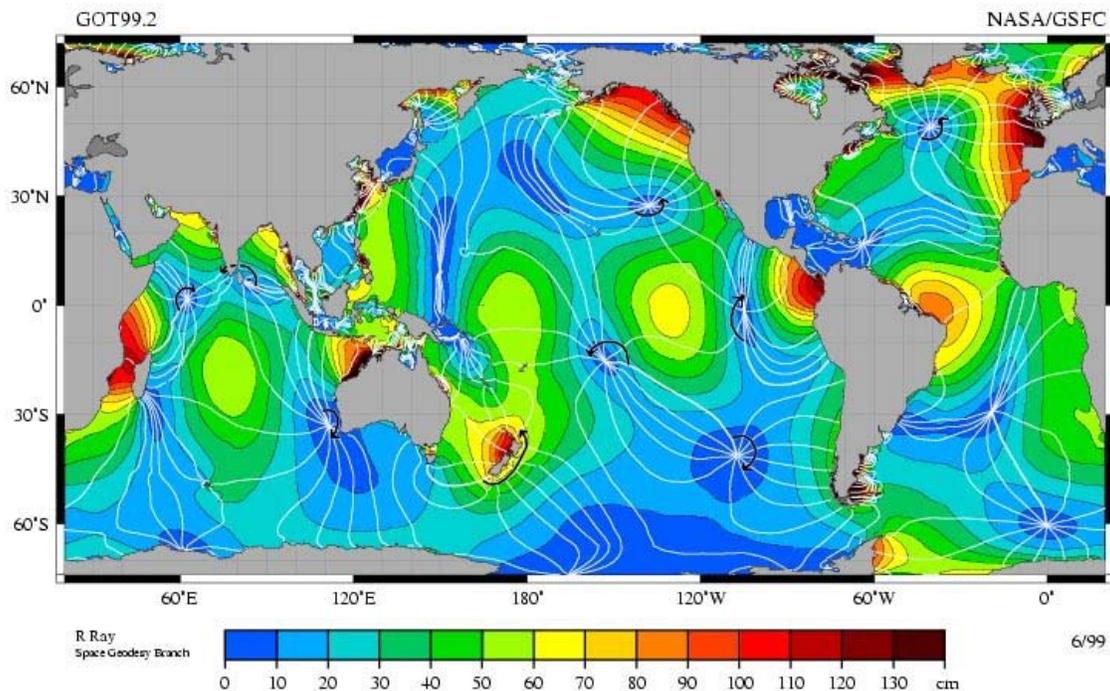
Fig. 4: The M_2 tidal constituent. Amplitude is indicated by color, and the white lines are cotidal differing by 1 hour. The curved arcs around the amphidromic points show the direction of the tides, each indicating a synchronized 6-hour period.

Because the M_2 tidal constituent dominates in most locations, the stage or *phase* of a tide, denoted by the time in hours after high water is a useful concept. Tidal stage is also measured in degrees, with 360° per tidal cycle. Lines of constant tidal phase are called *cotidal lines*, analogous to lines on topographical maps. High water is reached simultaneously along the cotidal lines extending from the coast out into the ocean, and cotidal lines (and hence tidal phases) advance along the coast. Semidiurnal and long phase constituents are measured from high water, diurnal from maximum flood tide. This and the discussion that follows is precisely true only for a single tidal constituent.

For an ocean in the shape of a circular basin enclosed by a coastline, the *cotidal lines* point radially inward and must eventually meet at a common point, the amphidromic point. The amphidromic point is at once cotidal with high and low waters, which is satisfied by *zero* tidal motion. (The rare exception occurs when the tide encircles an island, as it does around New Zealand and Madagascar.) Tidal motion generally lessens moving away from continental coasts, so that crossing the cotidal lines are contours of constant *amplitude* (half the distance between high and low water) which decrease to zero at the amphidromic point. For a semidiurnal tide the amphidromic point can be thought of roughly like the center of a clock face, with the hour hand pointing in the direction of the high water cotidal line, which is directly opposite the low water cotidal line. High water

rotates about the amphidromic point once every 12 hours in the direction of rising cotidal lines, and away from ebbing cotidal lines. This rotation is generally clockwise in the southern hemisphere and counterclockwise in the northern hemisphere, and is caused by the Coriolis effect. The difference of cotidal phase from the phase of a reference tide is the *epoch*. The reference tide is the hypothetical constituent equilibrium tide on a landless Earth measured at 0° longitude, the Greenwich meridian.

In the North Atlantic, because the cotidal lines circulate counterclockwise around the amphidromic point, the high tide passes New York harbor approximately an hour ahead of Norfolk harbor. South of Cape Hatteras the tidal forces are more complex, and cannot be predicted reliably based on the North Atlantic cotidal lines.

Physics

History of tidal physics

Tidal physics was important in the early development of heliocentrism and celestial mechanics, with the existence of two daily tides being explained by the Moon's gravity. Later the daily tides were explained more precisely by the interaction of the Moon's gravity and the Sun's gravity to cause the variation of tides.

An early explanation of tides was given by Galileo Galilei in his 1632 *Dialogue Concerning the Two Chief World Systems,* whose working title was *Dialogue on the Tides*. However, the resulting theory was incorrect - he attributed the tides to water sloshing due to the Earth's movement around the Sun, hoping to provide mechanical proof of the Earth's movement - and the value of the theory is disputed, as discussed there. At the same time Johannes Kepler correctly suggested that the Moon caused the tides, based upon ancient observation and correlations, an explanation which was rejected by Galileo. It was originally mentioned in Ptolemy's Tetrabiblos as being derived from ancient observation.

Isaac Newton (1642–1727) was the first person to explain tides scientifically. His explanation of the tides (and many other phenomena) was published in the *Principia* (1687). and used his theory of universal gravitation to account for the tide-generating forces as due to the lunar and solar attractions. Newton and others before Pierre-Simon Laplace worked with an equilibrium theory, largely concerned with an approximation that describes the tides that would occur in a non-inertial ocean evenly covering the whole Earth. The tide-generating force (or its corresponding potential) is still relevant to tidal theory, but as an intermediate quantity rather than as a final result; theory has to consider also the Earth's accumulated dynamic tidal response to the force, a response that is influenced by bathymetry, Earth's rotation, and other factors.

In 1740, the Académie Royale des Sciences in Paris offered a prize for the best theoretical essay on tides. Daniel Bernoulli, Leonhard Euler, Colin Maclaurin and Antoine Cavalleri shared the prize.

Maclaurin used Newton's theory to show that a smooth sphere covered by a sufficiently deep ocean under the tidal force of a single deforming body is a prolate spheroid (essentially a three dimensional oval) with major axis directed toward the deforming body. Maclaurin was the first to write about the Earth's rotational effects on motion. Euler realized that the tidal force's *horizontal* component (more than the vertical) drives the tide. In 1744 Jean le Rond d'Alembert studied tidal equations for the atmosphere which did not include rotation.

Pierre-Simon Laplace formulated a system of partial differential equations relating the ocean's horizontal flow to its surface height, the first major dynamic theory for water tides. The Laplace tidal equations are still in use today. William Thomson, 1st Baron Kelvin, rewrote Laplace's equations in terms of vorticity which allowed for solutions describing tidally-driven coastally-trapped waves, known as Kelvin waves.

Others including Kelvin and Henri Poincaré further developed Laplace's theory. Based on these developments and the lunar theory of E W Brown describing the motions of the moon, Arthur Thomas Doodson developed and published in 1921 the first modern development of the tide-generating potential in harmonic form: Doodson distinguished 388 tidal frequencies. Some of his methods remain in use.

Forces

The tidal force produced by a massive object (Moon, hereafter) on a small particle located on or in an extensive body (Earth, hereafter) is the vector difference between the gravitational force exerted by the Moon on the particle, and the gravitational force that would be exerted on the particle if it were located at the Earth's center of mass. Thus, the tidal force depends not on the strength of the lunar gravitational field, but on its gradient (which falls off approximately as the inverse cube of the distance to the originating gravitational body). The solar *gravitational force* on the Earth is on average 179 times stronger than the lunar, but because the Sun is on average 389 times farther from the Earth, its field gradient is weaker. The solar tidal force is 46% as large as the lunar. More precisely, the lunar tidal acceleration (along the Moon-Earth axis, at the Earth's surface) is about 1.1×10^{-7} g, while the solar tidal acceleration (along the Sun-Earth axis, at the Earth's surface) is about 0.52×10^{-7} g, where g is the gravitational acceleration at the Earth's surface. Venus has the largest effect of the other planets, at 0.000113 times the solar effect.
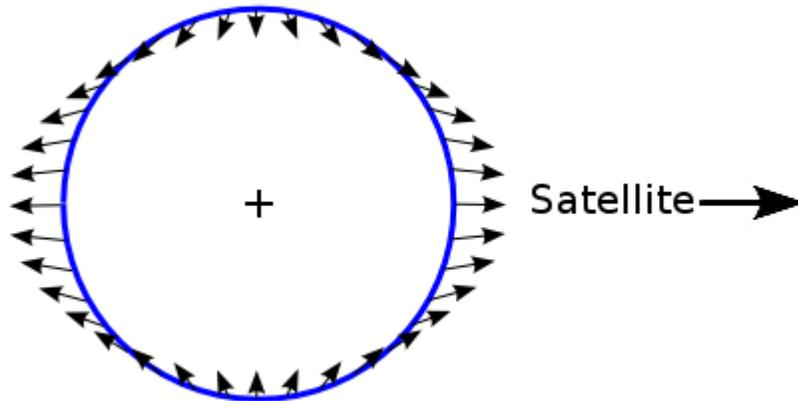
Fig. 6: The lunar gravity differential field at the Earth's surface is known as the tide-generating force. This is the primary mechanism that drives tidal action and explains two equipotential tidal bulges, accounting for two daily high waters.

Tidal forces can also be analyzed this way: each point of the Earth experiences the Moon's radially decreasing gravity differently; they are subject to the *tidal forces* of Figure 6, which dominate. Finally, most importantly, only the tidal forces' *horizontal* components actually tidally accelerate the water particles since there is small resistance. The tidal force on a particle equals about one ten millionth that of Earth's gravitational force.

The ocean's surface is closely approximated by an equipotential surface, (ignoring ocean currents) commonly referred to as the geoid. Since the gravitational force is equal to the potential's gradient, there are no tangential forces on such a surface, and the ocean surface is thus in gravitational equilibrium. Now consider the effect of massive external bodies such as the Moon and Sun. These bodies have strong gravitational fields that diminish with distance in space and which act to alter the shape of an equipotential surface on the Earth. This deformation has a fixed spatial orientation relative to the influencing body. The Earth's rotation relative to this shape causes the daily tidal cycle. Gravitational forces follow an inverse-square law (force is inversely proportional to the square of the distance), but tidal forces are inversely proportional to the cube of the distance. The ocean surface moves to adjust to changing tidal equipotential, tending to rise when the tidal potential is high, which occurs on the part of the Earth nearest to and furthest from the Moon. When the tidal equipotential changes, the ocean surface is no longer aligned with it, so that the apparent direction of the vertical shifts. The surface then experiences a down slope, in the direction that the equipotential has risen.

Laplace's tidal equations

Ocean depths are much smaller than their horizontal extent. Thus, the response to tidal forcing can be modelled using the Laplace tidal equations which incorporate the following features:

1. The vertical (or radial) velocity is negligible, and there is no vertical shear—this is a sheet flow.
2. The forcing is only horizontal (tangential).
3. The Coriolis effect appears as a fictitious lateral forcing proportional to velocity.
4. The surface height's rate of change is proportional to the negative divergence of velocity multiplied by the depth. As the horizontal velocity stretches or compresses the ocean as a sheet, the volume thins or thickens, respectively.

The boundary conditions dictate no flow across the coastline and free slip at the bottom.

The Coriolis effect steers waves to the right in the northern hemisphere and to the left in the southern allowing coastally trapped waves. Finally, a dissipation term can be added which is an analog to viscosity.

Amplitude and cycle time

The theoretical amplitude of oceanic tides caused by the Moon is about 54 centimetres (21 in) at the highest point, which corresponds to the amplitude that would be reached if the ocean possessed a uniform depth, there were no landmasses, and the Earth were rotating in step with the Moon's orbit. The Sun similarly causes tides, of which the theoretical amplitude is about 25 centimetres (9.8 in) (46% of that of the Moon) with a cycle time of 12 hours. At spring tide the two effects add to each other to a theoretical level of 79 centimetres (31 in), while at neap tide the theoretical level is reduced to 29 centimetres (11 in). Since the orbits of the Earth about the Sun, and the Moon about the Earth, are elliptical, tidal amplitudes change somewhat as a result of the varying Earth–Sun and Earth–Moon distances. This causes a variation in the tidal force and theoretical amplitude of about ±18% for the Moon and ±5% for the Sun. If both the Sun and Moon were at their closest positions and aligned at new moon, the theoretical amplitude would reach 93 centimetres (37 in).

Real amplitudes differ considerably, not only because of depth variations and continental obstacles, but also because wave propagation across the ocean has a natural period of the same order of magnitude as the rotation period: if there were no land masses, it would take about 30 hours for a long wavelength surface wave to propagate along the equator halfway around the Earth (by comparison, the Earth's lithosphere has a natural period of about 57 minutes). Earth tides, which raise and lower the bottom of the ocean, and the tide's own gravitational self attraction are both significant and further complicate the ocean's response to tidal forces.

Dissipation

Earth's tidal oscillations introduce dissipation at an average rate of about 3.75 terawatt. About 98% of this dissipation is by marine tidal movement. Dissipation arises as basin-scale tidal flows drive smaller-scale flows which experience turbulent dissipation. This tidal drag creates torque on the Moon that gradually transfers angular momentum to its orbit, and a gradual increase in Earth–Moon separation. The equal and opposite torque on the Earth correspondingly decreases its rotational velocity. Thus, over geologic time, the Moon recedes from the Earth, at about 3.8 centimetres (1.5 in)/year, lengthening the terrestrial day. Day length has increased by about 2 hours in the last 600 million years. Assuming (as a crude approximation) that the deceleration rate has been constant, this would imply that 70 million years ago, day length was on the order of 1% shorter with about 4 more days per year.

Observation and prediction

History
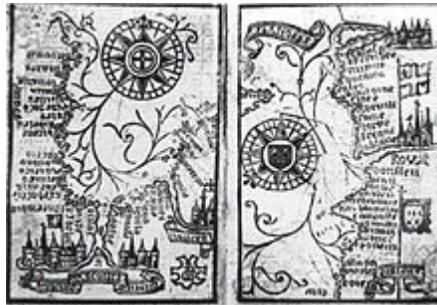
Brouscon's Almanach of 1546: Compass bearings of high waters in the Bay of Biscay (left) and the coast from Brittany to Dover (right).
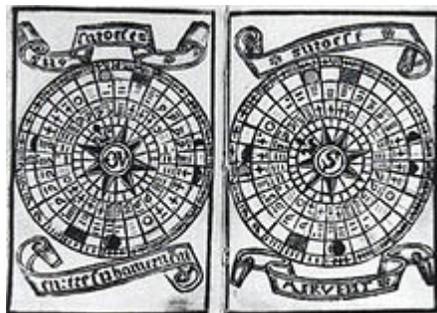
Brouscon's Almanach of 1546: Tidal diagrams "according to the age of the Moon".

From ancient times, tidal observation and discussion has increased in sophistication, first marking the daily recurrence, then tides' relationship to the Sun and Moon. Pytheas travelled to the British Isles about 325 BC and seems to be the first to have related spring tides to the phase of the Moon.

In the 2nd century BC, the Babylonian astronomer, Seleucus of Seleucia, correctly described the phenomenon of tides in order to support his heliocentric theory. He correctly theorized that tides were caused by the Moon, although he believed that the interaction was mediated by the pneuma. He noted that tides varied in time and strength in different parts of the world. According to Strabo (1.1.9), Seleucus was the first to link tides to the lunar attraction, and that the height of the tides depends on the Moon's position relative to the Sun.

In China, Wang Chong (27-100 AD) correlated tide to the moon's movement in the book entitled Lunheng. He noted that "tide's rise and fall follow the moon and vary in magnitude."

The *Naturalis Historia* of Pliny the Elder collates many tidal observations, e.g., the spring tides are a few days after (or before) new and full moon and are highest around the equinoxes, though Pliny noted many relationships now regarded as fanciful. In his *Geography*, Strabo described tides in the Persian Gulf having their greatest range when the Moon was furthest from the plane of the equator. All this despite the relatively small amplitude of Mediterranean basin tides. (The strong currents through the Strait of Messina and between Greece and the island of Euboea through the Euripus puzzled Aristotle). Philostratus discussed tides in Book Five of The Life of Apollonius of Tyana. Philostratus mentions the Moon, but attributes tides to "spirits". In Europe around 730 AD, the Venerable Bede described how the rising tide on one coast of the British Isles coincided with the fall on the other and described the time progression of high water along the Northumbrian coast.

In the 9th century, the Arabian earth-scientist, Al-Kindi (Alkindus), wrote a treatise entitled *Risala fi l-Illa al-Failali l-Madd wa l-Fazr* (*Treatise on the Efficient Cause of the Flow and Ebb*), in which he presents an argument on tides which "depends on the changes which take place in bodies owing to the rise and fall of temperature." He describes a precise laboratory experiment that proved his argument.

The first tide table in China was recorded in 1056 AD primarily for visitors wishing to see the famous tidal bore in the Qiantang River. The first known British tide table is thought to be that of John Wallingford, who died Abbot of St. Albans in 1213, based on high water occurring 48 minutes later each day, and three hours earlier at the Thames mouth than upriver at London.

William Thomson (Lord Kelvin) led the first systematic harmonic analysis of tidal records starting in 1867. The main result was the building of a tide-predicting machine using a system of pulleys to add together six harmonic time functions. It was

"programmed" by resetting gears and chains to adjust phasing and amplitudes. Similar machines were used until the 1960s.

The first known sea-level record of an entire spring–neap cycle was made in 1831 on the Navy Dock in the Thames Estuary. Many large ports had automatic tide gage stations by 1850.

William Whewell first mapped co-tidal lines ending with a nearly global chart in 1836. In order to make these maps consistent, he hypothesized the existence of amphidromes where co-tidal lines meet in the mid-ocean. These points of no tide were confirmed by measurement in 1840 by Captain Hewett, RN, from careful soundings in the North Sea.

Timing
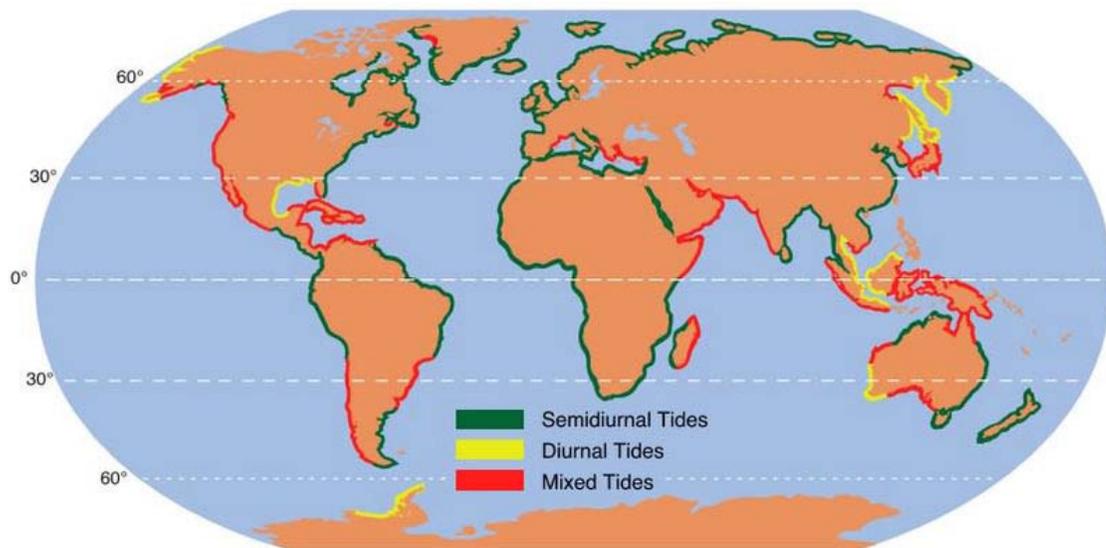
Fig. 7: The same tidal forcing has different results depending on many factors, including coast orientation, continental shelf margin, water body dimensions.

There is a delay between the phases of the Moon and the effect on the tide. Springs and neaps in the North Sea, for example, are two days behind the new/full moon and first/third quarter moon. This is called the tide's *age*.

The local bathymetry greatly influences the tide's exact time and height at a particular coastal point. There are some extreme cases: the Bay of Fundy, on the east coast of Canada, features the world's largest well-documented tidal ranges, 16 metres (52 ft) because of its shape. Some experts believe Ungava Bay in northern Quebec to have even higher tidal ranges, but it is free of pack ice for only about four months every year, while the Bay of Fundy rarely freezes.

Southampton in the United Kingdom has a double high water caused by the interaction between the region's different tidal harmonics. This is contrary to the popular belief that

the flow of water around the Isle of Wight creates two high waters. The Isle of Wight is important, however, since it is responsible for the 'Young Flood Stand', which describes the pause of the incoming tide about three hours after low water.

Because the oscillation modes of the Mediterranean Sea and the Baltic Sea do not coincide with any significant astronomical forcing period, the largest tides are close to their narrow connections with the Atlantic Ocean. Extremely small tides also occur for the same reason in the Gulf of Mexico and Sea of Japan. Elsewhere, as along the southern coast of Australia, low tides can be due to the presence of a nearby amphidrome (see figure 4).

Analysis
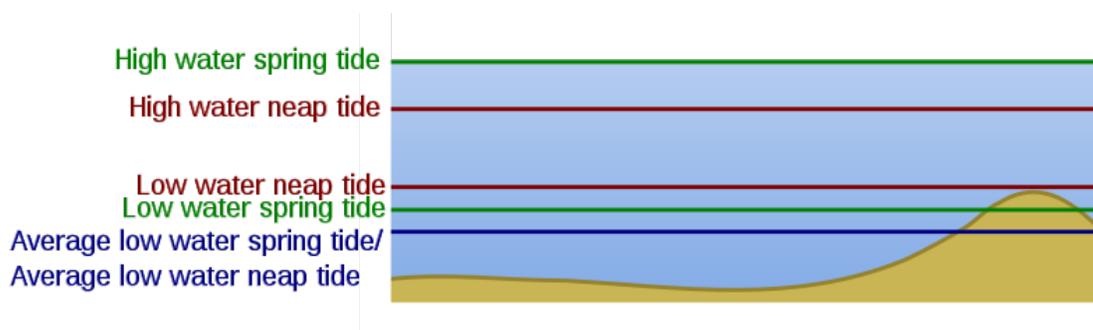
A regular water level chart

Isaac Newton's theory of gravitation first enabled an explanation of why there were generally two tides a day, not one, and offered hope for detailed understanding. Although it may seem that tides could be predicted via a sufficiently detailed knowledge of the instantaneous astronomical forcings, the actual tide at a given location is determined by astronomical forces accumulated over many days. Precise results require detailed knowledge of the shape of all the ocean basins—their bathymetry and coastline shape.

Current procedure for analysing tides follows the method of harmonic analysis introduced in the 1860s by William Thomson. It is based on the principle that the astronomical theories of the motions of Sun and Moon determine a large number of component frequencies, and at each frequency there is a component of force tending to produce tidal motion, but that at each place of interest on the Earth, the tides respond at each frequency with an amplitude and phase peculiar to that locality. At each place of interest, the tide heights are therefore measured for a period of time sufficiently long (usually more than a year in the case of a new port not previously studied) to enable the response at each significant tide-generating frequency to be distinguished by analysis, and to extract the tidal constants for a sufficient number of the strongest known components of the astronomical tidal forces to enable practical tide prediction. The tide heights are expected to follow the tidal force, with a constant amplitude and phase delay for each component. Because astronomical frequencies and phases can be calculated with

certainty, the tide height at other times can then be predicted once the response to the harmonic components of the astronomical tide-generating forces has been found.

The main patterns in the tides are

- the twice-daily variation
- the difference between the first and second tide of a day
- the spring–neap cycle
- the annual variation

The *Highest Astronomical Tide* is the perigean spring tide when both the Sun and the Moon are closest to the Earth.

When confronted by a periodically varying function, the standard approach is to employ Fourier series, a form of analysis that uses sinusoidal functions as a *basis* set, having frequencies that are zero, one, two, three, etc. times the frequency of a particular fundamental cycle. These multiples are called *harmonics* of the fundamental frequency, and the process is termed harmonic analysis. If the basis set of sinusoidal functions suit the behaviour being modelled, relatively few harmonic terms need to be added. Orbital paths are very nearly circular, so sinusoidal variations are suitable for tides.

For the analysis of tide heights, the Fourier series approach has in practice to be made more elaborate than the use of a single frequency and its harmonics. The tidal patterns are decomposed into many sinusoids having many fundamental frequencies, corresponding (as in the lunar theory) to many different combinations of the motions of the Earth, the Moon, and the angles that define the shape and location of their orbits.

For tides, then, *harmonic analysis* is not limited to harmonics of a single frequency. In other words, the harmonies are multiples of many fundamental frequencies, not just of the fundamental frequency of the simpler Fourier series approach. Their representation as a Fourier series having only one fundamental frequency and its (integer) multiples would require many terms, and would be severely limited in the time-range for which it would be valid.

The study of tide height by harmonic analysis was begun by Laplace, William Thomson (Lord Kelvin), and George Darwin. A.T. Doodson extended their work, introducing the *Doodson Number* notation to organise the hundreds of resulting terms. This approach has been the international standard ever since, and the complications arise as follows: the tide-raising force is notionally given by sums of several terms. Each term is of the form

$$A \cdot \cos(w \cdot t + p)$$

where A is the amplitude, w is the angular frequency usually given in degrees per hour corresponding to t measured in hours, and p is the phase offset with regard to the astronomical state at time $t = 0$. There is one term for the Moon and a second term for the Sun. The phase p of the first harmonic for the Moon term is called the lunitidal

interval or high water interval. The next step is to accommodate the harmonic terms due to the elliptical shape of the orbits. Accordingly, the value of A is not a constant but also varying with time, slightly, about some average figure. Replace it then by $A(t)$ where A is another sinusoid, similar to the cycles and epicycles of Ptolemaic theory. Accordingly,

$$A(t) = A \cdot (1 + A_a \cdot \cos(w_a \cdot t + p_a)) \, ,$$

which is to say an average value A with a sinusoidal variation about it of magnitude A_a , with frequency w_a and phase p_a . Thus the simple term is now the product of two cosine factors:

$$A \cdot [1 + A_a \cdot \cos(w_a + p_a)] \cdot \cos(w \cdot t + p)$$

Given that for any x and y

$$\cos(x) \cdot \cos(y) = \tfrac{1}{2} \cdot \cos(\, x + y \,) + \tfrac{1}{2} \cdot \cos(\, x{-}y \,) \, ,$$

it is clear that a compound term involving the product of two cosine terms each with their own frequency is the same as *three* simple cosine terms that are to be added at the original frequency and also at frequencies which are the sum and difference of the two frequencies of the product term. (Three, not two terms, since the whole expression is $(1 + \cos(x)) \cdot \cos(y)$.) Consider further that the tidal force on a location depends also on whether the Moon (or the Sun) is above or below the plane of the equator, and that these attributes have their own periods also incommensurable with a day and a month, and it is clear that many combinations result. With a careful choice of the basic astronomical frequencies, the Doodson Number annotates the particular additions and differences to form the frequency of each simple cosine term.
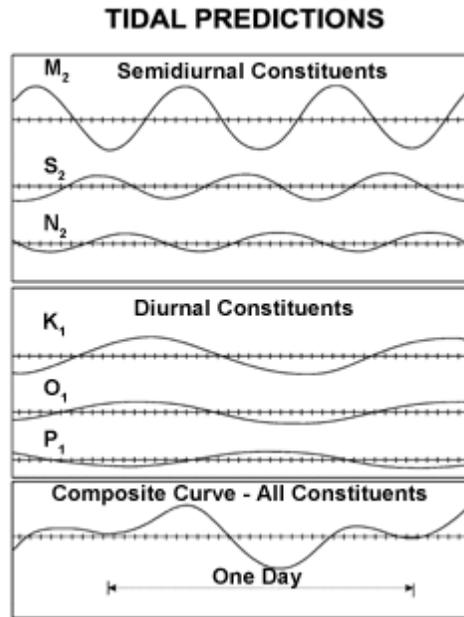
TIDAL PREDICTIONS

Fig. 8: Tidal prediction summing constituent parts.

Remember that astronomical tides do *not* include weather effects. Also, changes to local conditions (sandbank movement, dredging harbour mouths, etc.) away from those prevailing at the measurement time affect the tide's actual timing and magnitude. Organisations quoting a "highest astronomical tide" for some location may exaggerate the figure as a safety factor against analytical uncertainties, distance from the nearest measurement point, changes since the last observation time, ground subsidence, etc., to avert liability should an engineering work be overtopped. Special care is needed when assessing the size of a "weather surge" by subtracting the astronomical tide from the observed tide.

Careful Fourier data analysis over a nineteen-year period (the *National Tidal Datum Epoch* in the U.S.) uses frequencies called the *tidal harmonic constituents*. Nineteen years is preferred because the Earth, Moon and Sun's relative positions repeat almost exactly in the Metonic cycle of 19 years, which is long enough to include the 18.613 year lunar nodal tidal constituent. This analysis can be done using only the knowledge of the forcing *period*, but without detailed understanding of the mathematical derivation, which means that useful tidal tables have been constructed for centuries. The resulting amplitudes and phases can then be used to predict the expected tides. These are usually dominated by the constituents near 12 hours (the *semidiurnal* constituents), but there are major constituents near 24 hours (*diurnal*) as well. Longer term constituents are 14 day or *fortnightly*, monthly, and semiannual. Semidiurnal tides dominated coastline, but some areas such as the South China Sea and the Gulf of Mexico are primarily diurnal. In the semidiurnal areas, the primary constituents M_2 (lunar) and S_2 (solar) periods differ slightly, so that the relative phases, and thus the amplitude of the combined tide, change fortnightly (14 day period).

In the M_2 plot above, each cotidal line differs by one hour from its neighbors, and the thicker lines show tides in phase with equilibrium at Greenwich. The lines rotate around the amphidromic points counterclockwise in the northern hemisphere so that from Baja California Peninsula to Alaska and from France to Ireland the M_2 tide propagates northward. In the southern hemisphere this direction is clockwise. On the other hand M_2 tide propagates counterclockwise around New Zealand, but this is because the islands act as a dam and permit the tides to have different heights on the islands' opposite sides. (The tides do propagate northward on the east side and southward on the west coast, as predicted by theory.)

The exception is at Cook Strait where the tidal currents periodically link high to low water. This is because cotidal lines 180° around the amphidromes are in opposite phase, for example high water across from low water at each end of Cook Strait. Each tidal constituent has a different pattern of amplitudes, phases, and amphidromic points, so the M_2 patterns cannot be used for other tide components.

Example calculation
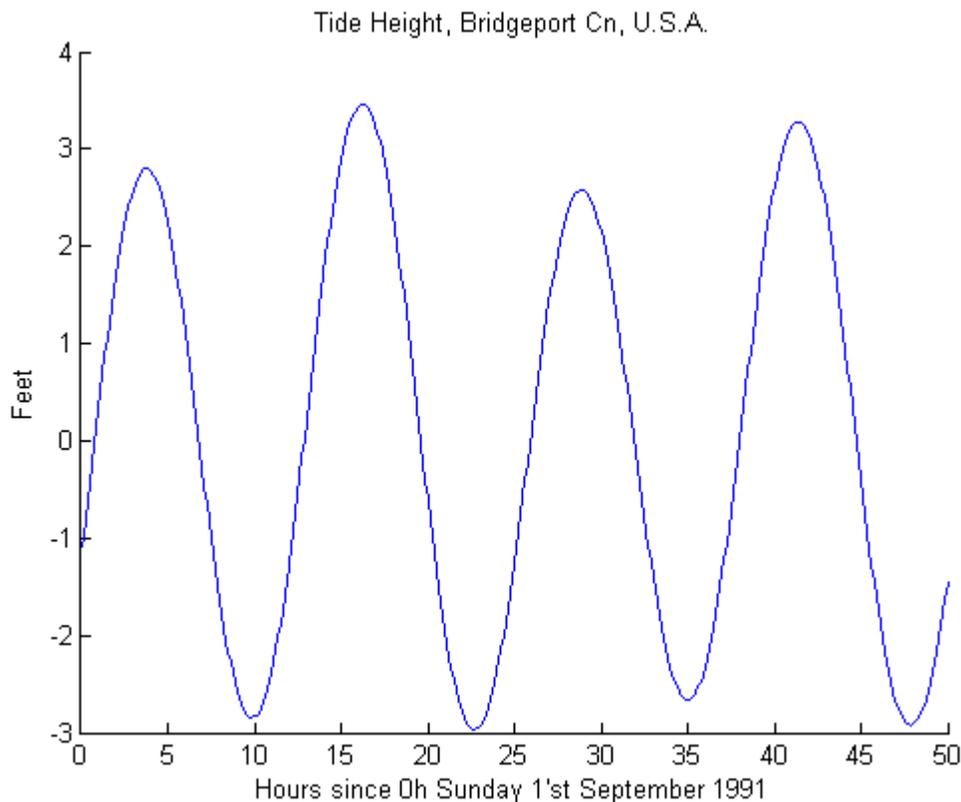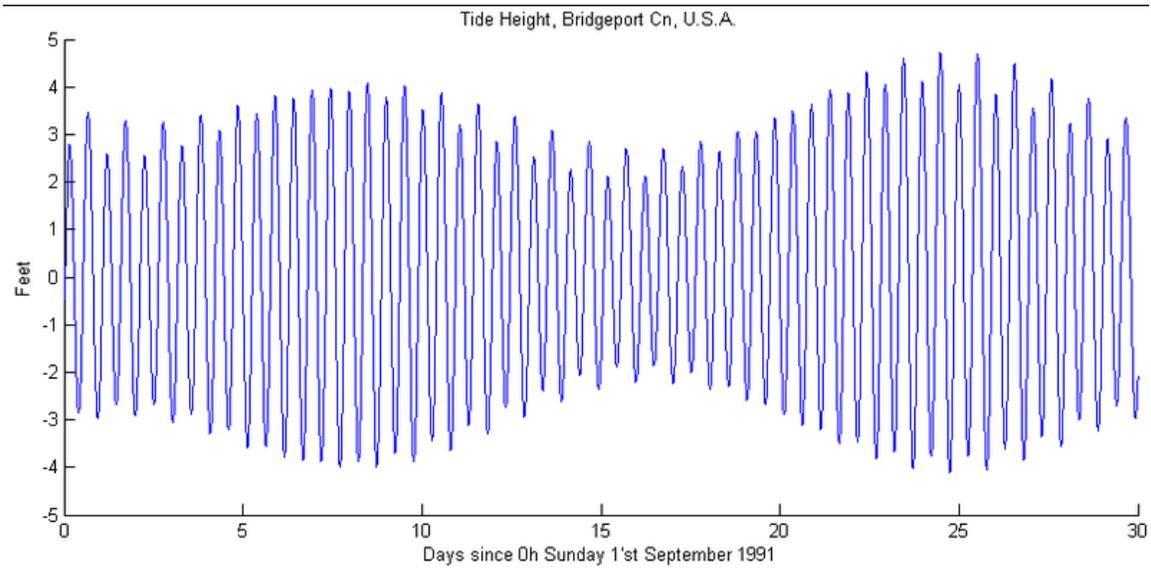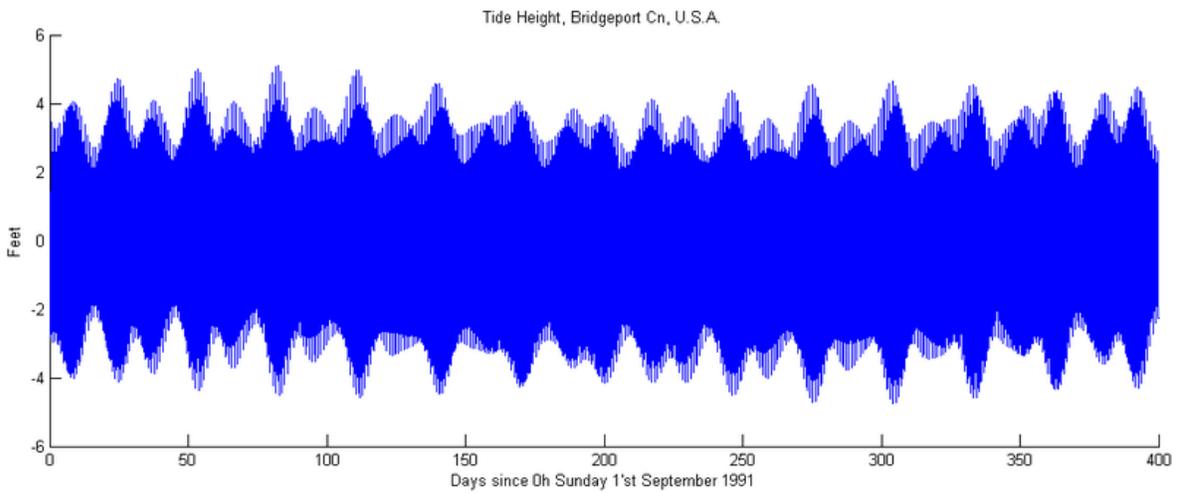

Fig. 9: Tides at Bridgeport, Connecticut, U.S.A. during a 50 hour period.

Fig. 10: Tides at Bridgeport, Connecticut, U.S.A. during a 30 day period.

Fig. 11: Tides at Bridgeport, Connecticut, U.S.A. during a 400 day period.
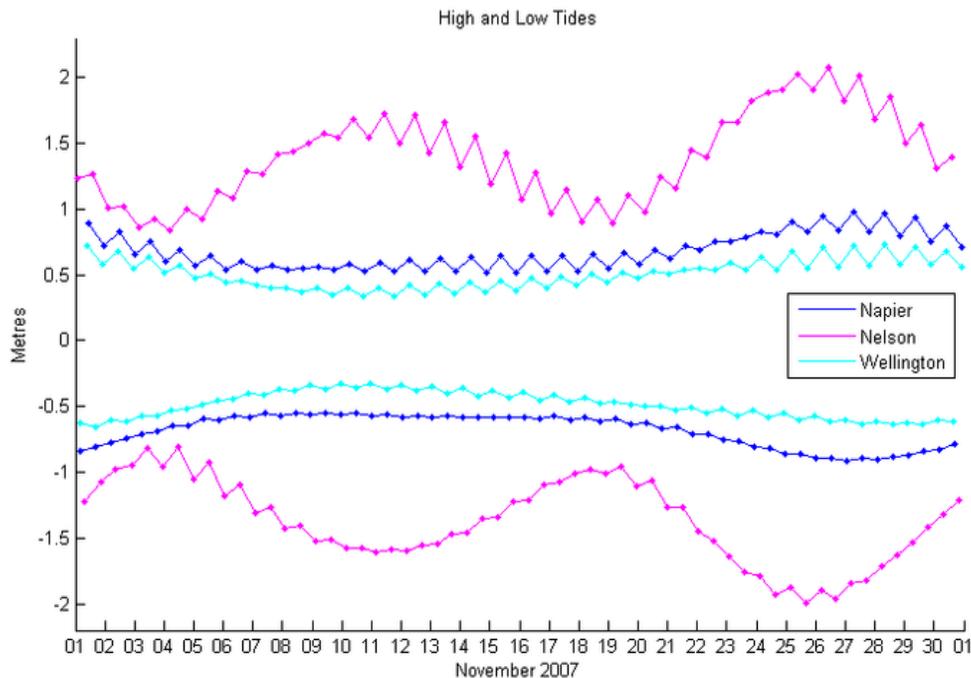
Fig. 12: Two spring tides per month vs. one.

Figure 9 shows the common pattern of two tidal peaks a day as the earth rotates under the moon; because the moon is also moving in its orbit around the earth and in the same sense as the earth's rotation, a point on the earth must rotate slightly further to catch up so that the cycle time is not twelve but 12.4206 hours - a bit over twenty-five minutes extra. The two peaks are not equal: the twin tidal bulges beneath the Moon and on the opposite side of the Earth align with the Moon. Bridgeport is north of the equator, so when the Moon is north of the equator also and shining upon Bridgeport, Bridgeport is closer to its maximum tide than approximately twelve hours later when Bridgeport is on the opposite side of the Earth from the Moon and the high tide bulge at Bridgeport's longitude has its maximum south of the equator. Thus the two high tides a day alternate in maximum heights: lower high (just under three feet), higher high (just over three feet), and again. Likewise for the low tides.

Figure 10 shows the spring tide/neap tide cycle in tidal amplitudes as the Moon orbits the Earth from being in line (Sun–Earth–Moon, or Sun–Moon–Earth) when the two main influences combine to give the spring tides, to when the two forces are opposing each other as when the angle Moon–Earth–Sun is close to ninety degrees, producing the neap tides. As the Moon moves around its orbit it changes from north of the equator to south of the equator. The alternation in high tide heights becomes smaller, until they are the same (at the lunar equinox, the Moon is above the equator), then redevelops but with the other polarity, waxing to a maximum difference and then waning again.

Figure 11 shows just over a year's worth of tidal height calculations. The Sun also cycles from north to south of the equator, while the Earth–Sun and Earth–Moon distances change on their own cycles. None of the various cycle periods are commensurate.

Current

The tides' influence on current flow is much more difficult to analyse, and data is much more difficult to collect. A tidal height is a simple number which applies to a wide region simultaneously. A flow has both a magnitude and a direction, both of which can vary substantially with depth and over short distances due to local bathymetry. Also, although a water channel's center is the most useful measuring site, mariners object when current-measuring equipment obstructs waterways. A flow proceeding up a curved channel is the same flow, even though its direction varies continuously along the channel. Surprisingly, flood and ebb flows are often not in opposite directions. Flow direction is determined by the upstream channel's shape, not the downstream channel's shape. Likewise, eddies may form in only one flow direction.

Nevertheless, current analysis is similar to tidal analysis: in the simple case, at a given location the flood flow is in mostly one direction, and the ebb flow in another direction. Flood velocities are given positive sign, and ebb velocities negative sign. Analysis proceeds as though these are tide heights.

In more complex situations, the main ebb and flood flows do not dominate. Instead, the flow direction and magnitude trace an ellipse over a tidal cycle (on a polar plot) instead of along the ebb and flood lines. In this case, analysis might proceed along pairs of directions, with the primary and secondary directions at right angles. An alternative is to treat the tidal flows as complex numbers, as each value has both a magnitude and a direction.

Tide flow information is most commonly seen on nautical charts, presented as a table of flow speeds and bearings at hourly intervals, with separate tables for spring and neap tides. The timing is relative to high water at some harbour where the tidal behaviour is similar in pattern, though it may be far away.

As with tide height predictions, tide flow predictions based only on astronomical factors do not incorporate weather conditions, which can *completely* change the outcome.

The tidal flow through Cook Strait between the two main islands of New Zealand is particularly interesting, as the tides on each side of the strait are almost exactly out of phase, so that one side's high water is simultaneous with the other's low water. Strong currents result, with almost zero tidal height change in the strait's center. Yet, although the tidal surge normally flows in one direction for six hours and in the reverse direction for six hours, a particular surge might last eight or ten hours with the reverse surge enfeebled. In especially boisterous weather conditions, the reverse surge might be entirely overcome so that the flow continues in the same direction through three or more surge periods.

A further complication for Cook Strait's flow pattern is that the tide at the north side (e.g. at Nelson) follows the common bi-weekly spring–neap tide cycle (as found along the west side of the country), but the south side's tidal pattern has only *one* cycle per month, as on the east side: Wellington, and Napier.

Figure 12 shows separately the high water and low water height and time, through November 2007; these are *not* measured values but instead are calculated from tidal parameters derived from years-old measurements. Cook Strait's nautical chart offers tidal current information. For instance the January 1979 edition for 41°13·9'S 174°29·6'E (north west of Cape Terawhiti) refers timings to Westport while the January 2004 issue refers to Wellington. Near Cape Terawhiti in the middle of Cook Strait the tidal height variation is almost nil while the tidal current reaches its maximum, especially near the notorious Karori Rip. Aside from weather effects, the actual currents through Cook Strait are influenced by the tidal height differences between the two ends of the strait and as can be seen, only one of the two spring tides at the north end (Nelson) has a counterpart spring tide at the south end (Wellington), so the resulting behaviour follows neither reference harbour.

Power generation

Tidal energy can be extracted by two means: inserting a water turbine into a tidal current, or building ponds that release/admit water through a turbine. In the first case, the energy amount is entirely determined by the timing and tidal current magnitude. However, the best currents may be unavailable because the turbines would obstruct ships. In the second, the impoundment dams are expensive to construct, natural water cycles are completely disrupted, ship navigation is disrupted. However, with multiple ponds, power can be generated at chosen times. So far, there are few installed systems for tidal power generation (most famously, La Rance by Saint Malo, France) which faces many difficulties. Aside from environmental issues, simply withstanding corrosion and biological fouling pose engineering challenges.

Tidal power proponents point out that, unlike wind power systems, generation levels can be reliably predicted, save for weather effects. While some generation is possible for most of the tidal cycle, in practice turbines lose efficiency at lower operating rates. Since the power available from a flow is proportional to the cube of the flow speed, the times during which high power generation is possible are brief.
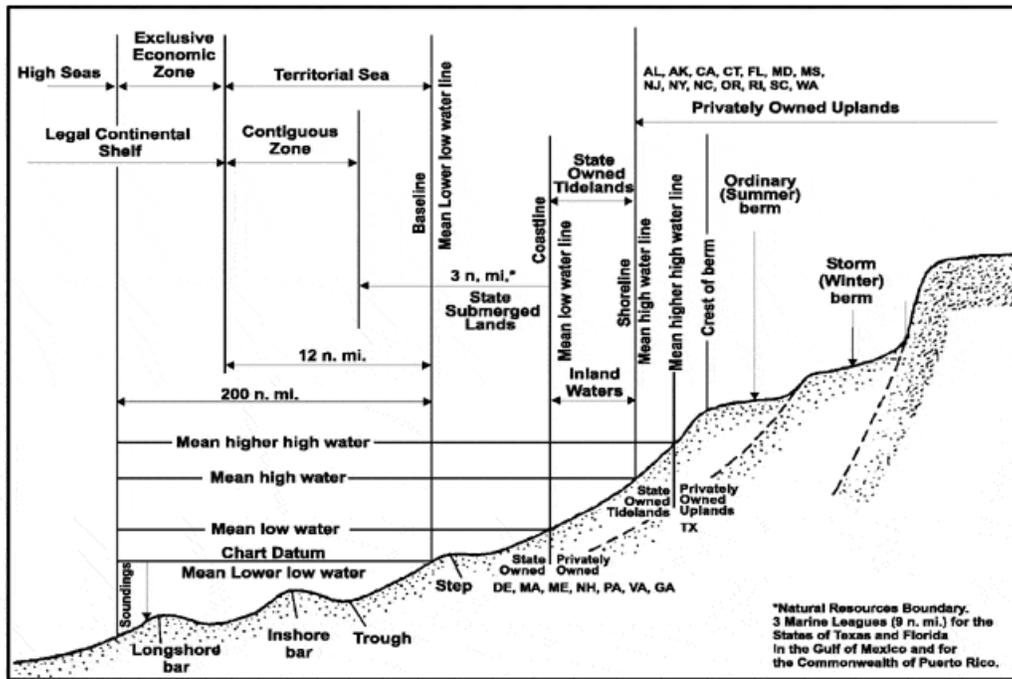
Navigation

DATUMS

Fig. 13: Civil and maritime uses of tidal data

Tidal flows are important for navigation, and significant errors in position occur if they are not accommodated. Tidal heights are also important; for example many rivers and harbours have a shallow "bar" at the entrance which prevents boats with significant draft from entering at low tide.

Until the advent of automated navigation, competence in calculating tidal effects was important to naval officers. The certificate of examination for lieutenants in the Royal Navy once declared that the prospective officer was able to "shift his tides".

Tidal flow timings and velocities appear in *tide charts* or a tidal stream atlas. Tide charts come in sets. Each chart covers a single hour between one high water and another (they ignore the leftover 24 minutes) and show the average tidal flow for that hour. An arrow on the tidal chart indicates the direction and the average flow speed (usually in knots) for spring and neap tides. If a tide chart is not available, most nautical charts have "tidal diamonds" which relate specific points on the chart to a table giving tidal flow direction and speed.

The standard procedure to counteract tidal effects on navigation is to (1) calculate a "dead reckoning" position (or DR) from travel distance and direction, (2) mark the chart (with a

vertical cross like a plus sign) and (3) draw a line from the DR in the tide's direction. The distance the tide moves the boat along this line is computed by the tidal speed, and this gives an "estimated position" or EP (traditionally marked with a dot in a triangle).

Nautical charts display the water's "charted depth" at specific locations with "soundings" and the use of bathymetric contour lines to depict the submerged surface's shape. These depths are relative to a "chart datum", which is typically the water level at the lowest possible astronomical tide (tides may be lower or higher for meteorological reasons) and are therefore the minimum possible water depth during the tidal cycle. "Drying heights" may also be shown on the chart, which are the heights of the exposed seabed at the lowest astronomical tide.

Tide tables list each day's high and low water heights and times. To calculate the actual water depth, add the charted depth to the published tide height. Depth for other times can be derived from tidal curves published for major ports. The rule of twelfths can suffice if an accurate curve is not available. This approximation presumes that the increase in depth in the six hours between low and high water is: first hour — 1/12, second — 2/12, third — 3/12, fourth — 3/12, fifth — 2/12, sixth — 1/12.

Biological aspects

Intertidal ecology

Fig. 14: A rock, seen at low water, exhibiting typical intertidal zonation.

Intertidal ecology is the study of intertidal ecosystems, where organisms live between the low and high water lines. At low water, the intertidal is exposed (or 'emersed') whereas at high water, the intertidal is underwater (or 'immersed'). Intertidal ecologists therefore study the interactions between intertidal organisms and their environment, as well as among the different species. The most important interactions may vary according to the

type of intertidal community. The broadest classifications are based on substrates — rocky shore or soft bottom.

Intertidal organisms experience a highly variable and often hostile environment, and have adapted to cope with and even exploit these conditions. One easily visible feature is vertical zonation, in which the community divides into distinct horizontal bands of specific species at each elevation above low water. A species' ability to cope with desiccation determines its upper limit, while competition with other species sets its lower limit.

Humans use intertidal regions for food and recreation. Overexploitation can damage intertidals directly. Other anthropogenic actions such as introducing invasive species and climate change have large negative effects. Marine Protected Areas are one option communities can apply to protect these areas and aid scientific research.

Biological rhythms

The approximately fortnightly tidal cycle has large effects on intertidal organisms. Hence their biological rhythms tend to occur in rough multiples of this period. Many other animals such as the vertebrates, display similar rhythms. Examples include gestation and egg hatching. In humans, the menstrual cycle lasts roughly a month, an even multiple of the tidal period. Such parallels at least hint at the common descent of all animals from a marine ancestor.

Other tides

When oscillating tidal currents in the stratified ocean flow over uneven bottom topography, they generate internal waves with tidal frequencies. Such waves are called *internal tides*.

In addition to oceanic tides, large lakes can experience small tides and even planets can experience *atmospheric tides* and *Earth tides*. These are continuum mechanical phenomena. The first two take place in fluids. The third affects the Earth's thin solid crust surrounding its semi-liquid interior (with various modifications).

Lake tides

Large lakes such as Superior and Erie can experience tides of 1 to 4 cm, but these can be masked by meteorologically induced phenomena such as seiche. The tide in Lake Michigan is described as 0.5 inches to 1.5 inches or 1 and 3/4 inches.

Atmospheric tides

Atmospheric tides are negligible at ground level and aviation altitudes, masked by weather's much more important effects. Atmospheric tides are both gravitational and

thermal in origin and are the dominant dynamics from about 80–120 kilometres (50–75 mi) above which the molecular density becomes too low to support fluid behavior.

Earth tides

Earth tides or terrestrial tides affect the entire Earth's mass, which acts similarly to a liquid gyroscope with a very thin crust. The Earth's crust shifts (in/out, east/west, north/south) in response to lunar and solar gravitation, ocean tides, and atmospheric loading. While negligible for most human activities, terrestrial tides' semidiurnal amplitude can reach about 55 centimetres (22 in) at the equator—15 centimetres (5.9 in) is due to the Sun—which is important in GPS calibration and VLBI measurements. Precise astronomical angular measurements require knowledge of the Earth's rotation rate and nutation, both of which are influenced by Earth tides. The semi-diurnal M_2 Earth tides are nearly in phase with the Moon with a lag of about two hours.

Some particle physics experiments must adjust for terrestrial tides. For instance, at CERN and SLAC, the very large particle accelerators account for terrestrial tides. Among the relevant effects are circumference deformation for circular accelerators and particle beam energy. Since tidal forces generate currents in conducting fluids in the Earth's interior, they in turn affect the Earth's magnetic field. Earth tides have also been linked to earthquakes.

Galactic tides

Galactic tides are the tidal forces exerted by galaxies on stars within them and satellite galaxies orbiting them. The galactic tide's effects on the Solar System's Oort cloud are believed to cause 90 percent of long-period comets.

Misapplications

Tsunamis, the large waves that occur after earthquakes, are sometimes called *tidal waves*, but this name is given by their *resemblance* to the tide, rather than any actual link to the tide. Other phenomena unrelated to tides but using the word *tide* are rip tide, storm tide, hurricane tide, and black or red tides.

Chapter- 13

Tidal Acceleration

A picture of the Earth and the Moon from Mars. The presence of the moon (which has about 1/81 the mass of the Earth), is slowing Earth's rotation and lengthening the day by about 2 ms every one hundred years.

Tidal acceleration is an effect of the tidal forces between an orbiting natural satellite (*e.g.* the Moon), and the primary planet that it orbits (*e.g.* the Earth). The "acceleration" is usually negative, as it causes a gradual slowing and recession of a satellite in a prograde orbit away from the primary, and a corresponding slowdown of the primary's rotation. The process eventually leads to tidal locking of first the smaller, and later the larger body. The Earth-Moon system is the best studied case.

The similar process of **tidal deceleration** occurs for satellites that have an orbital period that is shorter than the primary's rotation period, or that orbit in a retrograde direction.
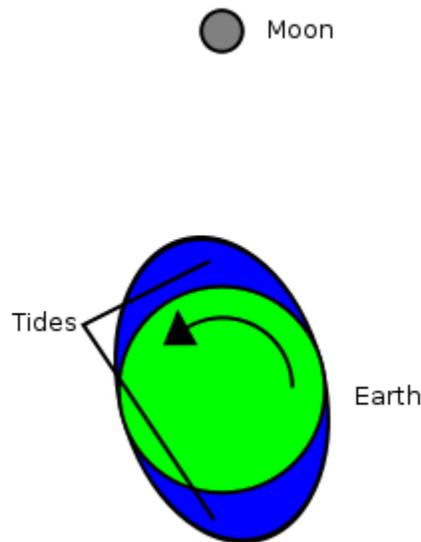
Earth-Moon system

Discovery history of the secular acceleration

Edmond Halley was the first to suggest, in 1695, that the mean motion of the Moon was apparently getting faster, by comparison with ancient eclipse observations, but he gave no data. (It was not yet known in Halley's time that what is actually occurring includes a slowing-down of the Earth's rate of rotation: Ephemeris time - History. When measured as a function of mean solar time rather than uniform time, the effect appears as a positive acceleration.) In 1749 Richard Dunthorne confirmed Halley's suspicion after re-examining ancient records, and produced the first quantitative estimate for the size of this apparent effect: a centurial rate of +10" (arcseconds) in lunar longitude (a surprisingly good result for its time, not far different from values assessed later, e.g. in 1786 by de Lalande, and to compare with values from about 10" to nearly 13" being derived about century later.)

Pierre-Simon Laplace produced in 1786 a theoretical analysis giving a basis on which the Moon's mean motion should accelerate in response to perturbational changes in the eccentricity of the orbit of the Earth around the Sun. Laplace's initial computation accounted for the whole effect, thus seeming to tie up the theory neatly with both modern and ancient observations.

However, in 1854, J C Adams caused the question to be re-opened by finding an error in Laplace's computations: it turned out that only about half of the Moon's apparent acceleration could be accounted for on Laplace's basis by the change in the Earth's orbital eccentricity. Adams' finding provoked a sharp astronomical controversy that lasted some years, but the correctness of his result, agreed by other mathematical astronomers including C E Delaunay, was eventually accepted. The question depended on correct analysis of the lunar motions, and received a further complication with another discovery, around the same time, that another significant long-term perturbation that had been calculated for the Moon (supposedly due to the action of Venus) was also in error, was found on re-examination to be almost negligible, and practically had to disappear from the theory. A part of the answer was suggested independently in the 1860s by Delaunay and by William Ferrel: tidal retardation of the Earth's rotation rate was lengthening the unit of time and causing a lunar acceleration that was only apparent.

It took some time for the astronomical community to accept the reality and the scale of tidal effects. But eventually it became clear that three effects are involved, when measured in terms of mean solar time. Beside the effects of perturbational changes in the Earth's orbital eccentricity, as found by Laplace and corrected by Adams, there are two tidal effects (a combination first suggested by Emmanuel Liais). First there is a real retardation of the Moon's angular rate of orbital motion, due to tidal exchange of angular momentum between the Earth and Moon. This increases the Moon's angular momentum around the Earth (and moves the Moon to a higher orbit with a slower period). Secondly there is an apparent increase in the Moon's angular rate of orbital motion (when measured in terms of mean solar time). This arises from the Earth's loss of angular momentum and the consequent increase in length of day.

A diagram of the Earth-Moon system showing how the tidal bulge is pushed ahead by the Earth's rotation. This offset bulge exerts a net torque on the Moon, boosting it while slowing the Earth's rotation.

Effects of Moon's gravity

Because the Moon's mass is a considerable fraction of that of the Earth (about 1:81), the two bodies can be regarded as a double planet system, rather than as a planet with a satellite. The plane of the Moon's orbit around the Earth lies close to the plane of the Earth's orbit around the Sun (the ecliptic), rather than in the plane perpendicular to the axis of rotation of the Earth (the equator) as is usually the case with planetary satellites. The mass of the Moon is sufficiently large, and it is sufficiently close, to raise tides in the matter of the Earth. In particular, the water of the oceans bulges out along both ends of an axis passing through the centers of the Earth and Moon. The average tidal bulge closely follows the Moon in its orbit, and the Earth rotates under this tidal bulge in just over a day. However, the rotation drags the position of the tidal bulge ahead of the position directly under the Moon. As a consequence, there exists a substantial amount of mass in the bulge that is offset from the line through the centers of the Earth and Moon. Because

of this offset, a portion of the gravitational pull between Earth's tidal bulges and the Moon is perpendicular to the Earth-Moon line, *i.e.* there exists a torque between the Earth and the Moon. This boosts the Moon in its orbit, and decelerates the rotation of the Earth.

So the result is that the mean solar day, which is nominally 86400 seconds long, is actually getting longer when measured in SI seconds with stable atomic clocks. (The SI second, when adopted, was already a little shorter than the current value of the second of mean solar time.) The small difference accumulates every day, which leads to an increasing difference between our clock time (Universal Time) on the one hand, and Atomic Time and Ephemeris Time on the other hand. This makes it necessary to insert a leap second at irregular intervals.

If other effects were ignored, tidal acceleration would continue until the rotational period of the Earth matched the orbital period of the Moon. At that time, the Moon would always be overhead of a single fixed place on Earth. Such a situation already exists in the Pluto-Charon system. However, the slowdown of the Earth's rotation is not occurring fast enough for the rotation to lengthen to a month before other effects make this irrelevant: About 2.1 billion years from now, the continual increase of the Sun's radiation will cause the Earth's oceans to vaporize, removing the bulk of the tidal friction and acceleration. Even without this, the slowdown to a month-long day would still not have been completed by 4.5 billion years from now when the Sun will evolve into a red giant and possibly destroy both the Earth and Moon. (Tidal acceleration and solar mass loss is also moving the Earth outward from the Sun, but it is unknown whether it will be enough to save it from destruction.)

Tidal acceleration is one of the few examples in the dynamics of the solar system of a so-called **secular perturbation** of an orbit, *i.e.* a perturbation that continuously increases with time and is not periodic. Up to a high order of approximation, mutual gravitational perturbations between major or minor planets only cause periodic variations in their orbits, that is, parameters oscillate between maximum and minimum values. The tidal effect gives rise to a quadratic term in the equations, which leads to unbounded growth. In the mathematical theories of the planetary orbits that form the basis of ephemerides, quadratic and higher order secular terms do occur, but these are mostly Taylor expansions of very long time periodic terms. The reason that tidal effects are different is that unlike distant gravitational perturbations, friction is an essential part of tidal acceleration, and leads to permanent loss of energy from the dynamical system in the form of heat. In other words, we do not have a Hamiltonian system here.

Angular momentum and energy

The gravitational torque between the Moon and the tidal bulge of the Earth causes the Moon to be promoted in its orbit, and the Earth to be decelerated in its rotation. As in any physical process within an isolated system, total energy and angular momentum are conserved. Effectively, energy and angular momentum are transferred from the rotation of the Earth to the orbital motion of the Moon (however, most of the energy lost by the Earth is converted to heat, and only about one 30th is transferred to the Moon). The

Moon moves farther away from the Earth, so its potential energy (in the Earth's gravity well) increases. It stays in orbit, and from Kepler's 3rd law it follows that its velocity actually decreases, so the tidal action on the Moon actually causes a deceleration of its motion across the celestial sphere. Although its kinetic energy decreases, its potential energy increases by a larger amount. The tidal force has a component in the direction of the Moon's motion, and therefore increases its energy, but the non-tidal part of the Earth's gravity pulls (on average) slightly backwards on the Moon (which on average has a slight outward velocity), so the net result is that the Moon slows down. The Moon's orbital angular momentum increases.

The rotational angular momentum of the Earth decreases and consequently the length of the day increases. The *net* tide raised on Earth by the Moon is dragged ahead of the Moon by Earth's much faster rotation. **Tidal friction** is required to drag and maintain the bulge ahead of the Moon, and it dissipates the excess energy of the exchange of rotational and orbital energy between the Earth and Moon as heat. If the friction and heat dissipation were not present, the Moon's gravitational force on the tidal bulge would rapidly (within two days) bring the tide back into synchronization with the Moon, and the Moon would no longer recede. Most of the dissipation occurs in a turbulent bottom boundary layer in shallow seas such as the European shelf around the British Isles, the Patagonian shelf off Argentina, and the Bering Sea.

The dissipation of energy by tidal friction averages about 3.75 terawatts, of which 2.5 terawatts are from the principal M_2 lunar component and the remainder from other components, both lunar and solar.

An *equilibrium tidal bulge* does not really exist on Earth because the continents do not allow this mathematical solution to take place. Oceanic tides actually rotate around the oceans basin as vast *gyres* around several *amphidromic points* where no tide exists. The Moon pulls on each individual undulation as Earth rotates—some undulations are ahead of the Moon, others are behind it, while still others are on either side. The "bulges" that actually do exist for the Moon to pull on (and which pull on the Moon) are the net result of integrating the actual undulations over all the world's oceans. Earth's *net* (or *equivalent*) equilibrium tide has an amplitude of only 3.23 cm, which is totally swamped by oceanic tides that can exceed one metre.

Historical evidence

This mechanism has been working for 4.5 billion years, since oceans first formed on the Earth. There is geological and paleontological evidence that the Earth rotated faster and that the Moon was closer to the Earth in the remote past. *Tidal rhythmites* are alternating layers of sand and silt laid down offshore from estuaries having great tidal flows. Daily, monthly and seasonal cycles can be found in the deposits. This geological record is consistent with these conditions 620 million years ago: the day was 21.9±0.4 hours, and there were 13.1±0.1 synodic months/year and 400±7 solar days/year. The length of the year has remained virtually unchanged during this period because no evidence exists that

the constant of gravitation has changed. The average recession rate of the Moon between then and now has been 2.17±0.31 cm/year, which is about half the present rate.

Quantitative description of the Earth-Moon case

The motion of the Moon can be followed with an accuracy of a few centimeters by lunar laser ranging (LLR). Laser pulses are bounced off mirrors on the surface of the moon, emplaced during the Apollo missions of 1969 to 1972 and by Lunokhod 2 in 1973. Measuring the return time of the pulse yields a very accurate measure of the distance. These measurements are fitted to the equations of motion. This yields numerical values for the Moon's secular acceleration in longitude and the rate of change of the semimajor axis of the Earth-Moon ellipse. From the period 1970–2007, the results are:

−25.85"/cy² in ecliptic longitude
(*cy* is centuries, here taken to the square)
+38.14 mm/yr in the mean Earth-Moon distance

This is consistent with results from satellite laser ranging (SLR), a similar technique applied to artificial satellites orbiting the Earth, which yields a model for the gravitational field of the Earth, including that of the tides. The model accurately predicts the changes in the motion of the Moon.

Finally, ancient observations of solar eclipses give fairly accurate positions for the Moon at those moments. Studies of these observations give results consistent with the value quoted above.

The other consequence of tidal acceleration is the deceleration of the rotation of the Earth. The rotation of the Earth is somewhat erratic on all time scales (from hours to centuries) due to various causes. The small tidal effect cannot be observed in a short period, but the cumulative effect on the Earth's rotation as measured with a stable clock (ephemeris time, atomic time) of a shortfall of even a few milliseconds every day becomes readily noticeable in a few centuries. Since some event in the remote past, more days and hours have passed (as measured in full rotations of the Earth) (Universal Time) than as measured with stable clocks calibrated to the present, longer length of the day (ephemeris time). This is known as ΔT. Recent values can be obtained from the International Earth Rotation and Reference Systems Service (IERS). A table of the actual length of the day in the past few centuries is also available.

From the observed change in the Moon's orbit, the corresponding change in the length of the day can be computed:

+2.3 ms/cy
(*cy* is centuries).

However, from historical records over the past 2700 years the following average value is found:

+1.70 ± 0.05 ms/cy

The corresponding cumulative value is a parabola having a coefficient of T² (time in centuries squared) of:

ΔT = +31 s/cy²

Opposing the tidal deceleration of the Earth is a mechanism that is in fact accelerating the rotation. The Earth is not a sphere, but rather an ellipsoid that is flattened at the poles. SLR has shown that this flattening is decreasing. The explanation is, that during the ice age large masses of ice collected at the poles, and depressed the underlying rocks. The ice mass started disappearing over 10000 years ago, but the Earth's crust is still not in hydrostatic equilibrium and is still rebounding (the relaxation time is estimated to be about 4000 years). As a consequence, the polar diameter of the Earth increases, and since the mass and density remain the same, the volume remains the same; therefore the equatorial diameter is decreasing. As a consequence, mass moves closer to the rotation axis of the Earth. This means that its moment of inertia is decreasing. Because its total angular momentum remains the same during this process, the rotation rate increases. This is the well-known phenomenon of a spinning figure skater who spins ever faster as she retracts her arms. From the observed change in the moment of inertia the acceleration of rotation can be computed: the average value over the historical period must have been about −0.6 ms/cy. This largely explains the historical observations.

Other cases of tidal acceleration

Most natural satellites of the planets undergo tidal acceleration to some degree (usually small), except for the two classes of tidally decelerated bodies. In most cases, however, the effect is small enough that even after billions of years most satellites will not actually be lost. The effect is probably most pronounced for Mars' second moon Deimos, which may become an Earth-crossing asteroid after it leaks out of Mars' grip. The effect also arises between different components in a binary star.

Tidal deceleration

This comes in two varieties:

1. *Fast satellites*: Some inner moons of the gas giant planets and Phobos orbit within the synchronous orbit radius so that their orbital period is shorter than their planet's rotation. In this case the tidal bulges raised by the moon on their planet lag behind the moon, and act to *decelerate* it in its orbit. The net effect is a decay of that moon's orbit as it gradually spirals towards the planet. The planet's rotation also speeds up slightly in the process. In the distant future these moons will impact the planet or cross within their Roche limit and be tidally disrupted into fragments. However, all such moons in the solar system are very small bodies and

the tidal bulges raised by them on the planet are also small, so the effect is usually weak and the orbit decays slowly. The moons affected are:

- *Around Mars*: Phobos
- *Around Jupiter*: Metis and Adrastea
- *Around Saturn*: none, except for the ring particles (like Jupiter, Saturn is a very rapid rotator but has no satellites close enough)
- *Around Uranus*: Cordelia, Ophelia, Bianca, Cressida, Desdemona, Juliet, Portia, Rosalind, Cupid, Belinda, and Perdita
- *Around Neptune*: Naiad, Thalassa, Despina, Galatea and Larissa

2. *Retrograde satellites*: All retrograde satellites experience tidal deceleration to some degree because the moon's orbital motion and the planet's rotation are in opposite directions, causing restoring forces from their tidal bulges. A difference to the previous "fast satellite" case here is that the planet's rotation is also slowed down rather than sped up (angular momentum is still conserved because in such a case the values for the planet's rotation and the moon's revolution have opposite signs). The only satellite in the Solar System for which this effect is non-negligible is Neptune's moon Triton. All the other retrograde satellites are on distant orbits and tidal forces between them and the planet are negligible.

The planet Venus is believed to have no satellites chiefly because any hypothetical satellites would have suffered deceleration long ago, from either cause; Venus has a very slow *and* retrograde rotation.

Chapter- 14

Tidal Power

Tidal power, also called **tidal energy**, is a form of hydropower that converts the energy of tides into electricity or other useful forms of power. The first large-scale tidal power plant (the Rance Tidal Power Station) started operation in 1966.

Although not yet widely used, tidal power has potential for future electricity generation. Tides are more predictable than wind energy and solar power. Among sources of renewable energy, tidal power has traditionally suffered from relatively high cost and limited availability of sites with sufficiently high tidal ranges or flow velocities, thus constricting its total availability. However, many recent technological developments and improvements, both in design (e.g. dynamic tidal power, tidal lagoons) and turbine technology (e.g. new axial turbines, crossflow turbines), indicate that the total availability of tidal power may be much higher than previously assumed, and that economic and environmental costs may be brought down to competitive levels.

Historically, tide mills have been used, both in Europe and on the Atlantic coast of North America. The earliest occurrences date from the Middle Ages, or even from Roman times.

Generation of tidal energy
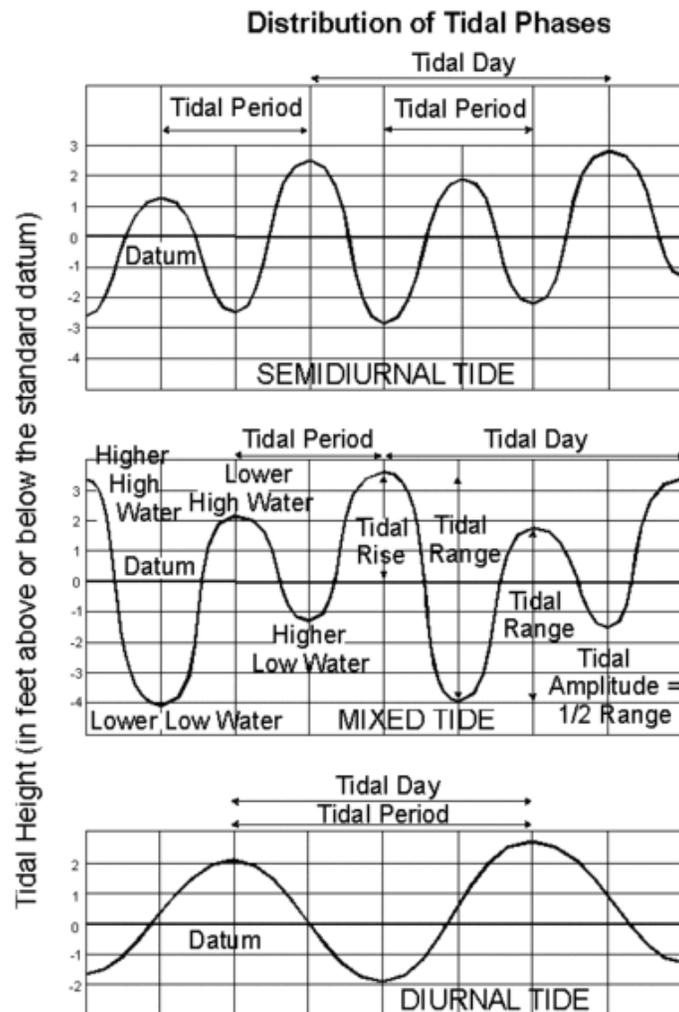
Variation of tides over a day

Tidal power is the only form of energy which derives directly from the relative motions of the Earth–Moon system, and to a lesser extent from the Earth–Sun system. Tidal forces produced by the Moon and Sun, in combination with Earth's rotation, are responsible for the generation of the tides. Other sources of energy originate directly or indirectly from the Sun, including fossil fuels, conventional hydroelectric, wind, biofuels, wave power and solar. Nuclear energy makes use of Earth's mineral deposits of fissile elements, while geothermal power uses the Earth's internal heat which comes from a combination of residual heat from planetary accretion (about 20%) and heat produced through radioactive decay (80%).

Tidal energy is extracted from the relative motion of large bodies of water. Periodic changes of water levels, and associated tidal currents, are due to the gravitational

attraction of the Sun and Moon. Magnitude of the tide at a location is the result of the changing positions of the Moon and Sun relative to the Earth, the effects of Earth rotation, and the local geography of the sea floor and coastlines.

Because the Earth's tides are ultimately due to gravitational interaction with the Moon and Sun and the Earth's rotation, tidal power is practically inexhaustible and classified as a renewable energy resource.

A tidal generator uses this phenomenon to generate electricity. Greater tidal variation or tidal current velocities can dramatically increase the potential for tidal electricity generation.

The movement of the tides causes a continual loss of mechanical energy in the Earth–Moon system due to pumping of water through the natural restrictions around coastlines, and consequent viscous dissipation at the seabed and in turbulence. This loss of energy has caused the rotation of the Earth to slow in the 4.5 billion years since formation. During the last 620 million years the period of rotation has increased from 21.9 hours to the 24 hours we see now; in this period the Earth has lost 17% of its rotational energy. While tidal power may take additional energy from the system, increasing the rate of slowdown, the effect would be noticeable over millions of years only, thus being negligible.

Generating methods

The world's first commercial-scale and grid-connected tidal stream generator – SeaGen – in Strangford Lough. The strong wake shows the power in the tidal current.
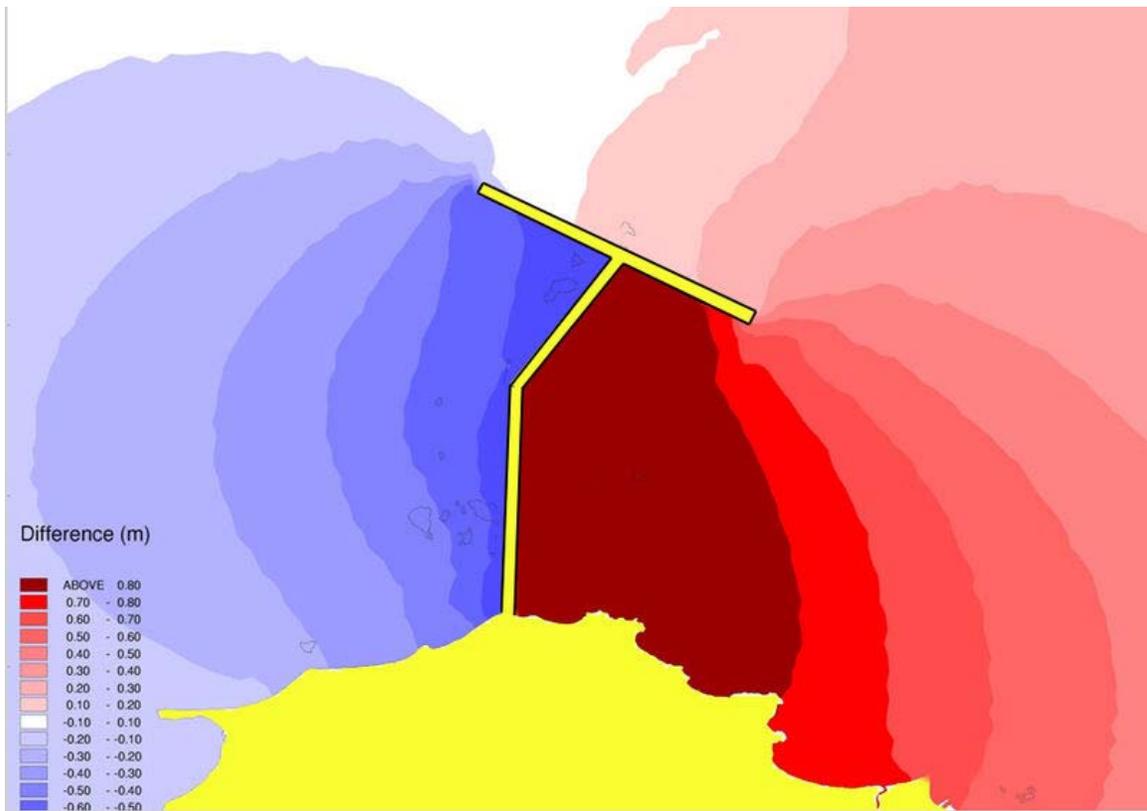
Top-down view of a DTP dam. Blue and dark red colors indicate low and high tides, respectively.

Tidal power can be classified into three generating methods:

Tidal stream generator

Tidal stream generators (or TSGs) make use of the kinetic energy of moving water to power turbines, in a similar way to wind turbines that use moving air. This method is gaining in popularity because of the lower cost and lower ecological impact compared to tidal barrages.

Tidal barrage

Tidal barrages make use of the potential energy in the difference in height (or *head*) between high and low tides. Barrages are essentially dams across the full width of a tidal estuary, and suffer from very high civil infrastructure costs, a worldwide shortage of viable sites and environmental issues.

Dynamic tidal power

Dynamic tidal power (or DTP) is a theoretical generation technology that would exploit an interaction between potential and kinetic energies in tidal flows. It proposes that very long dams (for example: 30–50 km length) be built from coasts straight out into the sea or ocean, without enclosing an area. Tidal phase differences are introduced by the dam, leading to a significant water level differential (at least 2–3 meters) in shallow coastal seas featuring strong coast-parallel oscillating tidal currents such as found in the UK, China and Korea. Each dam would generate power at a scale of 6 - 15 GW.

Current and future tidal power schemes

- The first tidal power station was the Rance tidal power plant built over a period of 6 years from 1960 to 1966 at La Rance, France. It has 240 MW installed capacity.
- The first tidal power site in North America is the Annapolis Royal Generating Station, Annapolis Royal, Nova Scotia, which opened in 1984 on an inlet of the Bay of Fundy. It has 20 MW installed capacity.
- The Jiangxia Tidal Power Station, south of Hangzhou in China has been operational since 1985, with current installed capacity of 3.2 MW. More tidal power is planned near the mouth of the Yalu River.
- The first in-stream tidal current generator in North America (Race Rocks Tidal Power Demonstration Project) was installed at Race Rocks on southern Vancouver Island in September 2006. The next phase in the development of this tidal current generator will be in Nova Scotia.
- A small project was built by the Soviet Union at Kislaya Guba on the Barents Sea. It has 0.4 MW installed capacity. In 2006 it was upgraded with a 1.2MW experimental advanced orthogonal turbine.
- Jindo Uldolmok Tidal Power Plant in South Korea is a tidal stream generation scheme planned to be expanded progressively to 90 MW of capacity by 2013. The first 1 MW was installed in May 2009.
- A 1.2 MW SeaGen system became operational in late 2008 on Strangford Lough in Northern Ireland.
- 254 MW Sihwa Lake Tidal Power Plant in South Korea is under construction and planned to be completed by the end of 2010.
- The contract for an 812 MW tidal barrage near Ganghwa Island north-west of Incheon has been signed by Daewoo. Completion is planned for 2015.

- A 1,320 MW barrage built around islands west of Incheon is proposed by the Korean government, with projected construction start in 2017.

- Other South Korean projects include barrages planned for Garorim Bay, Ansanman, and Swaseongho, and tidal generation associated with the Saemangeum reclamation project. The barrages are all in the multiple-hundred megawatts range.

- The Indian state of Gujarat is planning to host South Asia's first commercial-scale tidal power station. The company Atlantis Resources is to install a 50MW tidal farm in the Gulf of Kutch on India's west coast, with construction starting early in 2012.

- Estimates for new tidal barrages in England give the potential generation at 5.6GW mean power.

Country	Place	Mean tidal range (m)	Area of basin (km²)	Maximum capacity (MW)
🇬🇧 United Kingdom	River Severn	7.8	450	8,640
🇷🇺 Russia	Penzhinskaya Bay	6.0	20,500	87,000

Chapter- 15

Tidal Range & Amphidromic Point

Tidal Range
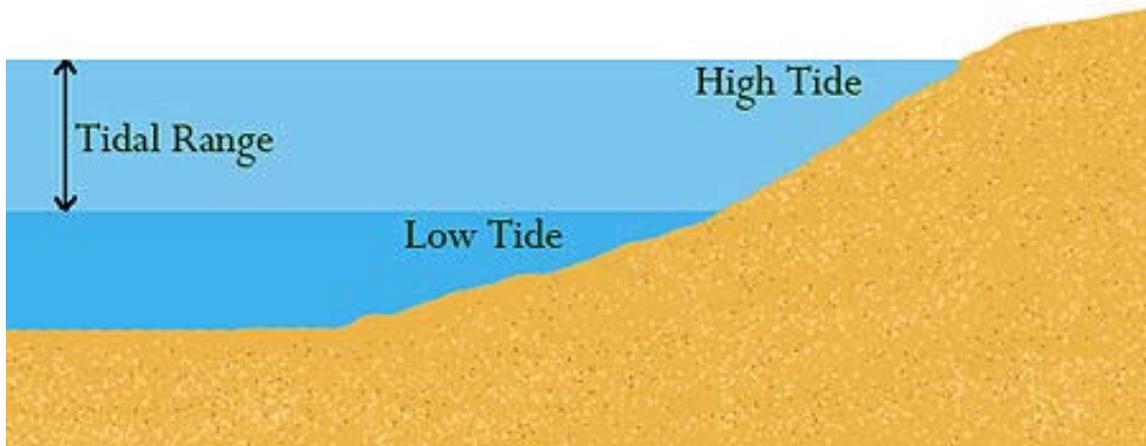
The tidal range is difference between the high tide and the low tide.

The **tidal range** is the vertical difference between the high tide and the succeeding low tide. Tides are the rise and fall of sea levels caused by the combined effects of the gravitational forces exerted by the Moon and the Sun and the rotation of the Earth. The tidal range is not constant, but changes depending on where the sun and the moon are.

The most extreme tidal range occurs around the time of the full or new moons, when the gravitational forces of both the Sun and Moon are in phase reinforcing each other in the same direction (new moon), or are exactly the opposite phase (full). This type of tide is known as a spring tide. During neap tides, when the Moon and Sun's gravitational force vectors act in quadrature (making a right angle to the Earth's orbit), the difference between high and low tides is smaller. Neap tides occur during the first and last quarters of the moon's phases. The largest annual tidal range can be expected around the time of the Equinox, if coincidental with a spring tide.

Tidal data for coastal areas is published by the National Hydrographic service of the country concerned Tidal data is based on astronomical phenomena and is predictable.

Storm force winds blowing from a steady direction for a prolonged time interval combined with low barometric pressure can increase the tidal range particularly in narrow bays. Such weather related effects on the tide, which can cause ranges in excess of predicted values and can cause localized flooding are not calculable in advance.

Geography

The typical tidal range in the open ocean is about 0.6 meters (2 feet). Closer to the coast, this range is much greater. Coastal tidal ranges vary globally and can differ anywhere from near zero to over 11 meters (38 feet). The exact range depends on the volume of water adjacent to the coast, and the geography of the basin the water sits in. Larger bodies of water have higher ranges, and the geography can act as a funnel amplifying or dispersing the tide. The world's largest tidal range of 11.7 meters (38.4 feet) occurs at Burntcoat Head in the Bay of Fundy,Eastern Canada. The Bristol Channel, between England and Wales, regularly experiences tidal ranges of up to 14 meters. The top 50 locations with the largest tidal ranges world-wide are listed by the National Oceanic and Atmospheric Administration of the US.

Some of the smallest tidal ranges occur in the Mediterranean, Baltic, and Caribbean Seas. A point within a tidal system where the tidal range is almost zero is called an amphidromic point.

Classification

The tidal range has been classified as:

- **Micromareal**, when the tidal range is lower than 2 meters.
- **Mesomareal**, when the tidal range is between 2 meters and 4 meters.
- **Macromareal**, when the tidal range is higher than 4 meters.

Amphidromic Point

An **amphidromic point** is a point within a tidal system where the tidal range is almost zero. The tidal range (the height difference between high tide and low tide) is zero at the amphidromic point and increases with distance from this point. These points are called nodes.
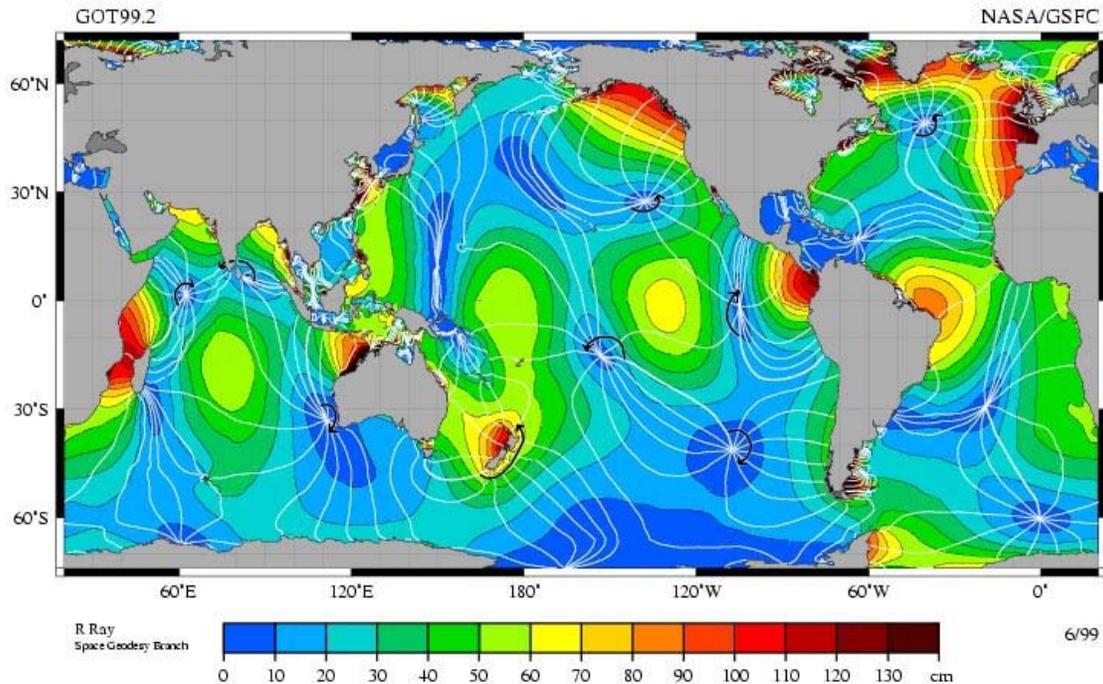
The M_2 tidal constituent, the amplitude indicated by color. The white lines are cotidal lines spaced at phase intervals of 30° (a bit over 1 hr). The amphidromic points are the dark blue areas where the lines come together.

Amphidromic points occur because of the Coriolis effect and interference within oceanic basins, seas and bays creating a wave pattern — called an **amphidromic system** — which rotates around the amphidromic point. At the amphidromic point, there is no vertical movement from tidal action. There can be tidal currents as the water levels on either side of the amphidromic point are not the same.

In most locations M_2 is the largest (semidiurnal) tidal constituent, with an amplitude of roughly half of the full tidal range. Cotidal points means they reach high tide at the same time and low tide at the same time. In the accompanying figure, the low tide lags or leads by 1 hr 2 min from its neighboring lines. Where the lines meet are amphidromes and the tide rotates around them; for example: along the Chilean coast, and from southern Mexico to Peru the tide propagates southward, while from Baja California to Alaska the tide propagates northward.

Amphidromic points in the M_2 tidal constituent

Based on the accompanying figure, the set of clockwise amphidromic points includes:

- north of the Seychelles
- near Enderby Land
- off Perth

- east of New Guinea
- south of Easter Island
- west of the Galapagos Islands
- north of Queen Maud Land

Anti-clockwise amphidromic points include:

- near Sri Lanka
- north of New Guinea
- at Tahiti
- between Mexico and Hawaii
- near the Leeward Islands
- east of Newfoundland
- midway between Rio de Janeiro and Angola
- east of Iceland

The islands of Madagascar and New Zealand are amphidromic points in the sense that the tide goes around them (counterclockwise in both cases) in about 12 and a half hours, but the amplitude of the tides on their coasts is in some places large.